CHAOS IN YANG-MILLS MATRIX MODELS

A THESIS SUBMITTED TO
THE GRADUATE SCHOOL OF NATURAL AND APPLIED SCIENCES
OF
MIDDLE EAST TECHNICAL UNIVERSITY

BY

KAĞAN BAŞKAN

IN PARTIAL FULFILLMENT OF THE REQUIREMENTS
FOR
THE DEGREE OF MASTER OF SCIENCE
IN
PHYSICS

JULY 2019

Approval of the thesis:

CHAOS IN YANG-MILLS MATRIX MODELS

submitted by **KAĞAN BAŞKAN** in partial fulfillment of the requirements for the degree of **Master of Science in Physics Department, Middle East Technical University** by,

Prof. Dr. Halil Kalıpçılar
Dean, Graduate School of **Natural and Applied Sciences** _____

Prof. Dr. Altuğ Özpineci
Head of Department, **Physics** _____

Prof. Dr. Seçkin Kürkcüoğlu
Supervisor, **Physics, METU** _____

Assoc. Prof. Dr. İsmet Yurduşen
Co-supervisor, **Mathematics, Hacettepe University** _____

Examining Committee Members:

Prof. Dr. Sadi Turgut
Physics, METU _____

Prof. Dr. Seçkin Kürkcüoğlu
Physics, METU _____

Assoc. Prof. Dr. İsmet Yurduşen
Mathematics, Hacettepe University _____

Prof. Dr. İsmail Turan
Physics, METU _____

Assoc. Prof. Dr. Yusuf İpekoğlu
Physics, METU _____

Date:

I hereby declare that all information in this document has been obtained and presented in accordance with academic rules and ethical conduct. I also declare that, as required by these rules and conduct, I have fully cited and referenced all material and results that are not original to this work.

Name, Surname: Kağan Başkan

Signature :

ABSTRACT

CHAOS IN YANG-MILLS MATRIX MODELS

Başkan, Kağan
M.S., Department of Physics
Supervisor: Prof. Dr. Seçkin Kürkcüoğlu
Co-Supervisor: Assoc. Prof. Dr. İsmet Yurduşen

July 2019, 81 pages

In this thesis, chaotic dynamics emerging from Yang-Mills matrix models are investigated. Firstly, we investigate the Yang-Mills two-matrix models with Chern-Simons term using both analytical and numerical methods. In particular, we obtain the Poincaré sections and Lyapunov exponents at several different values of the parameters of the model, revealing the detailed structure of the chaotic dynamics. In the second part of the thesis, we focus on a massive deformation of the bosonic part of the Banks-Fischler-Shenker-Susskind (BFSS) matrix model. Using an ansatz involving fuzzy-2 and fuzzy-4 sphere configurations we determine reduced effective Hamiltonians through which we study the emerging chaotic dynamics.

Keywords: Yang Mills Matrix Models, BFSS Matrix Model, Chern-Simons Theory in Matrix Models, Chaos in Matrix Models

ÖZ

YANG-MILLS MATRİS MODELLERİNDE KAOS

Başkan, Kağan
Yüksek Lisans, Fizik Bölümü
Tez Yöneticisi: Prof. Dr. Seçkin Kürkcüoğlu
Ortak Tez Yöneticisi: Doç. Dr. İsmet Yurduşen

Temmuz 2019 , 81 sayfa

Bu tezde Yang-Mills matris modellerinden ortaya çıkan kaotik dinamik yapılar incelenmiştir. İlk olarak, Chern-Simons teriminin ekli olduğu Yang-Mills iki-matris modeli analitik ve sayısal metotlarla incelenmiştir. Modelin parametrelerinin çeşitli değerlerinde Poincaré kesitleri ve Lyapunov üsleri elde edilerek kaotik dinamiğin detaylı yapısı ortaya konulmuştur. Tezin ikinci kısmında, Banks-Fischler-Shenker-Susskind (BFSS) matris modelinin bozonik kısmının kütle deformasyonlu durumlarına odaklanılmıştır. Fuzzy-2 ve fuzzy-4 küre konfigürasyonlarını içeren bir yaklaşım kullanılarak indirgenmiş etkin Hamiltonianlar elde edilip bunların vasıtasıyla modelin kaotik yapıları incelenmiştir.

Anahtar Kelimeler: Yang Mills Matris Modelleri, BFSS Matris Modeli, Matris Modellerinde Chern-Simons Teorisi, Matris Modellerinde Kaos

To my family

ACKNOWLEDGMENTS

I would like to thank my advisor Prof. Dr. Seçkin Kürkcüoğlu for his continuous support, patience and motivation. His immense knowledge have guided me throughout my M.S. study and related research. It was a great opportunity for me to study under his supervision.

I would also like to thank Onur Oktay for his help, illuminating discussions and collaboration during the process of the research.

I would like to express my gratitude to my parents. They have encouraged me during my most difficult times and supported me continuously. This accomplishment would not have been possible without them.

TABLE OF CONTENTS

LIST OF TABLES

TABLES

LIST OF FIGURES

FIGURES

CHAPTER 1

INTRODUCTION

Matrix gauge theories, which are also called matrix quantum mechanics in the literature continue to attract significant attention and being explored from several perspectives ever since their discovery over twenty years ago. Among these, the matrix model proposed by Banks-Fischler-Shenker-Susskind (BFSS) model[1] is essentially supersymmetric gauge theory consisting of nine $N \times N$ matrices and a single $U(N)$ gauge field, in its bosonic part, whose matrix elements depend on time only. This model can be obtained by dimensionally reducing the $\mathcal{N} = 1$ SUSY Yang-Mills theory in 9+1 dimensions to zero volume, in other words to 0+1 dimensions. The BFSS model has an important role in superstring theory and M-theory. In the context of superstring theory it may be interpreted to describe the dynamics of N-coincident D0-branes[1, 2, 3]. The latter are point like objects in string theory with certain properties and generalize to D-p branes with $p \leq 9$ [4, 5]. Due to gauge-gravity correspondence this description of the BFSS gauge theory has a gravity dual at large N, which describes a so called blackbrane that is a string theoretical black hole[2, 3, 6, 7].

In this thesis, our focus will be on the bosonic part of the BFSS model and related models. We will make no formal attempt to connect the developments in this work to a broader perspective in string theory and limit ourselves to make only qualitative remarks in that context whenever needed. As already noted, the bosonic sector of the BFSS model consists of nine $N \times N$ Hermitian matrices and a Hermitian $U(N)$ (or $SU(N)$) gauge field. The action for the model is invariant under the $SU(N)$ gauge symmetry as well as a $SO(9)$ global symmetry, which is responsible for rigidly rotating the nine matrices among themselves. Due to the large number of interacting degrees of freedom through a quartic Yang-Mills potential it does not seem possible

to obtain a general solution of this model. It is possible to consider smaller matrix models that is matrix models with less number of matrices and a smaller gauge group by considering various degrees of freedom in the BFSS model to be frozen or motivate such matrix models as emerging from dimensionally reducing Yang-Mills theories in d+1-dimensions with $d \leq 9$.

One of the recent focuses in this context has been to explore the chaotic dynamics emerging from the BFSS and related matrix models[8, 9, 10]. In [8], the minimal bosonic matrix model, which is a model with two 2×2 matrices and $SU(2)$ gauge and $SO(2)$ global symmetry has been put under investigation. Even in this simplest case, it does not appear possible to obtain the general solution of the equations of motion. After transforming the model to new set of coordinates using analytical methods and taking advantage of the gauge and global symmetries the authors of [8] have successfully studied the chaotic dynamics in this model by obtaining the Poincaré sections and Lyapunov spectrum. They show how as the value of a conserved component of angular momentum is modified from zero to non-zero values, the system evolves from a chaotic dynamical phase to eventually a non-chaotic phase. They also comment in what sense these results may be useful to explain the passage from black hole phase to a no-black hole phase in the gravity dual of related models with larger number of degrees of freedom. A considerable part of chapter 2 is devoted to the review of this article. After these brief remarks on the recent literature we can present the main developments contained in this thesis.

In chapter 3, we investigate how the addition of a Chern-Simons term affects the minimal matrix model of Berenstein and Kawai[8]. To be more precise, we first analyze in detail the structural changes in the model upon supplementing the action with a Chern-Simons term, which is first order in time derivatives. This eventually leads us to model physical changes in the dynamics, from chaos to no-chaos when, in addition to the conserved component of angular momentum, the Chern-Simons coupling is modified to assume different values. The latter can only assume values, which are integer multiples of $\frac{1}{4\pi}$ as a consequence of level quantization in the non-abelian Chern-Simons theory[11]. We study this model by obtaining the Poincaré sections and also by numerically evaluating the Lyapunov spectrum. These results are obtained in collaboration with my supervisor S. Kürkcüoğlu[12]

Consequences of the deformation of the Berenstein-Kawai model via a mass term respecting the gauge and global symmetries are discussed in chapter 4. Poincaré sections' and Lyapunov spectrum's responses to the variation of the mass parameter are given in this chapter.

In chapter 5, we study a double mass deformation of the BFSS matrix model. In this study, we focus on massive deformations which break the $SO(9)$ global symmetry down to $SO(5) \times SO(4)$ and eventually to $SO(5) \times SO(3) \times \mathbb{Z}_2$ upon choosing a certain ansatz configuration to obtain effective actions, whose chaotic dynamics can be studied in detail. The aforementioned ansatz configuration is selected to be composed of matrices forming fuzzy four and two spheres with collective time-dependence. Similar ansatz involving fuzzy two spheres have been used in the work of Asano, Kawai and Yoshida[9] studying chaos in BMN model and inspired us to consider an ansatz with larger dimensional fuzzy spaces. By using the ansatz at several different matrix levels we obtain a family of reduced effective actions, whose dynamics are studied in detail. Finally, after showing the presence of chaotic dynamics by evaluating the Poincaré sections and Lyapunov spectrum, we also make a numerical study revealing that the largest exponent increases logarithmically with increasing energy in these models. The results of this chapter are a part of results obtained in collaboration with O. Oktay and C. Taşcı and my supervisor S. Kürkcüoğlu[13].

Chapter 6 summarizes our original findings in this thesis and states our conclusions. Some related supplemental materials on the definition, evaluation and properties of Poincaré sections and Lyapunov exponents are given in appendices.

CHAPTER 2

BFSS MATRIX MODEL

In this chapter, we introduce the bosonic sector of the BFSS matrix model[1] and present its basic features and properties. BFSS matrix model can be obtained from the dimensional reduction of the $U(N)$, $\mathcal{N} = 1$ supersymmetric Yang-Mills theory from 9+1 dimensions to 0+1. This model holds an important place in string theory and M-theory. Since the string theoretic foundations and features of this model are beyond the scope of this thesis, we are going to focus mainly on the classical dynamics of BFSS model. The simplest but yet non-integrable submodel is $SU(2)$ 2-Yang-Mills matrix model, i.e. the matrix model with only two 2×2 matrices and with $SU(2)$ gauge symmetry. In section 2.3 we focus on this model, and present a review of the study of [8].

2.1 Bosonic Sector of the BFSS Matrix Model

The BFSS action has two parts, which are bosonic and fermionic. The resulting action has $SU(N)$ gauge symmetry and $SO(9)$ global symmetry. In this thesis, only the bosonic part of the model will be studied and its action is given as[2]

$$S_{BFSS} = \int \mathrm{d}t L_{BFSS}\,, \tag{2.1.1a}$$

$$L_{BFSS} = \frac{1}{g^2}\,\mathrm{Tr}\left(\frac{1}{2}(D_0 X_i)^2 + \frac{1}{4}[X_i, X_j]^2\right), \tag{2.1.1b}$$

where $i, j = 1, ..., 9$ and the bosonic degrees of freedom X_i are $N \times N$ Hermitian matrices. g is the Yang-Mills coupling[1] which has a dimension of $(length)^{-3/2}$ since

[1] Since we use classical physics, g only changes the energy scale. We take $g = 1$.

A_0, X_i are of dimension $\frac{1}{length}$. The covariant derivative D_0 is given as

$$D_0 X_i = \partial_0 X_i - i[A_0, X_i]\,, \tag{2.1.2}$$

where A_0 is the gauge field, which is also an $N \times N$ Hermitian matrix.

SU(N) gauge symmetry of the action in (2.1.1a) can be seen by substituting the following transformations

$$X_i \to X_i' = U^\dagger X_i U\,, \tag{2.1.3a}$$

$$A_0 \to A_0' = U^\dagger A_0 U + iU^\dagger \partial_0 U\,, \tag{2.1.3b}$$

into the Lagrangian in (2.1.1b). We first show that $D_0 X_i$ transforms covariantly under the action of the local gauge group $SU(N)$.

$$\begin{aligned} D_0(U^\dagger X_i U) =& \partial_0(U^\dagger X_i U) - i\big[U^\dagger A_0 U + iU^\dagger \partial_0 U, U^\dagger X_i U\big] \\ =& \partial_0(U^\dagger X_i U) - i\big[U^\dagger A_0 U, U^\dagger X_i U\big] \\ &+ \big[U^\dagger \partial_0 U, U^\dagger X_i U\big] \\ =& (\partial_0 U^\dagger) X_i U + U^\dagger(\partial_0 X_i)U + \cancel{U^\dagger X_i (\partial_0 U)} \\ &- iU^\dagger[A_0, X_i]U + U^\dagger(\partial_0 U)U^\dagger X_i U - \cancel{U^\dagger X_i U U^\dagger \partial_0 U} \\ =& (\partial_0 U^\dagger) X_i U + U^\dagger(\partial_0 X_i)U + U^\dagger(\partial_0 U)U^\dagger X_i U \\ &- iU^\dagger[A_0, X_i]U\,, \end{aligned} \tag{2.1.4}$$

where we used $UU^\dagger = 1$. Substituting the following identity

$$\begin{aligned} \partial_0(UU^\dagger) = (\partial_0 U)U^\dagger + U(\partial_0 U^\dagger) = 0 \\ \Rightarrow U(\partial_0 U^\dagger) = -(\partial_0 U)U^\dagger \\ \Rightarrow \partial_0 U^\dagger = -U^\dagger(\partial_0 U)U^\dagger\,, \end{aligned} \tag{2.1.5}$$

into the last line in (2.1.4) gives

$$U^\dagger(\partial_0 X_i)U - iU^\dagger[A_0, X_i]U - \cancel{U^\dagger(\partial_0 U)U^\dagger X_i U} + \cancel{U^\dagger(\partial_0 U)U^\dagger X_i U}\,. \tag{2.1.6}$$

Therefore, we have

$$\begin{aligned} \mathrm{Tr}\,\frac{1}{2}(D_0 X_i)^2 \to \mathrm{Tr}\,\frac{1}{2}U^\dagger(D_0 X_i)UU^\dagger(D_0 X_i)U \\ = \mathrm{Tr}\,\frac{1}{2}(D_0 X_i)^2\,, \end{aligned} \tag{2.1.7}$$

where we have used the cyclicity of the trace verifying the invariance of the kinetic term under $SU(2)$ gauge transformations. The potential term in the Lagrangian transforms under the $SU(N)$ gauge transformations as follows

$$\begin{aligned}\mathrm{Tr}\big([X_i, X_j]^2\big) &= \big[U^\dagger X_i U, U^\dagger X_j U\big]^2 \\ &= \mathrm{Tr}\big(\big[U^\dagger X_i U, U^\dagger X_j U\big]\big[U^\dagger X_i U, U^\dagger X_j U\big]\big) \\ &= \mathrm{Tr}\big(U^\dagger [X_i, X_j] U U^\dagger [X_i, X_j] U\big) \\ &= \mathrm{Tr}\big(U^\dagger [X_i, X_j]^2 U\big) \\ &= \mathrm{Tr}\big([X_i, X_j]^2\big)\,.\end{aligned} \tag{2.1.8}$$

Equations (2.1.7) and (2.1.8) together show that the Lagrangian L_{BFSS} is invariant under the $SU(N)$ gauge transformations.

In addition to the local gauge symmetry, the action has also a global $SO(9)$ symmetry i.e. it is invariant under the rigid $SO(9)$ rotations of X_i among each other. To see this property, consider 9×9 orthogonal matrices $R_{ij} \in SO(9)$ and the rotation

$$X_i' = R_{ij} X_j\,. \tag{2.1.9}$$

The covariant derivative transforms as

$$\begin{aligned}D_0(R_{ij}X_j) =& \partial_0(R_{ij}X_j) - i[A_0, R_{ij}X_j] \\ =& R_{ij}(\partial_0 X_j - i[A_0, X_j]) \\ =& R_{ij}(D_0 X_j)\,.\end{aligned} \tag{2.1.10}$$

Therefore, the kinetic term in the Lagrangian remains invariant under $R \in SO(9)$:

$$\begin{aligned}\frac{1}{2}D_0(R_{ij}X_j)D_0(R_{ik}X_k) =& \frac{1}{2}R_{ij}R_{ik}(D_0X_j)(D_0X_k) \\ =& \frac{1}{2}\delta_{jk}(D_0X_j)(D_0X_k) \\ =& \frac{1}{2}(D_0X_j)^2\,,\end{aligned} \tag{2.1.11}$$

where we have used the fact that $RR^T = R^T R$ since R is an orthogonal matrix. The second term in L_{BFSS} transforms as

$$\begin{aligned}\frac{1}{4}[R_{ij}X_j, R_{kl}X_l][R_{im}X_m, R_{kn}X_n] =& R_{ij}R_{kl}R_{im}R_{kn}[X_j, X_l][X_m, X_n] \\ =& \frac{1}{4}\delta_{jm}\delta_{ln}[X_j, X_l][X_m, X_n] \\ =& \frac{1}{4}[X_j, X_l]^2 \\ =& \frac{1}{4}[X_i, X_j]^2\,.\end{aligned} \tag{2.1.12}$$

In the above equation the last line is obtained after relabeling the dummy indices. Equations (2.1.11) and (2.1.12) together indicate that the Lagrangian is invariant under the $SO(9)$ transformations.

Since there is no $\dot{A}_0 = \partial_0 A_0$ term in the L_{BFSS}, its equation of motion is purely algebraic and therefore A_0 is not a dynamical variable. Nevertheless, the algebraic equation of motion of A_0 imposes a constraint on the system which is usually called the Gauss law constraint. The variation

$$A_0 \to A_0 + \delta A_0 \tag{2.1.13}$$

gives the equation of motion with respect to A_0 as follows

$$\begin{aligned}
\frac{1}{2}\,\mathrm{Tr}(D_0 X_i)^2 &\to \frac{1}{2}\,\mathrm{Tr}((\partial_0 X_i - i[A_0 + \delta A_0, X_i])(\partial_0 X_i - i[A_0 + \delta A_0, X_i])) \\
&= \frac{1}{2}\,\mathrm{Tr}((\partial_0 X_i - i[A_0, X_i] - i[\delta A_0, X_i])(\partial_0 X_i - i[A_0, X_i] - i[\delta A_0, X_i])) \\
&= \frac{1}{2}\,\mathrm{Tr}\big((D_0 X_i - i[\delta A_0, X_i])(D_0 X_i - i[\delta A_0, X_i]) + O((\delta A_0)^2)\big) \\
&= \frac{1}{2}\,\mathrm{Tr}(-iD_0 X_i[\delta A_0, X_i] - i[\delta A_0, X_i] D_0 X_i) \\
&= \mathrm{Tr}(-iD_0 X_i[\delta A_0, X_i]) \\
&= \mathrm{Tr}(-iD_0 X_i(\delta A_0 X_i - X_i \delta A_0)) \\
&= \mathrm{Tr}(-i\delta A_0 X_i(D_0 X_i) - i\delta A_0 (D_0 X_i) X_i) \\
&= \mathrm{Tr}(-i\delta A_0 [X_i, D_0 X_i])\,,
\end{aligned} \tag{2.1.14}$$

where we have used the cyclicity of the trace while rearranging the terms. The variation of the action with respect to A_0 is therefore given as

$$\begin{aligned}
\delta S = \int \mathrm{d}t\,\mathrm{Tr}(-i\delta A_0 [X_i, D_0 X_i]) = 0\,, \\
-i[X_i, D_0 X_i] = 0\,.
\end{aligned} \tag{2.1.15}$$

This implies that the equation of motion in the $A_0 = 0$ gauge is

$$\left[X_i, \dot{X}_i\right] = 0\,, \tag{2.1.16}$$

where overdot denotes derivatives with respect to time. (2.1.16) is usually called the Gauss law constraint, in the literature [1].

The BFSS equation of motion can be obtained from the following variation

$$X_i \to X_i + \delta X_i \,. \tag{2.1.17}$$

The variation of the action is

$$\delta S = \int_{-\infty}^{\infty} \mathrm{d}t \,\mathrm{Tr}\left(\frac{1}{2}\frac{\mathrm{d}}{\mathrm{d}t}(X_i + \delta X_i)\frac{\mathrm{d}}{\mathrm{d}t}(X_i + \delta X_i) + \frac{1}{4}[X_i + \delta X_i, X_j + \delta X_j]^2\right). \tag{2.1.18}$$

The first term in the variation of the action takes the form

$$\begin{aligned}\mathrm{Tr}\left(\frac{1}{2}\frac{\mathrm{d}}{\mathrm{d}t}(X_i + \delta X_i)\frac{\mathrm{d}}{\mathrm{d}t}(X_i + \delta X_i)\right) &= \mathrm{Tr}\left(\frac{1}{2}(\dot{X}_i + \delta\dot{X}_i)(\dot{X}_j + \delta\dot{X}_j)\right) \\ &= \mathrm{Tr}\left(\frac{1}{2}(\dot{X}_i\delta\dot{X}_i + \delta\dot{X}_i\dot{X}_i)\right) \\ &= \mathrm{Tr}\left(\dot{X}_i\delta\dot{X}_i\right),\end{aligned} \tag{2.1.19}$$

where we have used the cyclicity of the trace and kept only the first order variations. This equation can be further simplified by using integration by parts as follows

$$\begin{aligned}\int_{-\infty}^{\infty} \mathrm{d}t \,\mathrm{Tr}\left(\dot{X}_i\delta\dot{X}_i\right) &= \dot{X}_i\delta X_i\Big|_{-\infty}^{\infty} - \int_{-\infty}^{\infty} \mathrm{d}t \,\mathrm{Tr}\left(\ddot{X}_i\delta X_i\right) \\ &= -\int_{-\infty}^{\infty} \mathrm{d}t \,\mathrm{Tr}\left(\ddot{X}_i\delta X_i\right).\end{aligned} \tag{2.1.20}$$

To first order in δX_i, the second term in the action can be written as follows

$$
\begin{aligned}
&\frac{1}{4}[X_i+\delta X_i, X_j+\delta X_j]^2 \\
&=\frac{1}{4}([X_i,X_j]+[X_i,\delta X_j]+[\delta X_i,X_j]+[\delta X_i,\delta X_j])^2 \\
&=\frac{1}{4}([X_i,X_j]([X_i,\delta X_j]+[\delta X_i,X_j])+([X_i,\delta X_j]+[\delta X_i,X_j])[X_i,X_j]) \\
&=\frac{1}{2}[X_i,X_j]([X_i,\delta X_j]+[\delta X_i,X_j]) \\
&=\frac{1}{2}(X_iX_j-X_jX_i)(X_i\delta X_j-\delta X_jX_i+\delta X_iX_j-X_j\delta X_i) \\
&=\frac{1}{2}(X_iX_jX_i\delta X_j-X_iX_j\delta X_jX_i+X_iX_j\delta X_iX_j-X_iX_jX_j\delta X_i \\
&-X_jX_iX_i\delta X_j+X_jX_i\delta X_jX_i-X_jX_i\delta X_iX_j+X_jX_iX_j\delta X_i) \\
&=\frac{1}{2}\delta X_i(X_jX_iX_j-X_iX_jX_j-X_jX_jX_i+X_jX_iX_j) \\
&+\frac{1}{2}\delta X_j(X_iX_jX_i-X_iX_iX_j-X_jX_iX_i+X_iX_jX_i) \\
&=\delta X_i(X_jX_iX_j-X_iX_jX_j-X_jX_jX_i+X_jX_iX_j) \\
&=\delta X_i(X_j[X_i,X_j]-[X_i,X_j]X_j) \\
&=\delta X_i[X_j,[X_i,X_j]]\,.
\end{aligned}
\tag{2.1.21}
$$

Since the indices i and j are dummy, we have interchanged i with j in the 9^{th} line. Putting the results obtained in (2.1.20) and (2.1.21) together we find that the variation of the action becomes

$$
\delta S=\int_{-\infty}^{\infty}\mathrm{d}t\,\mathrm{Tr}\Big(\delta X_i(-\ddot{X}+[X_j,[X_i,X_j]])\Big)=0\,. \tag{2.1.22}
$$

Therefore, the BFSS equation of motion is given as

$$
\ddot{X}_i+[[X_i,X_j],X_j]=0\,. \tag{2.1.23}
$$

2.2 The BFSS Matrix Model From Dimensional Reduction

In this section, the BFSS matrix model will be obtained from the dimensional reduction of pure $SU(N)$ Yang-Mills theory in 9+1 dimensions to 0+1 dimensions[2].

In 9+1 dimensions we can work with the metric $\eta^{\mu\nu}=(-1,1,1,...,1)$. The Yang-

Mills action can be written as

$$S = \frac{1}{g^2} \int \mathrm{d}^{10}x \, \mathrm{Tr}\left(-\frac{1}{4} F_{\mu\nu} F^{\mu\nu} \right), \tag{2.2.1}$$

where $\mu, \nu = 0, 1, ..., 9$ and sum over repeated indices are implied. The electromagnetic field tensor is given as

$$F_{\mu\nu} = \partial_\mu A_\nu - \partial_\nu A_\mu - i[A_\mu, A_\nu] \,, \tag{2.2.2}$$

where $A_\mu = A_\mu(\vec{\mathbf{x}}, t) = (A_0(\vec{\mathbf{x}}, t), A_i(\vec{\mathbf{x}}, t))$ for $i = 1, ..., 9$ is the gauge field. It transforms under $SU(N)$ gauge transformation as

$$A_\mu \to A'_\mu = U^\dagger A_\mu U + i U^\dagger \partial_\mu U \,, \tag{2.2.3}$$

where $U = U(\vec{\mathbf{x}}, t) \in SU(N)$. The idea of dimensional reduction from 9+1 to 0+1 dimensions can be simply explained as follows. We consider all the components of the gauge field A_μ and all the gauge transformations U, to be independent of the spatial coordinates $x^i = 1, ..., 9$ and depend only on $x^0 = t$. Thus we write $A_\mu \equiv A_\mu(t) = (A_0(t), A_i(t))$ and $U \equiv U(t)$. From (2.2.3), we see that this implies for the spatial components $A_i(t)$ the gauge transformations

$$A'_i(t) = U^\dagger A_i U \tag{2.2.4}$$

and for $A_0(t)$ the gauge transformations are given in (2.1.3b). This shows that A_i transform adjointly under $SU(N)$ gauge transformations. That is, just like an adjoint non-abelian scalar field with $SU(N)$ gauge symmetry. Therefore, we may devise the new notation

$$A_\mu \to (A_0(t), X_i(t)) \tag{2.2.5}$$

as the constituent fields. Inserting (2.2.5) to (2.2.2) we find for the components of the electromagnetic field tensor

$$\begin{aligned} F_{ij} &= \partial_i X_j - \partial_j X_i - i[X_i, X_j] \\ &= -i[X_i, X_j] \,, \end{aligned} \qquad \begin{aligned} F_{0i} &= \partial_0 X_i - \partial_i A_0 - i[A_0, X_i] \\ &= \partial_0 X_i - i[A_0, X_i] \\ &= D_0 X_i \,, \end{aligned} \tag{2.2.6}$$

where we have used the fact that all spatial derivatives are vanishing. Thus the La-

grangian takes the form

$$\begin{aligned} L = -\frac{1}{4g^2}\,\mathrm{Tr}(F_{\mu\nu}F^{\mu\nu}) &= \mathrm{Tr}\left(-\frac{1}{4g^2}(F_{0i}F^{0i} + F_{i0}F^{i0} + F_{ij}F^{ij}\right) \\ &= \mathrm{Tr}\left(-\frac{1}{4g^2}(2F_{0i}F^{0i} + F_{ij}F^{ij})\right) \\ &= \mathrm{Tr}\left(-\frac{1}{4g^2}(2(D_0X_i)(-D_0X_i) - [X_i,X_j]^2)\right) \\ &= \frac{1}{g^2}\,\mathrm{Tr}\left(\frac{1}{2}(D_0X_i)^2 + \frac{1}{4}[X_i,X_j]^2\right) \end{aligned} \tag{2.2.7}$$

and the action is

$$S = \frac{1}{g^2}\int \mathrm{d}t\,\mathrm{Tr}\left(\frac{1}{2}(D_0X_i)^2 + \frac{1}{4}[X_i,X_j]^2\right), \tag{2.2.8}$$

which is the BFSS action that we have introduced in equation (2.1.1).

2.3 Two Matrix Model

We will now concentrate on the structure of the Yang-Mills two matrix model with $SU(2)$ gauge symmetry. This model can be obtained by dimensionally reducing the pure $SU(2)$ Yang Mills theory in 2+1 dimensions to 0+1 along the same lines as described in the previous section or equally by considering (2.2.8) with only $X_i : i = 1, 2$. The Lagrangian has the form

$$L = \frac{1}{2}\,\mathrm{Tr}\big((D_0X_1)^2 + (D_0X_2)^2 + [X_1,X_2]^2\big), \tag{2.3.1}$$

which has the $SU(2)$ gauge symmetry and $SO(2)$ global symmetry. X_1 and X_2 are 2×2 matrices which are traceless and hermitian. Since they are in a triplet of $SU(2)$, we can use Pauli matrices to write X_1 and X_2 as

$$\begin{aligned} X_i = N\vec{\mathbf{x}}_i\cdot\vec{\sigma} &= Nx_i^\alpha\sigma^\alpha \\ &= N\begin{pmatrix} x_i^3 & x_i^1 - ix_i^2 \\ x_i^1 + ix_i^2 & -x_i^3 \end{pmatrix}, \end{aligned} \tag{2.3.2}$$

where $\alpha = 1, 2, 3$ and N is the normalization constant which will be determined now. Working in the $A_0 = 0$ gauge, N can be fixed by requiring that $\mathrm{Tr}\left(\dot{X}_1^2 + \dot{X}_2^2\right) =$

$\sum_\alpha (\dot{x}_1^\alpha \dot{x}_1^\alpha) + (\dot{x}_2^\alpha \dot{x}_2^\alpha)$. To satisfy this requirement, we see that we must have

$$\begin{aligned}\frac{1}{2}\,\mathrm{Tr}\Big(\dot{X}_i^2\Big) &= \frac{1}{2}N^2\,\mathrm{Tr}\Big(\dot{x}_i^\alpha \sigma^\alpha \dot{x}_i^\beta \sigma^\beta\Big) \\ &= \frac{1}{2}N^2 \dot{x}_i^\alpha \dot{x}_i^\beta\,\mathrm{Tr}\big(\sigma^\alpha \sigma^\beta\big) \\ &= \frac{1}{2}N^2 \dot{x}_i^\alpha \dot{x}_i^\beta 2\delta^{\alpha\beta} \\ &= N^2 \dot{x}_i^\alpha \dot{x}_i^\alpha\,,\end{aligned} \tag{2.3.3}$$

which therefore implies that we must take $N = \dfrac{1}{\sqrt{2}}$. Let us now insert X_i given in (2.3.3) into the Lagrangian (2.3.1) in the $A_0 = 0$ gauge and evaluate the traces. This yields

$$\begin{aligned}L &= \frac{1}{2}\,\mathrm{Tr}\left(\left(\frac{1}{\sqrt{2}}\dot{x}_1^\alpha \sigma^\alpha\right)^2 + \left(\frac{1}{\sqrt{2}}\dot{x}_1^\beta \sigma^\beta\right)^2 + \left[\frac{1}{\sqrt{2}}x_1^\alpha \sigma^\alpha, \frac{1}{\sqrt{2}}x_1^\beta \sigma^\beta\right]^2\right) \\ &= \frac{1}{2}\,\mathrm{Tr}\left(\frac{1}{2}(\dot{x}_1^\alpha)^2 \mathbb{1}_2 + \frac{1}{2}(\dot{x}_2^\beta)^2 \mathbb{1}_2 + \left(\frac{1}{2}2i\epsilon^{\alpha\beta\gamma}x_1^\alpha x_2^\beta \sigma^\gamma\right)^2\right) \\ &= \frac{1}{2}\,\mathrm{Tr}\left(\frac{1}{2}(\dot{x}_1^\alpha)^2 \mathbb{1}_2 + \frac{1}{2}(\dot{x}_2^\beta)^2 \mathbb{1}_2 - (\vec{\mathbf{x}}_1 \times \vec{\mathbf{x}}_2)^2 \mathbb{1}_2\right) \\ &= \frac{1}{2}(\dot{\vec{\mathbf{x}}}_1)^2 + \frac{1}{2}(\dot{\vec{\mathbf{x}}}_2)^2 - (\vec{\mathbf{x}}_1 \times \vec{\mathbf{x}}_2)^2\,.\end{aligned} \tag{2.3.4}$$

We see that the Lagrangian is analogous to that of two point particles with coordinates $\vec{\mathbf{x}}_1$ and $\vec{\mathbf{x}}_2$ of unit mass and the interaction potential is $V(x_1, x_2) = (\vec{\mathbf{x}}_1 \times \vec{\mathbf{x}}_2)^2$. Drawing from our knowledge of analytical mechanics we can write down the canonically conjugate momenta for $\vec{\mathbf{x}}_1$ and $\vec{\mathbf{x}}_2$ as

$$\vec{\mathbf{p}}_1 := \frac{\partial L}{\partial \dot{\vec{\mathbf{x}}}_1} = \dot{\vec{\mathbf{x}}}_1\,, \quad \vec{\mathbf{p}}_2 := \frac{\partial L}{\partial \dot{\vec{\mathbf{x}}}_2} = \dot{\vec{\mathbf{x}}}_2\,. \tag{2.3.5}$$

Then the Hamiltonian is found as follows

$$\begin{aligned}H &= \dot{\vec{\mathbf{x}}} \cdot \vec{\mathbf{p}} - L \\ &= \vec{\mathbf{p}}_i^2 - \frac{1}{2}\vec{\mathbf{p}}_i^2 + (\vec{\mathbf{x}}_1 \times \vec{\mathbf{x}}_2)^2 \\ &= \frac{1}{2}\vec{\mathbf{p}}_i^2 + (\vec{\mathbf{x}}_1 \times \vec{\mathbf{x}}_2)^2\,.\end{aligned} \tag{2.3.6}$$

Using (2.3.6) we may determine the Hamiltonian's equations of motion as

$$\begin{aligned}
\dot{\vec{\mathbf{p}}}_1 &:= -\frac{\partial H}{\partial \vec{\mathbf{x}}_1} = 2\vec{\mathbf{x}}_2 \times (\vec{\mathbf{x}}_1 \times \vec{\mathbf{x}}_2)\,, \\
\dot{\vec{\mathbf{p}}}_2 &:= -\frac{\partial H}{\partial \vec{\mathbf{x}}_2} = -2\vec{\mathbf{x}}_2 \times (\vec{\mathbf{x}}_1 \times \vec{\mathbf{x}}_2)\,, \\
\dot{\vec{\mathbf{x}}}_1 &:= \frac{\partial H}{\partial \vec{\mathbf{p}}_1} = \vec{\mathbf{p_1}}\,, \\
\dot{\vec{\mathbf{x}}}_1 &:= \frac{\partial H}{\partial \vec{\mathbf{p}}_2} = \vec{\mathbf{p_2}}\,.
\end{aligned} \tag{2.3.7}$$

Although these equations look superficially simple enough to yield the general solutions, it turns out that they are still too complicated to be solved exactly. In order to simplify the problem by taking advantage of its symmetries, we may first express $(\vec{\mathbf{x}}_1, \vec{\mathbf{x}}_2)$ as a single 3×2 matrix as

$$X = \begin{pmatrix} x_1^1 & x_2^1 \\ x_1^2 & x_2^2 \\ x_1^3 & x_2^3 \end{pmatrix}\,. \tag{2.3.8}$$

We can implement the $SU(2) \simeq SO(3)$ gauge symmetry of the model by left multiplying with $D(g) \equiv R \in SO(3)$, while the right multiplication implements the rigid $SO(2)$ symmetry of the model. Thus we have

$$X = \begin{pmatrix} x_1^1 & x_2^1 \\ x_1^2 & x_2^2 \\ x_1^3 & x_2^3 \end{pmatrix} \longrightarrow R_{SO(3)} \cdot \begin{pmatrix} x_1^1 & x_2^1 \\ x_1^2 & x_2^2 \\ x_1^3 & x_2^3 \end{pmatrix} \cdot \begin{pmatrix} \cos(\phi) & -\sin(\phi) \\ \sin(\phi) & \cos(\phi) \end{pmatrix}\,. \tag{2.3.9}$$

We can always make a gauge transformation, that is choose $D(g) \equiv R_{SO(3)}$ such that the vector $\vec{\mathbf{x}}_1$ is rotated to point in the 1-direction. In other words, if we start with $\vec{\mathbf{x}}_1' = (x_1^{1'}, x_1^{2'}, x_1^{3'})^T$ we can always find a gauge transformation such that $\vec{\mathbf{x}}_1' \to \vec{\mathbf{x}}_1 = (x_1^1, 0, 0)^T$. This vector does not change under a $SO(2) \subset SO(3)$ subgroup and that residual gauge symmetry can be used to take $\vec{\mathbf{x}}_2' \to \vec{\mathbf{x}}_2 = (x_2^1, x_2^2, 0)^T$. Nevertheless, rigid $SO(2)$ rotations which are acting from the right on X, would allow us to keep only the last row of X to be zero but rotates x_1^2 to a non-zero value in general. The final outcome of this analysis is that out of 6 degrees of freedom only 4 remains due to the local and global symmetries of the problem. The question we need to answer is whether this analysis is preserved as the system is evolving in time. To do so, we inspect the Gauss law constraint.

In the previous section we have determined the Gauss law constraint of the BFSS theory in the $A_0 = 0$ gauge as given in (2.1.16), and for the two matrix model this takes the form

$$\begin{aligned}
&\Big[X_1, \dot{X}_1\Big] + \Big[X_2, \dot{X}_2\Big] = 0, \\
&= \frac{1}{2}\Big[x_1^\alpha \sigma^\alpha, \dot{x}_1^\beta \sigma^\beta\Big] + \frac{1}{2}[x_2^\mu \sigma^\mu, \dot{x}_1^\nu \sigma^\nu] = 0 \\
&= \frac{1}{2}(2i\epsilon^{\alpha\beta\gamma} x_1^\alpha \dot{x}_1^\beta \sigma^\gamma + 2i\epsilon^{\mu\nu\rho} x_2^\mu \dot{x}_2^\nu \sigma^\rho) = 0 \\
&= i(\vec{\mathbf{x}}_1 \times \dot{\vec{\mathbf{x}}}_1 + \vec{\mathbf{x}}_2 \times \dot{\vec{\mathbf{x}}}_2) \cdot \vec{\sigma} = 0 \\
&=: i(\vec{\mathbf{L}}_1 + \vec{\mathbf{L}}_2) \cdot \vec{\sigma} = 0\,.
\end{aligned} \tag{2.3.10}$$

This implies that $\vec{\mathbf{L}} := \vec{\mathbf{L}}_1 + \vec{\mathbf{L}}_2 = 0$. Continuing with the point particle dynamics interpretation of the system we can identify $\vec{\mathbf{L}}_i$ with the angular momentum of the i$^{\text{th}}$ particle and $\vec{\mathbf{L}}$ as the total angular momentum of the system. Let us, however note that for the two matrix model described by the action (2.3.1), $\vec{\mathbf{L}}$ is the generator of $SU(2)$ gauge transformations. Constraint equation means that the total angular momentum is vanishing. Time derivative of $\vec{\mathbf{L}}_1$ is

$$\begin{aligned}
\dot{\vec{\mathbf{L}}}_1 &= \dot{\vec{\mathbf{x}}}_1 \times \vec{\mathbf{p}}_1 + \vec{\mathbf{x}}_1 \times \dot{\vec{\mathbf{p}}}_1 \\
&= 2\vec{\mathbf{x}}_1 \times (\vec{\mathbf{x}}_2 \times (\vec{\mathbf{x}}_1 \times \vec{\mathbf{x}}_2))\,.
\end{aligned} \tag{2.3.11}$$

In the first line of (2.3.11), the first term is vanishing since $\dot{\vec{\mathbf{x}}}_1 \times \vec{\mathbf{p}}_1 = \vec{\mathbf{p}}_1 \times \vec{\mathbf{p}}_1 = 0$. The second term is found by inserting the $\dot{\vec{\mathbf{p}}}_1$ in the (2.3.7) into this equation. Since $\vec{\mathbf{x}}_1$ and $\vec{\mathbf{x}}_2$ are orthogonal to $\vec{\mathbf{L}}_1$, $(\vec{\mathbf{x}}_1 \times \vec{\mathbf{x}}_2)$ is aligned with $\vec{\mathbf{L}}_1$. Then $(\vec{\mathbf{x}}_2 \times (\vec{\mathbf{x}}_1 \times \vec{\mathbf{x}}_2))$ is orthogonal to $\vec{\mathbf{L}}_1$. It is now obvious that $\vec{\mathbf{x}}_1 \times (\vec{\mathbf{x}}_2 \times (\vec{\mathbf{x}}_1 \times \vec{\mathbf{x}}_2))$ is aligned with $\vec{\mathbf{L}}_1$.

Equation (2.3.11) shows that $\vec{\mathbf{L}}_1$ and $\dot{\vec{\mathbf{L}}}_1$ are in the same direction. That is also valid for $\vec{\mathbf{L}}_2$ since they are anti-parallel vectors.

This angular momentum analysis shows that $\vec{\mathbf{x}}_1$, $\vec{\mathbf{x}}_2$, $\vec{\mathbf{p}}_1$ and $\vec{\mathbf{p}}_2$ are orthogonal to $\vec{\mathbf{L}}$ and the direction of $\vec{\mathbf{L}}$ does not change in time. Therefore, the whole motion is orthogonal to the $\vec{\mathbf{L}}$-plane. The gauge choice we previously made, taking $x_1^3 = x_2^3 = 0$ is preserved with $\vec{\mathbf{L}}$ pointing in the x^3-direction. Therefore, the motion is confined to the $x^1 - x^2$ plane.

Deleting the row of zeros in (2.3.8) four dynamical degrees of freedom are arranged

into a 2×2 matrix.

$$X = \begin{pmatrix} x_1^1 & x_1^2 \\ x_2^1 & x_2^2 \end{pmatrix} . \tag{2.3.12}$$

Since the determinant of this matrix is simply given by

$$\det(X) = x_1^1 x_2^2 - x_2^1 x_1^2 \,, \tag{2.3.13}$$

we see that the potential part of the Lagrangian in (2.3.4) or the Hamiltonian in (2.3.6) can be written as follows

$$\begin{aligned} \vec{\mathbf{x}}_1 \times \vec{\mathbf{x}}_2 &= \epsilon^{\alpha\beta} x_1^\alpha x_2^\beta \\ &= x_1^1 x_2^2 - x_2^1 x_1^2 \\ &= \det(X) \,. \end{aligned} \tag{2.3.14}$$

In order to simplify the problem it would be best if we could transform to a new coordinate system in which the $\vec{\mathbf{L}} = 0$ constraint can be explicitly implemented. Furthermore, we note that since the potential is given in terms of a cross product, the relative angle, say θ, between the particles may be taken as one of the generalized coordinates. After these intuitive remarks, we may take a two step approach to determine such new coordinates.

Step 1

Let us suppose that the particles are at a distance $\frac{r}{\sqrt{2}}$ form an arbitrarily chosen origin and are making a relative angle θ. Then, we may write as intermediate step

$$X_0 = \frac{1}{\sqrt{2}} \begin{pmatrix} r & r\cos(\theta) \\ 0 & r\sin(\theta) \end{pmatrix} . \tag{2.3.15}$$

Step 2

X_0 itself cannot be the most general form of the transformation between the old and the new coordinates, since (2.3.15) involves only the new coordinates, while we need two more. The remaining two degrees of freedom can be introduced by performing a left $SO(2)$ rotation $R_{SO(2)}(\chi)$ and a right $SO(2)$ rotation $R_{SO(2)}(\phi)$ by angles χ and

ϕ, respectively. Therefore, we may write this parametrization of X in (2.3.9) as

$$\begin{aligned} X &= R(\chi) X_0 R(\phi) \\ &= \frac{1}{\sqrt{2}} \begin{pmatrix} \cos(\chi) & -\sin(\chi) \\ \sin(\chi) & \cos(\chi) \end{pmatrix} \begin{pmatrix} r & r\cos(\theta) \\ 0 & r\sin(\theta) \end{pmatrix} \begin{pmatrix} \cos(\phi) & \sin(\phi) \\ -\sin(\phi) & \cos(\phi) \end{pmatrix} . \end{aligned} \tag{2.3.16}$$

This gives us the complete transformation of the coordinates $(x_1^1, x_1^2, x_2^1, x_2^2)$ to the new coordinates (r, θ, ϕ, χ).

In (2.3.16), $R(\chi)$ acting from the left implements the rotations along the x^3-axis by an angle χ. Therefore, we infer that the corresponding conjugate momenta $p_\chi = \frac{\partial L}{\partial \dot{\chi}}$ will be identified as the total angular momentum $\vec{\mathbf{L}}$ of the system. The Gauss law constraint $\vec{\mathbf{L}} = 0$ can then be implemented by taking $p_\chi = 0$ after expressing the Hamiltonian in the new phase space variables. We will see this explicitly in what follows.

In order to understand the purpose and meaning of the $R_{SO(2)}(\phi)$ acting from right, first note that it only acts on X_0 as a 2×2 matrix and cannot possibly act on an individual column vector. This is because, $R_{SO(2)}(\phi)$ acts in a similar manner as the rigid global rotations of X_i's mixing them, except that for $R_{SO(2)}(\phi)$ the angle ϕ is in general time-dependent. Note that this does not preserve the length of the column vectors in X_0. Meanwhile, we see that neither the left nor the right rotations change the form of the potential $\vec{\mathbf{x}}_1 \times \vec{\mathbf{x}}_2 = \frac{1}{4} r^4 \sin^2(\theta)$ in the new coordinates since, $\det(X) = \det(X_0)$.

The new coordinates are then (r, θ, ϕ, χ) and the corresponding conjugate momenta are $(p_r, p_\theta, p_\phi, p_\chi)$. Hamiltonian can formally be expressed as

$$\begin{aligned} H &= \frac{1}{2} g^{ij} p_i p_j + (\det(X))^2 \\ &= \frac{1}{2} g_{ij}^{-1} p_i p_j + \frac{1}{4} r^4 \sin^2(\theta) , \end{aligned} \tag{2.3.17}$$

where g_{ij} is the metric in the new coordinates which can be evaluated from the expression

$$g_{ij} = \mathrm{Tr}\big(\partial_i X^\dagger \partial_j X\big) . \tag{2.3.18}$$

Using equation (2.3.16), the metric g_{ij} can be explicitly written as

$$g_{ij} = \begin{pmatrix} 1 & 0 & 0 & 0 \\ 0 & \frac{r^2}{2} & \frac{r^2\sin(\theta)}{2} & \frac{r^2}{2} \\ 0 & \frac{r^2\sin(\theta)}{2} & r^2 & r^2\sin(\theta) \\ 0 & \frac{r^2}{2} & r^2\sin(\theta) & r^2 \end{pmatrix}, \tag{2.3.19}$$

where the rows and columns are labeled in the order $p_r, p_\theta, p_\phi, p_\chi$. We have evaluated the components of g_{ij} both analytically and also using Mathematica. Using this metric, square of the line element can be written as

$$\begin{aligned} \mathrm{d}s^2 =& \mathrm{d}r^2 + \frac{r^2}{2}\,\mathrm{d}\theta^2 + r^2\,\mathrm{d}\phi^2 + r^2\,\mathrm{d}\chi^2 \\ &+ r^2\sin^2(\theta)\,\mathrm{d}\theta\,\mathrm{d}\phi + r^2\,\mathrm{d}\theta\,\mathrm{d}\chi + 2r^2\sin(\theta)\,\mathrm{d}\phi\,\mathrm{d}\chi\ . \end{aligned} \tag{2.3.20}$$

Then, the inverse metric g_{ij}^{-1} is

$$g_{ij}^{-1} = \begin{pmatrix} 1 & 0 & 0 & 0 \\ 0 & \frac{4}{r^2} & 0 & -\frac{2}{r^2} \\ 0 & 0 & \frac{1}{r^2\cos^2(\theta)} & -\frac{\sec(\theta)\tan(\theta)}{r^2} \\ 0 & -\frac{2}{r^2} & -\frac{\sec(\theta)\tan(\theta)}{r^2} & \frac{(3-\cos(2\theta))\sec^2(\theta)}{2r^2} \end{pmatrix}. \tag{2.3.21}$$

As we have argued previously, p_χ corresponds to the total angular momentum $\vec{\mathbf{L}}$, and therefore we set it zero in writing out the Hamiltonian (2.3.17) explicitly. Thus, we only need the first 3×3 block of (2.3.21) as

$$g_{ij}^{-1} = \begin{pmatrix} 1 & 0 & 0 \\ 0 & \frac{4}{r^2} & 0 \\ 0 & 0 & \frac{1}{r^2\cos^2(\theta)} \end{pmatrix} \tag{2.3.22}$$

and the Hamiltonian in (2.3.17) can be written as follows

$$H = \frac{1}{2}p_r^2 + \frac{2}{r^2}p_\theta^2 + \frac{p_\phi^2}{2r^2\cos^2(\theta)} + \frac{1}{4}r^4\sin^2(\theta)\,. \tag{2.3.23}$$

Since (2.3.23) is cyclic in ϕ, we immediately have $\dot{p}_\phi = 0$, meaning that p_ϕ is conserved, i.e. it is a constant of motion. Treating p_ϕ a constant, we can focus on only the phase space $(r, \theta, p_r, p_\theta)$. There are singularities at $r = 0$ and $\theta = k\frac{\pi}{2}$ where k is an odd integer. Then the motion will be in the range $\theta \in (\text{-}\frac{\pi}{2}, \frac{\pi}{2})$ and $r > 0$.

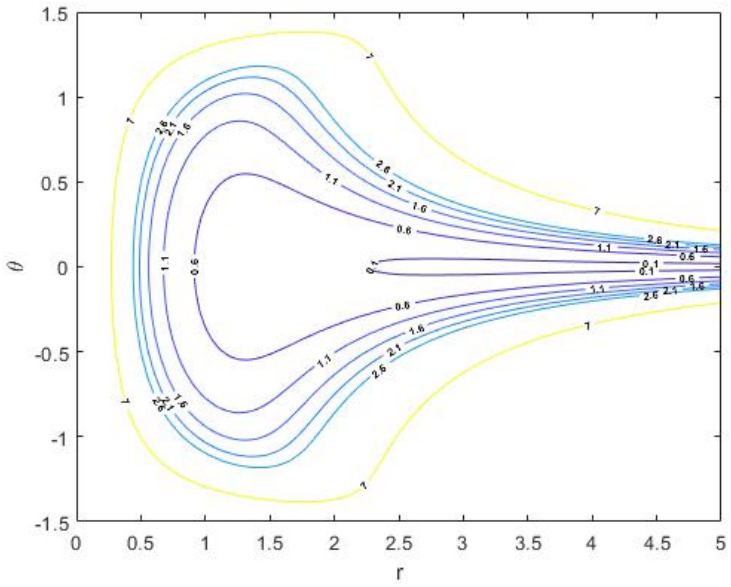

Figure 2.1: Potential contours at $p_\phi = 1$ and $V = 0.1, 0.6, 1.1, 1.6, 2.1, 2.6, 7$

The potential contours in figure 2.1, show that θ values will be in a very narrow region around $\theta = 0$ as we increase r for low energies. This is the region in which the commutator of the matrices are vanishingly small. Such configurations are called flat directions in the matrix model. They are lifted i.e. commutators do not vanish once quantum corrections are considered. Classical trajectories can spend a lot of time in this region and could become time consuming to compute numerically. In this region, θ exhibit harmonic motion. To see this, we recall that the general Hamiltonian for a simple harmonic oscillation

$$H_{S.H.O} = \frac{p^2}{2m} + \frac{1}{2}mw^2x^2\,. \tag{2.3.24}$$

Small angle approximation

$$\begin{aligned} \cos(\theta) &\simeq 1 - \frac{\theta^2}{2} + ... \\ \sin(\theta) &\simeq \theta + ... \\ \cos^{-2}(\theta) &\simeq 1 + \theta^2 + ... \end{aligned} \tag{2.3.25}$$

in θ-dependent part of the Hamiltonian gives us

$$\begin{aligned} H_\theta &= \frac{2}{r^2}p_\theta^2 + \frac{p_\phi^2}{2r^2}(1+\theta^2) + \frac{1}{4}r^4\theta^2 \\ &= \frac{2}{r^2}p_\theta^2 + \left(\frac{p_\phi^2}{2r^2} + \frac{1}{4}r^4\right)\theta^2 \,, \end{aligned} \tag{2.3.26}$$

where the binomial formula is used. From (2.3.24) and (2.3.26) we see that frequency of oscillations in θ is

$$w = \sqrt{\frac{4p_\phi^2}{r^4} + 2r^2} \,. \tag{2.3.27}$$

Figure 2.1 shows that the motion is adiabatic in θ at large r. In general the condition for an adiabatic motion is given as [14]

$$T\frac{\mathrm{d}\lambda}{\mathrm{d}t} \ll \lambda \,, \tag{2.3.28}$$

where λ is a slowly varying parameter and T is the period of motion. In our case, we may take the slowly varying parameter as the frequency w, and this gives the adiabatic condition as

$$\frac{\dot{w}}{w^2} \ll 1 \tag{2.3.29}$$

using (2.3.27), this takes the form

$$\frac{\dot{w}}{w^2} = \dot{r}\frac{-4p_\phi^2 + r^6}{\sqrt{2}r^5\left(\frac{2p_\phi^2}{r^4} + r^2\right)^{3/2}} \xrightarrow{r\to\infty} \simeq \dot{r}\frac{1}{r^2} \,. \tag{2.3.30}$$

Right hand side of (2.3.30) is vanishing at large r, then the motion is adiabatic in θ. Thus, a term $\hbar w \simeq \hbar r$ can be added to the potential to ease the numerics. Here $\hbar$ is just a parameter which will be set to a convenient number in the next section. The Hamiltonian can be written as follows

$$H = \frac{1}{2}p_r^2 + \frac{2}{r^2}p_\theta^2 + \frac{p_\phi^2}{2r^2\cos^2(\theta)} + \frac{1}{4}r^4\sin^2(\theta) + \hbar r \,. \tag{2.3.31}$$

The Hamiltonian equations of motion are

$$\begin{aligned} \dot{r} &= \frac{\partial H}{\partial p_r} = p_r \,, \\ \dot{p}_r &= -\frac{\partial H}{\partial r} = \frac{4}{r^3}p_\theta^2 - r^3\sin^2(\theta) + \frac{p_\phi^2}{r^3\cos^2(\theta)} - \hbar \,, \\ \dot{\theta} &= \frac{\partial H}{\partial p_\theta} = \frac{4}{r^2}p_\theta \,, \\ \dot{p_\theta} &= -\frac{\partial H}{\partial \theta} = -\frac{p_\phi^2\tan(\theta)}{r^2\cos^2(\theta)} - \frac{1}{2}r^4\sin(\theta)\cos(\theta) \,. \end{aligned} \tag{2.3.32}$$

2.3.1 Chaotic Dynamics From Poincaré Sections

Before presenting the results of Poincaré sections for this particular model, we digress a moment and give a brief explanation of the meaning of Poincaré sections in dynamical systems. Poincaré section is obtained by taking the intersection of the phase flow and a surface of section [9, 15, 16, 17]. Therefore, N dimensional phase space is reduced to $N-1$ dimensions, and in the Hamiltonian systems it can be reduced further when the energy is constant. In this way, the four dimensional phase space can be equally examined by focusing on the two dimensional Poincaré sections. The chaotic dynamics of a system can be understood from the Poincaré sections as follows. Randomly spread dots in Poincaré sections imply the existence of quasi periodic orbits. Contours in these figures, called as Kolmogorov, Arnold, Moser (KAM) tori [15], correspond to the quasi periodic orbits. The more detailed explanation of the Poincaré sections is given in appendix B.1.

In this section, we replicate the numerical results obtained by [8] using our own codes. We examine the chaotic behavior of this model for the various values of p_ϕ. In the Poincaré sections, we used 25 different initial condition sets. Initially we take $p_r = 0$ and $\theta = 0$ as a part of the all initial condition sets. For a given energy E, $r > 0$ is picked randomly so that p_θ, which is

$$p_\theta = \sqrt{\frac{r^2}{2}\left(E - \frac{p_\phi^2}{2r^2} - \hbar r\right)}\,, \tag{2.3.33}$$

takes a real value. Energy and the parameter $\hbar$ are taken to be equal to 1 and 0.1, respectively.

Poincaré sections given in figure 2.2, which are plotted in the $p_r - p_\theta$ plane at the intersection of $\theta = 0$, show that the system is more chaotic for the lower values of p_ϕ. At $p_\phi = 1$, KAM tori occurring in a relatively small region show that the phase space is quasi-periodic in this region, while the rest is fully chaotic. KAM tori grow at $p_\phi = 1.5$ and cover significant amount of the area in the $p_r - p_\theta$ section. This system appears to be fully quasi-periodic for $p_\phi \geq 2$. We depict the cases $p_\phi = 2$ and $p_\phi = 2.5$ for specific examples.

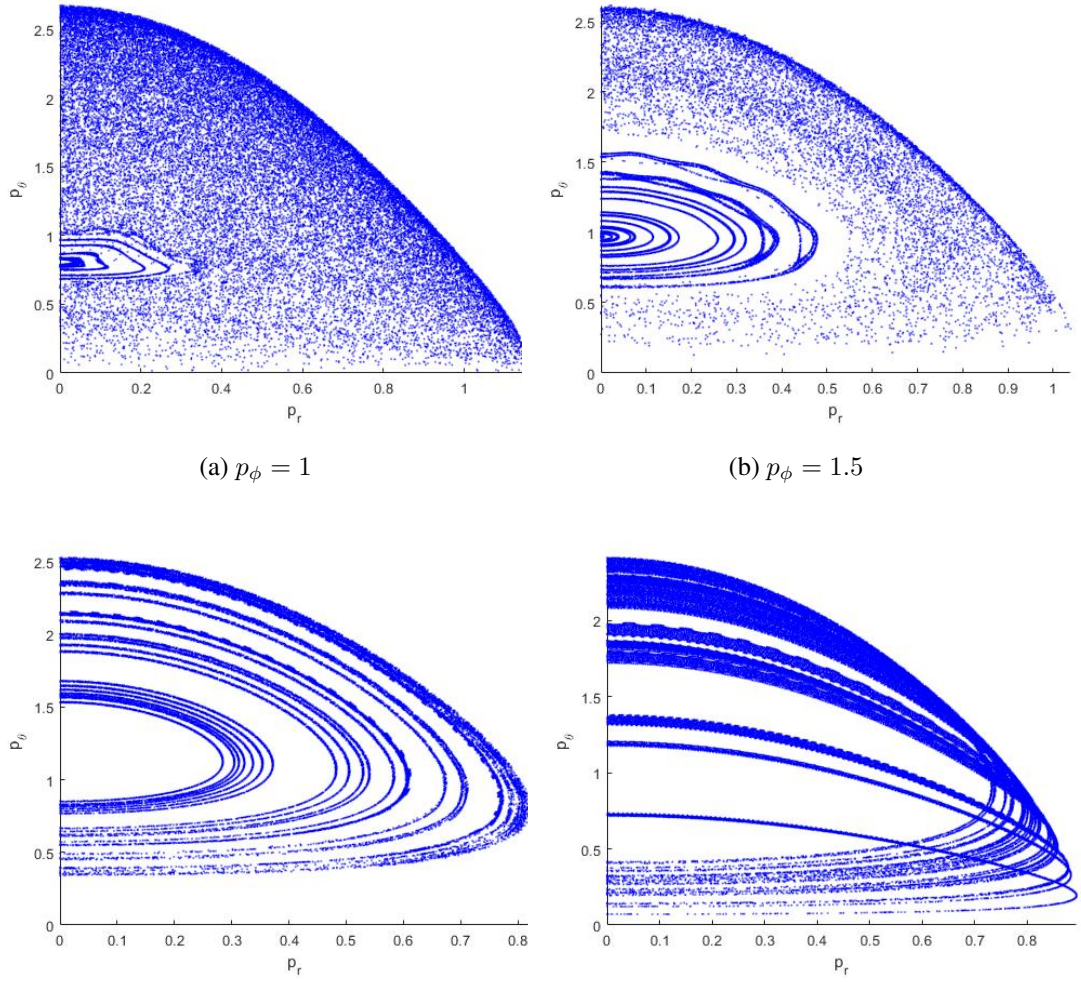

(a) $p_\phi = 1$ (b) $p_\phi = 1.5$

(c) $p_\phi = 2$ (d) $p_\phi = 2.5$

Figure 2.2: Poincaré sections

2.3.2 Chaotic Dynamics via Lyapunov Exponents

Another method for examining chaotic behavior in dynamical systems is the calculation of the Lyapunov exponents. For a given Hamiltonian system Lyapunov exponents are real numbers, which measure the divergence of the phase space trajectories starting from nearby initial conditions. There are as many Lyapunov exponents as the number of phase space variables. A positive Lyapunov exponent signifies that trajectories separated by infinitesimally separated initial conditions diverge exponentially. This is direct indication of chaotic behavior since it describes the high sensitivity of the system to initial conditions. One positive Lyapunov exponent is sufficient to con-

clude that the dynamical system has chaotic behavior. For Hamiltonian systems sum of all Lyapunov exponents is zero as a consequence of the Liouville's theorem, which states that the phase space volume does not change as the system evolves in time. Further analytical details of the definition and evolution of Lyapunov exponents are given in appendix B.2.

For consistency, in the calculation of Lyapunov exponents we pick the initial conditions, energy and parameter $\hbar$ as in the Poincaré sections. Lyapunov spectrum given in figure 2.3 are consistent with the Poincaré sections in terms of the transition from chaotic to non-chaotic behavior. Vertical axis is the average of the largest Lyapunov exponents which are numerically calculated for 25 different initial condition set for each p_ϕ and average of the 25 largest Lyapunov exponents are taken. Larger Lyapunov exponents indicate that the system is more chaotic at those p_ϕ values. Figure 2.3 shows that the system becomes less chaotic when we increase p_ϕ.

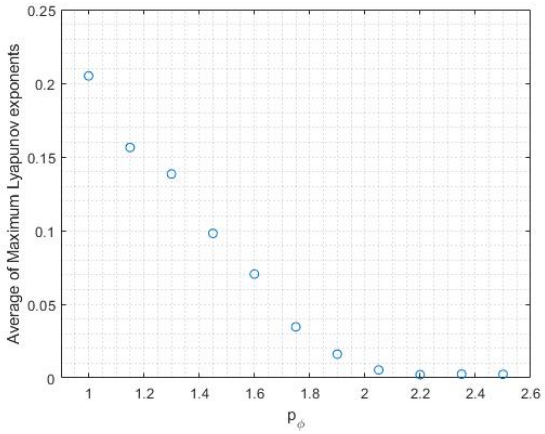

Figure 2.3: Lyapunov spectrum

Number of Lyapunov exponents are equal to the degrees of freedom in the system. In this model we have four Lyapunov exponents. One positive Lyapunov exponent is sufficient to show that the system is chaotic. For this reason, we take only average of the largest Lyapunov exponents in figure 2.3.

Lyapunov exponents versus time plot at $p_\phi = 0$ is given in figure 2.4. The largest Lyapunov exponent is approximately 0.4 which is the largest value among the largest Lyapunov exponents at different values of p_ϕ. Therefore, it is possible to conclude

that $p_\phi = 0$ is the most chaotic configuration. At $p_\phi = 0$, computational time for drawing Poincaré sections is very long and the plots does not yield sufficient intersection points. Nevertheless, Lyapunov spectrum is sufficient to conclude the behavior at $p_\phi = 0$.

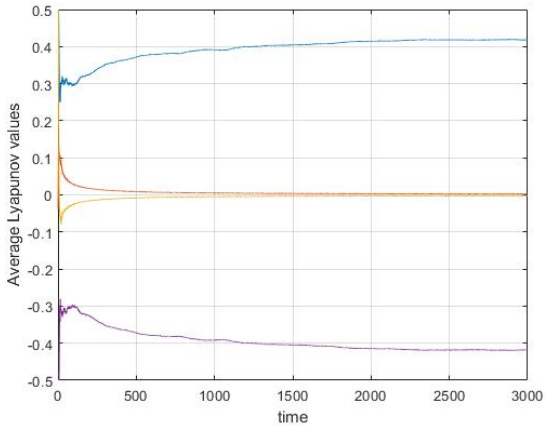

Figure 2.4: Lyapunov spectrum at $p_\phi = 0$

CHAPTER 3

TWO MATRIX MODEL WITH CHERN-SIMONS TERM

In this chapter, we will study the Yang-Mills two matrix model with the Chern-Simons term. For completeness we start the chapter by introducing the Chern-Simons action in 2+1 dimensions with $SU(2)$ gauge symmetry and obtain its dimensional reduction to 0+1 dimensions in a manner similar to the treatment presented in section 2.3 for the BFSS matrix model. This will allow us to explicitly write down the Yang-Mills Chern-Simons (YMCS) matrix model. We analyze the properties of this model. In particular, we discuss the meaning of the modified Gauss law constraint and determine the Hamiltonian of the new system. Using these developments and numerical methods we examine the chaotic dynamics emerging from this model.

3.1 Chern-Simons Action

Non-abelian Chern-Simons theory in 2+1 dimensions may be introduced by the Lagrangian [18]

$$L_{CS} = \kappa \epsilon^{\mu\nu\rho} \operatorname{Tr}\left(\tilde{A}_\mu \partial_\nu \tilde{A}_\rho + \frac{2}{3} \tilde{A}_\mu \tilde{A}_\nu \tilde{A}_\rho \right). \tag{3.1.1}$$

Neither the Lagrangian nor the action $S_{cs} = \int \mathrm{d}^3x \, L_{CS}$ is invariant under the $SU(N)$ gauge symmetry. In fact, under the $SU(N)$ action L_{CS} changes by two terms, one of which is of topological nature while the other is a total derivative [11]. The latter integrates to zero under proper boundary conditions over the fields, and therefore does not change the action S_{CS}, while the former is proportional to an integer, as a consequence of the topological conditions. Quantum physics, does not necessarily require that S is invariant under gauge symmetry but it is rather e^{iS} which is required to be gauge invariant, and this leads to the quantization of the Chern-Simons coupling.

For the $SU(2)$ gauge symmetry we have $\kappa = \frac{k}{4\pi}$, $k \in \mathbb{Z}$[11, 18]. In L_{CS}, $\tilde{A}_\mu$ are anti-Hermitian $SU(N)$ gauge fields i.e. $\tilde{A}_\mu^\dagger = -\tilde{A}_\mu$. Denoting the anti-Hermitian generator of $SU(N)$ by T^a we may write

$$\tilde{A}_\mu = \tilde{A}_\mu^a T^a\,, \quad \left[T^a, T^b\right] = f^{abc}T^c\,. \tag{3.1.2}$$

To comply with the conventions of the previous chapter, we want to work with the Hermitian gauge fields. We therefore would like to express (3.1.1) in terms of Hermitian gauge fields. To do so, we may write the Hermitian generators of $SU(N)$ as $S^a := iT^a$ and this gives

$$\begin{aligned}\left[S^a, S^b\right] &= \left[iT^a, iT^b\right] \\ &= i(i\left[T^a, T^b\right]) \\ &= i(f^{abc}iT^c) \\ &= if^{abc}S^c\,.\end{aligned} \tag{3.1.3}$$

We may now express the Hermitian gauge fields A_μ in terms of the anti-Hermitian $\tilde{A}_\mu$ as

$$\begin{aligned}A_\mu &= A_\mu^a S^a \\ &= A_\mu^a iT^a \\ &= i\tilde{A}_\mu\,.\end{aligned} \tag{3.1.4}$$

The non-abelian Chern-Simons Lagrangian expressed in terms of the Hermitian gauge fields A_μ takes the form

$$\begin{aligned}L_{CS} &= \kappa\epsilon^{\mu\nu\rho}\,\mathrm{Tr}\left(-iA_\mu\partial_\nu(-iA_\rho) + \frac{2}{3}(-i^3)A_\mu A_\nu A_\rho\right) \\ &= \kappa\epsilon^{\mu\nu\rho}\,\mathrm{Tr}\left(-A_\mu\partial_\nu A_\rho + \frac{2}{3}iA_\mu A_\nu A_\rho\right).\end{aligned} \tag{3.1.5}$$

3.2 Reduction to 0+1 dimensions

Let us now focus on the Chern-Simons term with $SU(2)$ gauge symmetry. Following the same steps as in section 2.2, we require that all spatial derivatives in the

Lagrangian vanish. Using the notation $A_\mu = (A_0, X_i)$, $i : 1, 2$ we have

$$\begin{aligned} L_{CS} &= \kappa \,\mathrm{Tr}\bigg(-\epsilon^{i0j} X_i \partial_0 X_j + \frac{2}{3} i(\epsilon^{0ij} A_0 X_i X_j + \epsilon^{i0j} X_i A_0 X_j + \epsilon^{ij0} X_i X_j A_0)\bigg) \\ &= \kappa \,\mathrm{Tr}\Big(\epsilon^{ij}(X_i \dot{X}_j + 2i A_0 X_i X_j)\Big)\,, \end{aligned} \tag{3.2.1}$$

where we used the cyclicity of the trace and wrote $\epsilon^{0ij} = \epsilon_{ij}$.

3.3 Two Matrix Model with Chern-Simons Terms

Coupling the Chern-Simons Lagrangian with the Yang-Mills two matrix model Lagrangian given in the equation (2.3.1) we have

$$L_{YMCS} = \mathrm{Tr}\left(\frac{1}{2}(D_0 X_i)^2 + \frac{1}{4}[X_i, X_j]^2 + \kappa \epsilon^{ij}(X_i \dot{X}_j + 2i A_0 X_i X_j)\right)\,. \tag{3.3.1}$$

Let's evaluate the variation of the action with respect to A_0. We have

$$\delta S_{YMCS} = \int \mathrm{d}t \,\mathrm{Tr}\big(-i[X_i, D_0 X_j] + 2i\kappa \epsilon^{ij} X_i X_j\big)\,. \tag{3.3.2}$$

Therefore, the A_0 equation of motion in the $A_0 = 0$ gauge reads

$$-\Big[X_i, \dot{X}_i\Big] + 2\kappa \epsilon^{ij} X_i X_j = 0\,. \tag{3.3.3}$$

This is the Gauss law constraint for the YMCS matrix model.

In the $A_0 = 0$ gauge (3.3.1) becomes

$$L_{YMCS} = \mathrm{Tr}\left(\frac{1}{2}(\dot{X}_i)^2 + \frac{1}{4}[X_i, X_j]^2 + \kappa \epsilon^{ij} X_i \dot{X}_j\right)\,. \tag{3.3.4}$$

We may now express the Lagrangian using the vectors $\vec{\mathbf{x}}_1$ and $\vec{\mathbf{x}}_2$ introduced in the previous chapter via the equation (2.3.2). The L_{YM} part of the Lagrangian reads just the same as in (2.3.4). For the L_{CS} term we find in terms of these vectors

$$\begin{aligned} L_{CS} &= \kappa \,\mathrm{Tr}\left(\frac{1}{2}\epsilon^{ij} x_i^\alpha \dot{x}_j^\beta \sigma^\alpha \sigma^\beta\right) \\ &= \kappa \,\mathrm{Tr}\left(\frac{1}{2}\epsilon^{ij} x_i^\alpha \dot{x}_j^\beta (\delta^{\alpha\beta} \mathbb{1}_2 + i\epsilon^{\alpha\beta\gamma}\sigma^\gamma)\right) \\ &= \kappa \,\mathrm{Tr}\left(\frac{1}{2}\epsilon^{ij} \vec{\mathbf{x}}_i \cdot \dot{\vec{\mathbf{x}}}_j \mathbb{1}_2\right) + \kappa \,\mathrm{Tr}\left(\frac{1}{2} i\epsilon^{ij}(\vec{\mathbf{x}}_i \times \dot{\vec{\mathbf{x}}}_j)\cdot \vec{\sigma}\right) \\ &= \kappa \epsilon^{ij} \vec{\mathbf{x}}_i \cdot \dot{\vec{\mathbf{x}}}_j \\ &= \kappa(\vec{\mathbf{x}}_1 \cdot \dot{\vec{\mathbf{x}}}_2 - \vec{\mathbf{x}}_2 \cdot \dot{\vec{\mathbf{x}}}_1)\,. \end{aligned} \tag{3.3.5}$$

The second term of the third line of (3.3.5) is vanishing since $\mathrm{Tr}\,\sigma_i = 0$. The L_{YMCS} is then

$$L_{YMCS} = \frac{1}{2}(\dot{\vec{\mathbf{x}}}_1^2 + \dot{\vec{\mathbf{x}}}_2^2) - (\vec{\mathbf{x}}_1 \times \vec{\mathbf{x}}_2)^2 + \kappa(\vec{\mathbf{x}}_1 \cdot \dot{\vec{\mathbf{x}}}_2 - \vec{\mathbf{x}}_2 \cdot \dot{\vec{\mathbf{x}}}_1)\,. \tag{3.3.6}$$

We can immediately find the conjugate momenta as

$$\begin{aligned} \vec{\mathbf{p}}_1 &= \frac{\partial L}{\partial \dot{\vec{\mathbf{x}}}_1} = \dot{\vec{\mathbf{x}}}_1 - \kappa \vec{\mathbf{x}}_2\,, \\ \vec{\mathbf{p}}_2 &= \frac{\partial L}{\partial \dot{\vec{\mathbf{x}}}_2} = \dot{\vec{\mathbf{x}}}_2 + \kappa \vec{\mathbf{x}}_1\,. \end{aligned} \tag{3.3.7}$$

Note that conjugate momenta $\vec{\mathbf{p}}_1$ and $\vec{\mathbf{p}}_2$ are no longer equal to the kinematical momenta $\dot{\vec{\mathbf{x}}}_1$ and $\dot{\vec{\mathbf{x}}}_2$ respectively due to the presence of the Chern-Simons term which is first order in time derivative.

The constraint equation, (3.3.3), expressed in terms of $\vec{\mathbf{x}}_1$, $\vec{\mathbf{x}}_2$ and their time derivatives is

$$\vec{\mathbf{x}}_1 \times \dot{\vec{\mathbf{x}}}_1 + \vec{\mathbf{x}}_2 \times \dot{\vec{\mathbf{x}}}_2 - 2\kappa \vec{\mathbf{x}}_1 \times \vec{\mathbf{x}}_2 = 0\,. \tag{3.3.8}$$

Solving for the kinematical momenta $\dot{\vec{\mathbf{x}}}_1$, $\dot{\vec{\mathbf{x}}}_2$ from (3.3.7) and inserting them in (3.3.8) yields

$$\begin{aligned} \vec{\mathbf{x}}_1 \times (\vec{\mathbf{p}}_1 + \kappa \vec{\mathbf{x}}_2) + \vec{\mathbf{x}}_2 \times (\vec{\mathbf{p}}_2 - \kappa \vec{\mathbf{x}}_1) - 2\kappa \vec{\mathbf{x}}_1 \times \vec{\mathbf{x}}_2 &= 0 \\ \vec{\mathbf{x}}_1 \times \vec{\mathbf{p}}_1 + \vec{\mathbf{x}}_2 \times \vec{\mathbf{p}}_2 + 2\kappa \vec{\mathbf{x}}_1 \times \vec{\mathbf{x}}_2 - 2\kappa \vec{\mathbf{x}}_1 \times \vec{\mathbf{x}}_2 &= 0 \\ \vec{\mathbf{L}}_1 + \vec{\mathbf{L}}_2 &= 0\,, \end{aligned} \tag{3.3.9}$$

where we have used $\vec{\mathbf{L}}_i = \vec{\mathbf{x}}_i \times \vec{\mathbf{p}}_i$ as the standard definition of angular momentum. This shows that the constraint equation has the same form as in (2.3.10). We will check the direction of time derivatives of $\vec{\mathbf{L}}_i$ after finding the Hamiltonian in Cartesian coordinates.

3.4 Lagrangian and Hamiltonian Mechanics with First Order Time Derivatives in the Lagrangian

In order to determine the Hamiltonian corresponding to the Lagrangian (3.3.6) let us digress a moment and inspect the structure of Lagrangians involving first order time derivatives and the transition to the Hamiltonian dynamics in such systems.

For a system with generalized coordinates q_i and velocities $\dot{q}_i$, Lagrangian involving first order time derivatives have the generic form

$$L = \frac{1}{2} g_{ij} \dot{q}_i \dot{q}_j + f_i \dot{q}_i - V \,, \tag{3.4.1}$$

where g_{ij} is the metric, f_i is some function of the generalized coordinates i.e. $f_i \equiv f_i(q_j)$ and V is a potential $V \equiv V(q_i)$. Canonical momenta are evaluated as

$$p_i = \frac{\partial L}{\partial \dot{q}_i} = g_{ij} \dot{q}_j + f_i \,. \tag{3.4.2}$$

In terms of p_i, $\dot{q}_i$ can be solved using the inverse metric in the form

$$\begin{aligned} \dot{q}_i &= g^{-1}_{ij}(p_j - f_j) \,, \\ &= g^{ij}(p_j - f_j) \,. \end{aligned} \tag{3.4.3}$$

The Hamiltonian is found as follows

$$\begin{aligned} H &= p_i \dot{q}_i - L \\ &= p_i g^{-1}_{ij}(p_j - f_j) - \frac{1}{2} \underbrace{g_{ij} g^{-1}_{ik}}_{\delta_{jk}} (p_k - f_k) g^{-1}_{jl}(p_l - f_l) - f_i g^{-1}_{ij}(p_j - f_j) + V \\ &= p_i g^{-1}_{ij}(p_j - f_j) - \frac{1}{2} g^{-1}_{jl}(p_j - f_j)(p_l - f_l) - f_i g^{-1}_{ij}(p_j - f_j) + V \\ &= p_i g^{-1}_{ij}(p_j - f_j) - \frac{1}{2} g^{-1}_{ij}(p_i - f_i)(p_j - f_j) - f_i g^{-1}_{ij}(p_j - f_j) + V \\ &= g^{-1}_{ij}(p_i p_j - p_i f_j - \frac{1}{2} p_i p_j + p_i f_j - \frac{1}{2} f_i f_j - p_i f_j + f_i f_j) + V \\ &= \frac{1}{2} g^{-1}_{ij} p_i p_j + \frac{1}{2} g^{-1}_{ij} f_i f_j - g^{-1}_{ij} p_i f_j + V \,, \end{aligned} \tag{3.4.4}$$

where we used $g_{ij} = g_{ji}$.

3.5 Hamiltonian Mechanics

Comparing (3.3.6) and (3.4.1) we read

$$\begin{aligned} g_{ij} &= g^{-1}_{ij} = \delta_{ij} \,, \\ \vec{\mathbf{q}}_i &= \vec{\mathbf{x}}_i \,, \\ f_i &= -\kappa \epsilon_{ij} x_j \,, \\ V &= (\vec{\mathbf{x}}_1 \times \vec{\mathbf{x}}_2)^2 \,, \end{aligned} \tag{3.5.1}$$

therefore the Hamiltonian is

$$\begin{aligned} H &= \frac{1}{2}\delta_{ij}p_i p_j + \frac{1}{2}\delta_{ij}\kappa^2\epsilon_{ik}x_k\epsilon_{jl}x_l - \delta_{ij}p_i(-\kappa\epsilon_{jl}x_l) + (\vec{\mathbf{x}}_1 \times \vec{\mathbf{x}}_2)^2 \\ &= \frac{1}{2}(\vec{\mathbf{p}}_1^2 + \vec{\mathbf{p}}_2^2) + \frac{1}{2}\kappa^2(\vec{\mathbf{x}}_1^2 + \vec{\mathbf{x}}_2^2) + \kappa(\vec{\mathbf{p}}_1 \cdot \vec{\mathbf{x}}_2 - \vec{\mathbf{p}}_2 \cdot \vec{\mathbf{x}}_1) + (\vec{\mathbf{x}}_1 \times \vec{\mathbf{x}}_2)^2 \,. \end{aligned} \tag{3.5.2}$$

We find that the Hamiltonian equations of motion are given as

$$\begin{aligned} \dot{\vec{\mathbf{x}}}_1 &= \frac{\partial H}{\partial \vec{\mathbf{p}}_1} = \vec{\mathbf{p}}_1 + \kappa\vec{\mathbf{x}}_2 \,, \\ \dot{\vec{\mathbf{p}}}_1 &= -\frac{\partial H}{\partial \vec{\mathbf{x}}_1} = \kappa^2\vec{\mathbf{x}}_1 - \kappa\vec{\mathbf{p}}_2 + 2\vec{\mathbf{x}}_2 \times (\vec{\mathbf{x}}_1 \times \vec{\mathbf{x}}_2) \,, \\ \dot{\vec{\mathbf{x}}}_2 &= \frac{\partial H}{\partial \vec{\mathbf{p}}_2} = \vec{\mathbf{p}}_2 - \kappa\vec{\mathbf{x}}_1 \,, \\ \dot{\vec{\mathbf{p}}}_2 &= -\frac{\partial H}{\partial \vec{\mathbf{x}}_2} = \kappa^2\vec{\mathbf{x}}_2 + \kappa\vec{\mathbf{p}}_1 - 2\vec{\mathbf{x}}_2 \times (\vec{\mathbf{x}}_1 \times \vec{\mathbf{x}}_2) \,. \end{aligned} \tag{3.5.3}$$

The time derivative of $\vec{\mathbf{L}}_1$ can be found by using these equations of motion as follows

$$\begin{aligned} \dot{\vec{\mathbf{L}}}_1 &= \vec{\mathbf{x}}_1 \times \dot{\vec{\mathbf{p}}} \\ &= \vec{\mathbf{x}}_1 \times (\kappa^2\vec{\mathbf{x}}_1 - \kappa\vec{\mathbf{p}}_2 + 2\vec{\mathbf{x}}_2 \times (\vec{\mathbf{x}}_1 \times \vec{\mathbf{x}}_2)) \\ &= -\kappa\vec{\mathbf{x}}_1 \times \vec{\mathbf{p}}_2 + 2\vec{\mathbf{x}}_1 \times (\vec{\mathbf{x}}_2 \times (\vec{\mathbf{x}}_1 \times \vec{\mathbf{x}}_2)) \,. \end{aligned} \tag{3.5.4}$$

The last term is the same as the one in section 2.3, it is parallel to $\vec{\mathbf{L}}_1$, but the first term does not have a definite direction. Therefore, $\dot{\vec{\mathbf{L}}}_1$ may not be parallel to $\vec{\mathbf{L}}_1$. The same situation is also valid for $\vec{\mathbf{L}}_2$. Since the time derivative of $\vec{\mathbf{L}}_i$ and $\dot{\vec{\mathbf{L}}}_i$ may not be in the same direction, it is not possible to immediately conclude that the motion remains confined to the $x_1 - x_2$ plane. However, we will see from our subsequent analysis that the motion remains confined to the $x_1 - x_2$ plane.

3.6 Coordinate Transformation

Next step in our analysis is to obtain a coordinate transformation from $\vec{\mathbf{x}}_1$ and $\vec{\mathbf{x}}_2$ to new variables as we did in the previous chapter in section 2.3. Compared to (2.3.15) keeping now the zeros we may start with the 3×2 matrix

$$X_0 = \frac{1}{\sqrt{2}} \begin{pmatrix} r & r\cos(\theta) \\ 0 & r\sin(\theta) \\ 0 & 0 \end{pmatrix} \,. \tag{3.6.1}$$

The reason for this is that, we need to be able to rotate both columns of this matrix by a general $SO(3)$ rotation not just by $SO(2)$ subgroup, since we cannot argue in advance that motion is confined to the $x_1 - x_2$ plane. A general $SO(3)$ rotation can be written using Euler's parametrization, which uses $z - x - z$ active rotation with the angles α, β, γ respectively and is given by[19]

$$R(\alpha,\beta,\gamma) = \begin{pmatrix} c(\alpha)c(\gamma) - s(\alpha)c(\beta)s(\gamma) & -s(\alpha)c(\beta)c(\gamma) - c(\alpha)s(\gamma) & s(\alpha)s(\beta) \\ c(\gamma)s(\alpha) + c(\alpha)c(\beta)s(\gamma) & c(\alpha)c(\beta)c(\gamma) - s(\alpha)s(\gamma) & -c(\alpha)s(\beta) \\ s(\beta)s(\gamma) & s(\beta)c(\gamma) & c(\beta) \end{pmatrix}, \tag{3.6.2}$$

where s and c stand for sine and cosine respectively. In order to obtain the coordinate transformation from $(\vec{\mathbf{x}}_1, \vec{\mathbf{x}}_2)$, we therefore write

$$X = \frac{1}{\sqrt{2}} R(\alpha,\beta,\gamma) \begin{pmatrix} r & r\cos(\theta) \\ 0 & r\sin(\theta) \\ 0 & 0 \end{pmatrix} \begin{pmatrix} \cos(\phi) & \sin(\phi) \\ -\sin(\phi) & \cos(\phi) \end{pmatrix}, \tag{3.6.3}$$

which can be compared to the equation (2.3.16). Explicit form of the components of the 3×2 matrix X are listed in the appendix A.1. The metric in these coordinate is evaluated from $g_{ij} = \mathrm{Tr}\big(\partial_i X^\dagger \partial_j X\big)$ and its components as well of those of its inverse g_{ij}^{-1} are also given in the appendix A.2.

There are six generalized coordinates $(r, \theta, \phi, \alpha, \beta, \gamma)$ and the corresponding six conjugate momenta given as $(p_r, p_\theta, p_\phi, p_\alpha, p_\beta, p_\gamma)$. Using these generalized coordinates and momenta and the inverse metric g_{ij}^{-1} given in the appendix, we have the first term

in the equation (3.4.4)

$$\begin{aligned}
\frac{1}{2}g_{ij}^{-1}p_ip_j = &-\frac{\csc^2(\beta)\cos(2\gamma)\csc^2(\theta)p_\alpha^2}{2r^2}\\
&-\frac{\csc^2(\beta)\csc^2(\theta)p_\alpha^2\cos(2(\gamma+\theta))}{2r^2}\\
&-\frac{2\cot(\beta)\csc(\beta)\csc^2(\theta)p_\alpha p_\gamma}{r^2}\\
&+\frac{\cot(\beta)\csc(\beta)\cos(2\gamma)\csc^2(\theta)p_\alpha p_\gamma}{r^2}\\
&+\frac{\cot(\beta)\csc(\beta)\csc^2(\theta)p_\alpha p_\gamma\cos(2(\gamma+\theta))}{r^2}\\
&+\frac{2\csc(\beta)\cot(\theta)\csc(\theta)p_\alpha p_\beta\sin(2\gamma+\theta)}{r^2}\\
&+\frac{\csc^2(\beta)\csc^2(\theta)p_\alpha^2}{r^2}+\frac{\cot^2(\beta)\csc^2(\theta)p_\gamma^2}{r^2}\\
&-\frac{\cot^2(\beta)\cot(\theta)\csc(\theta)p_\gamma^2\cos(2\gamma+\theta)}{r^2}\\
&+\frac{\cot(\theta)\csc(\theta)p_\beta^2\cos(2\gamma+\theta)}{r^2}\\
&-\frac{2\cot(\beta)\cot(\theta)\csc(\theta)p_\beta p_\gamma\sin(2\gamma+\theta)}{r^2}\\
&+\frac{\csc^2(\theta)p_\beta^2}{r^2}-\frac{\tan(\theta)\sec(\theta)p_\gamma p_\phi}{r^2}\\
&-\frac{2p_\gamma p_\theta}{r^2}+\frac{\sec^2(\theta)p_\gamma^2}{2r^2}+\frac{p_\gamma^2}{2r^2}\\
&+\frac{\sec^2(\theta)p_\phi^2}{2r^2}+\frac{2p_\theta^2}{r^2}+\frac{p_r^2}{2}\,.
\end{aligned} \tag{3.6.4}$$

In order to proceed, we need to know the form of $f_i = -\kappa\epsilon_{ij}x_j$ in the new coordinates. The function $f_i = f_i(q_j)$ and $\dot{q}_i$ in the Lagrangian (3.3.6) appear as

$$f_i\dot{q}_i \equiv \kappa\vec{\mathbf{x}}_1\cdot\dot{\vec{\mathbf{x}}}_2 - \kappa\vec{\mathbf{x}}_2\cdot\dot{\vec{\mathbf{x}}}_1\,. \tag{3.6.5}$$

Using the X matrix in (3.6.3) and time derivative $\dot{X}$ which is simply formed in terms of the time derivatives of the components of X, right hand side of (3.6.5) can be written by taking the inner products of the column vectors of X and $\dot{X}$ and can be written in this new coordinates as

$$f_i\dot{q}_i = -\frac{1}{2}r^2\kappa\left(2\dot{\phi}+\sin(\theta)(2\dot{\alpha}\cos(\beta)+2\dot{\gamma}+\dot{\theta})\right)\,. \tag{3.6.6}$$

Since $f_i\dot{q}_i = f_1\dot{r}+f_2\dot{\theta}+f_3\dot{\phi}+f_4\dot{\alpha}+f_5\dot{\beta}+f_6\dot{\gamma}$ in the new coordinates, $f_i(r,\theta,\phi,\alpha,\beta,\gamma)$,

$i : 1, ..., 6$ can be readily read out from this expression as

$$\begin{aligned} f_1 &= 0\,, \\ f_2 &= -\frac{1}{2}r^2\kappa\sin(\theta)\,, \\ f_3 &= -r^2\kappa\,, \\ f_4 &= -r^2\kappa\sin(\theta)\cos(\beta)\,, \\ f_5 &= 0\,, \\ f_6 &= -r^2\kappa\sin(\theta)\,. \end{aligned} \tag{3.6.7}$$

This allows us to determine both the second and the third terms in the Hamiltonian. We have for the second term

$$\frac{1}{2}g_{ij}^{-1}f_i f_j = \frac{1}{2}r^2\kappa^2\,, \tag{3.6.8}$$

and for the third term

$$\frac{1}{2}g_{ij}^{-1}p_i f_j = -p_\phi\kappa\,. \tag{3.6.9}$$

The potential term is

$$\frac{1}{2}(\vec{\mathbf{x}}_1 \times \vec{\mathbf{x}}_2)^2 = \frac{1}{4}r^4\sin^2(\theta)\,, \tag{3.6.10}$$

which is the same as in the case without the Chern-Simons term given in section 2.3 since the square of the cross product of vectors is a scalar and does not get affected by any gauge rotations.

Angular momentum vector $\vec{\mathbf{L}}$ for a general $SO(3)$ rotation can be expressed in terms of the Euler angles α, β, γ and the conjugate momenta p_α, p_β and p_γ as [20]

$$\vec{\mathbf{L}} = \begin{pmatrix} \sin(\alpha)(p_\gamma\csc(\beta) - p_\alpha\cot(\beta)) + p_\beta\cos(\alpha) \\ \cos(\alpha)\csc(\beta)(p_\alpha\cos(\beta) - p_\gamma) + p_\beta\sin(\alpha) \\ p_\alpha \end{pmatrix}\,, \tag{3.6.11}$$

whose details are given in the appendix A.3. The constraint, $\vec{\mathbf{L}} = 0$, is satisfied if and only if $p_\alpha = p_\beta = p_\gamma = 0$ in equation (3.6.11). Using this fact in (3.4.4), the calculation of the Hamiltonian is significantly simplified and we find

$$H = \frac{1}{2}p_r^2 + \frac{2}{r^2}p_\theta^2 + \frac{p_\phi^2}{2r^2\cos^2(\theta)} + \kappa p_\phi + \frac{\kappa^2 r^2}{2} + \frac{1}{4}r^4\sin^2(\theta)\,. \tag{3.6.12}$$

As noted previously, as a consequence of Chern-Simons level quantization we have $\kappa = \frac{k}{4\pi}$, where k is an integer. Therefore we can write (3.6.13) as

$$H = \frac{1}{2}p_r^2 + \frac{2}{r^2}p_\theta^2 + \frac{p_\phi^2}{2r^2\cos^2(\theta)} + \frac{kp_\phi}{4\pi} + \frac{k^2r^2}{32\pi^2} + \frac{1}{4}r^4\sin^2(\theta) + \hbar r\,, \qquad (3.6.13)$$

where we have added a term $\hbar r$ as in the pure Yang-Mills case since the θ-dependent terms in the Hamiltonian does not change compared to the pure Yang-Mills theory and therefore θ changes only adiabatically at large r. The contribution of the Chern-Simons term to the Hamiltonian are given by the terms proportional to k. Since $\frac{\partial H}{\partial \phi} = 0$, p_ϕ remains as a constant of motion and we can concentrate on the time evolution of the phase space variables r, θ, p_r, p_θ only.

Hamiltonian equations of motion are

$$\begin{aligned}
\dot{r} &= \frac{\partial H}{\partial p_r} = p_r\,,\\
\dot{p}_r &= -\frac{\partial H}{\partial r} = \frac{4p_\theta^2}{r^3} + \frac{p_\phi^2}{r^3\cos^2(\theta)} - \frac{k^2r}{16\pi^2} - r^3\sin^2(\theta) - \hbar\,,\\
\dot{\theta} &= \frac{\partial H}{\partial p_\theta} = \frac{4p_\theta}{r^2}\,,\\
\dot{p_\theta} &= -\frac{\partial H}{\partial \theta} = -\frac{1}{2}r^4\cos(\theta)\sin(\theta) - \frac{p_\phi^2\tan(\theta)}{\cos^2(\theta)r^2}\,.
\end{aligned} \qquad (3.6.14)$$

It is also interesting to note that the Hamiltonian can be expressed in the form

$$\begin{aligned}
H =& \frac{1}{2}p_r^2 + \frac{2}{r^2}p_\theta^2 + \frac{1}{2r^2\cos^2(\theta)}\left(p_\phi + \frac{k}{4\pi}r^2\cos^2(\theta)\right)^2\\
&+ \frac{1}{4}\left(r^2 + \frac{k^2}{16\pi^2}\right)^2\sin^2(\theta) - \frac{1}{4}\frac{k^4}{256\pi^4}\sin^2(\theta) + \hbar r\,.
\end{aligned} \qquad (3.6.15)$$

3.7 Numerical Results and Chaos

Compared to the pure Yang-Mills matrix model Hamiltonian there is no change in the phase space variables, they are still $(r, \theta, p_r, p_\theta)$ while the Hamiltonian and consequently the equations of motion have new contributions due to the Chern-Simons term. We now have in addition to p_ϕ another constant $k \in \mathbb{Z}$ which can be taken to assume different integer values, and we probe the emerging chaotic dynamics at different values of p_ϕ and k. The constants $(E = 1, \hbar = 0.1)$ and the algorithm choosing randomly initial conditions are same as in the section 2.3.

In the absence of the Chern-Simons term, the dynamics of the Hamiltonian (3.6.13) becomes almost completely chaotic, as $p_\phi \to 0$, while, chaos ceases to exist for $p_\phi \geq 2$. At $p_\phi = 1$, for instance, there is a small region in phase space filled with quasi periodic orbits, while the rest is chaotic. Here we study how chaotic dynamics changes for different choices of the Chern-Simons level at three different values of p_ϕ, which are $p_\phi = 0, 1, 2$.

The general effect of the additional terms is to reduce chaos with increasing Chern-Simons level. At $p_\phi = 0$, we see from figure 3.4a that as $|k|$ increases largest Lyapunov exponent (averaged over several initial conditions) quickly approaches to zero, indicating that the system becomes less and less chaotic as $|k|$ increases and almost no chaos exists for $|k| > 10$.

At $p_\phi = 1$, increasing the $|k|$ values suppresses the chaos except for the values of $k = -1$ to $k = -4$. Poincaré sections in figure 3.1 shows that the area of KAM tori takes the larger part of the phase space for the increasing positive k values. For negative k values in figure 3.2, the range of k that sustains chaotic dynamics is larger but chaos eventually disappears. The same trend can be seen in figure 3.4b. Lyapunov exponents tend to increase only slightly for $k < 0$ and $|k|$ small but they start to decrease and goes to zero at larger $|k|$ values. In order to understand the cause of small but interesting increase for $k = -1$ to $k = -4$ consider the following equation

$$E - \left(\frac{kp_\phi}{4\pi} + \frac{k^2r^2}{32\pi^2}\right) = \frac{1}{2}p_r^2 + \frac{2}{r^2}p_\theta^2 + \frac{p_\phi^2}{2r^2\cos^2(\theta)} + \frac{1}{4}r^4\sin^2(\theta) + \hbar r\,. \quad (3.7.1)$$

Here, we have just rearranged the equation (3.6.13) so that the right hand side of this equation is the Hamiltonian of the pure Yang-Mills case. For $-4 < k < -1$ of k values $kp_\phi + \frac{k^2r^2}{32\pi^2} < 0$. This has the same effect as increasing the energy of the pure Yang-Mills case which results in an increase for the value of the Lyapunov exponents.

At $p_\phi = 2$, we do not have much chaos left in the phase space and a nonzero value of $|k| \neq 0$ does not have any significant effect in this behavior as can be seen from the plot 3.4c which gives largest Lyapunov exponents to be very small, with the maximum values of approximately 0.03 at $k = -4$, and this number is not large enough to indicate appreciable chaotic dynamics in the phase space.

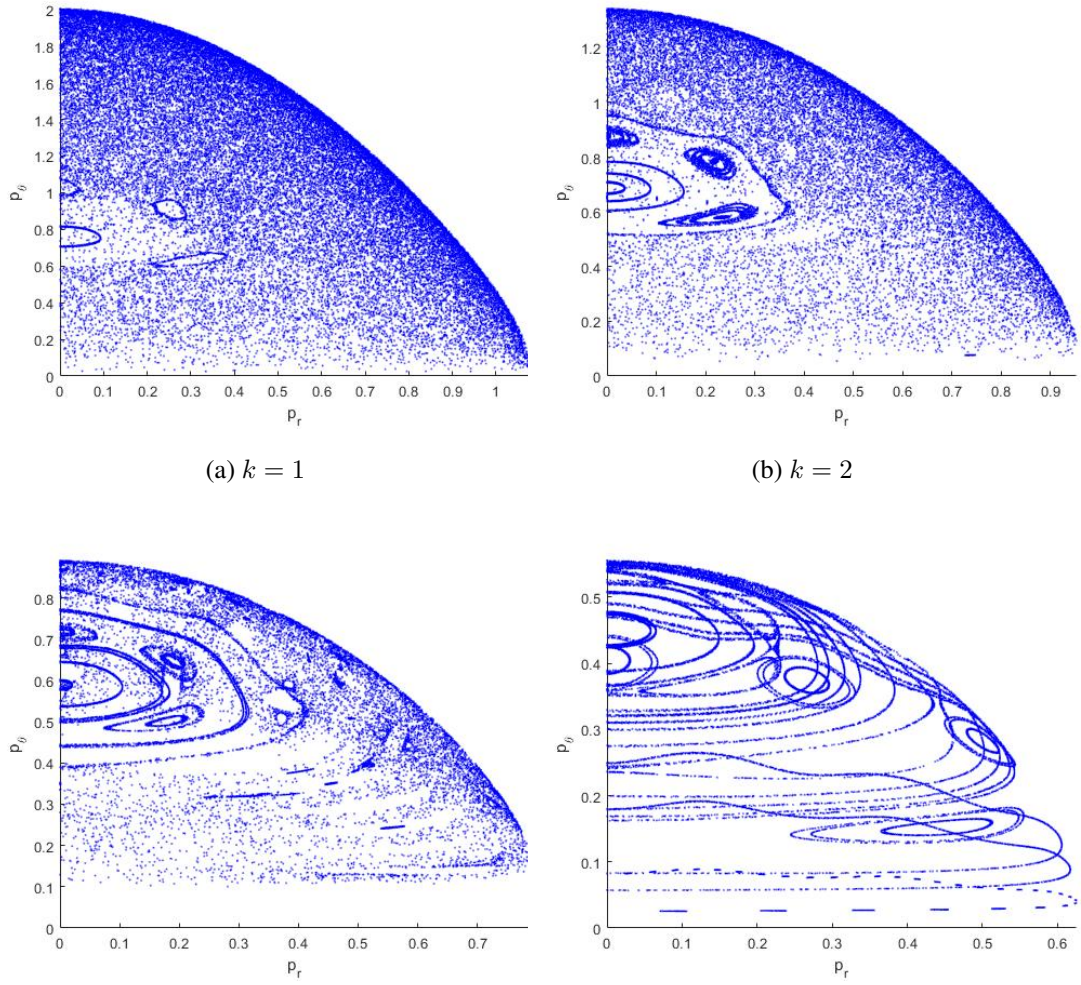

(a) $k = 1$ (b) $k = 2$

(c) $k = 3$ (d) $k = 4$

Figure 3.1: Poincaré sections at $p_\phi = 1$ for positive k values

Poincaré sections in figure 3.3 are in agreement with the conclusions drawn from the Lyapunov spectrum. Although the regions contain randomly scattered dots for $k = -1, -3, -5$ as can be seen in figures 3.3c, 3.3d, 3.3e, they appear due to a limited number of initial conditions and this does not cause an appreciable effect in the Lyapunov spectrum.

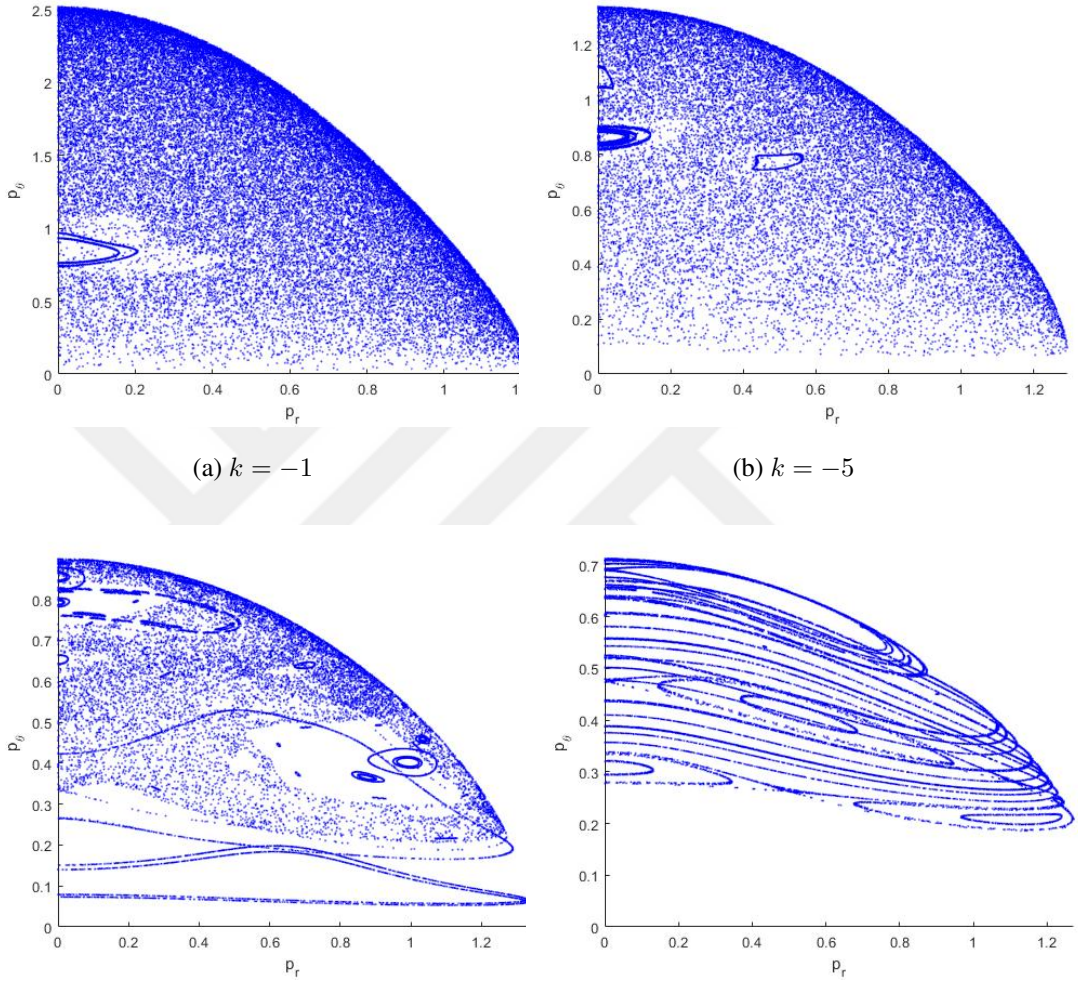

(a) $k = -1$ (b) $k = -5$

(c) $k = -10$ (d) $k = -15$

Figure 3.2: Poincaré sections at $p_\phi = 1$ for negative k values

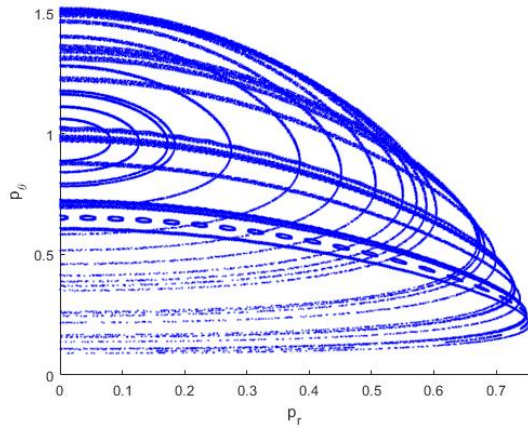

(a) $k = 1$

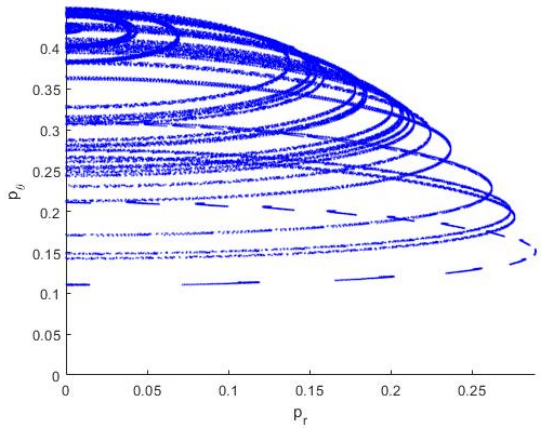

(b) $k = 2$

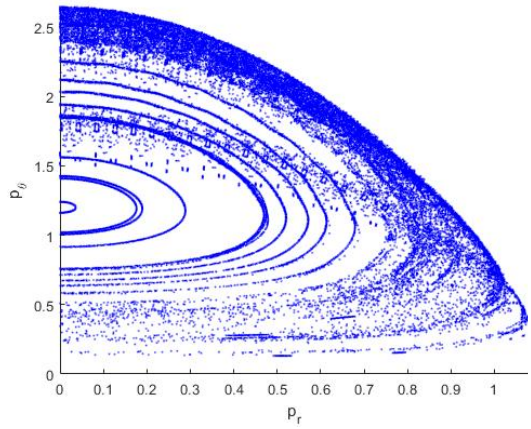

(c) $k = -1$

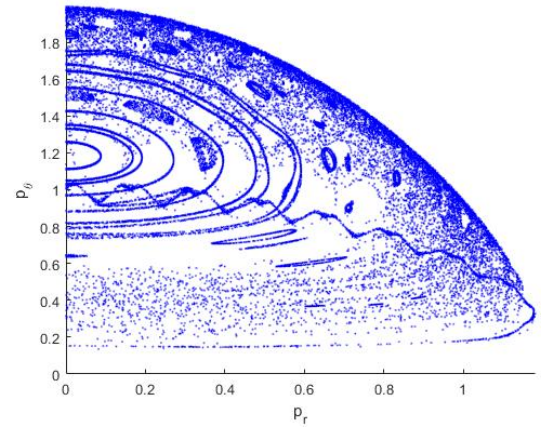

(d) $k = -3$

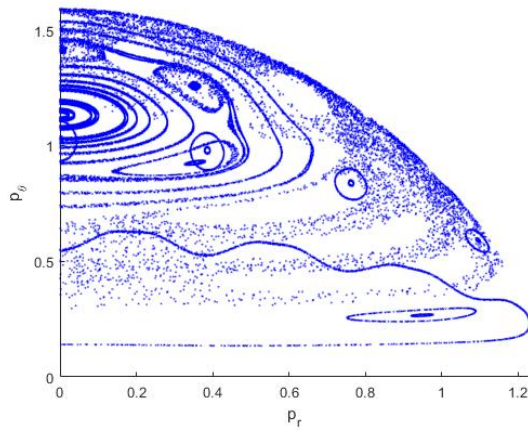

(e) $k = -5$

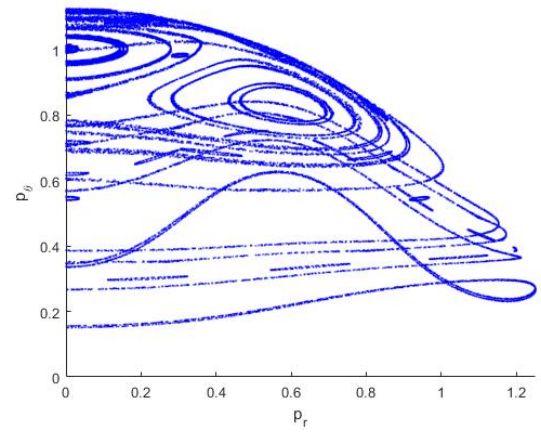

(f) $k = -10$

Figure 3.3: Poincaré sections at $p_\phi = 2$

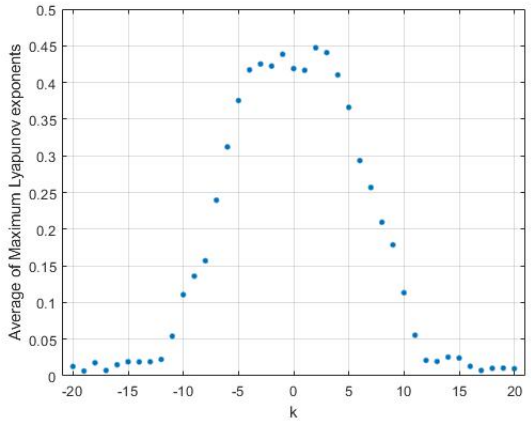

(a) $p_\phi = 0$

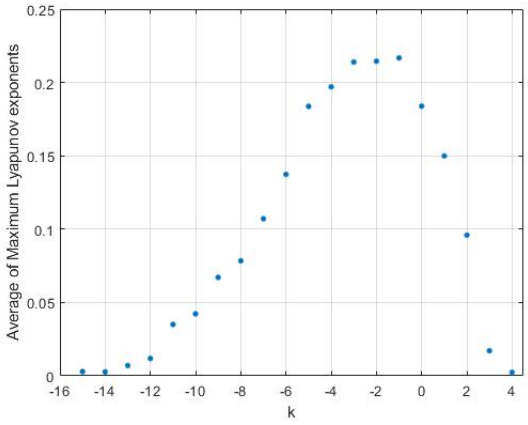

(b) $p_\phi = 1$

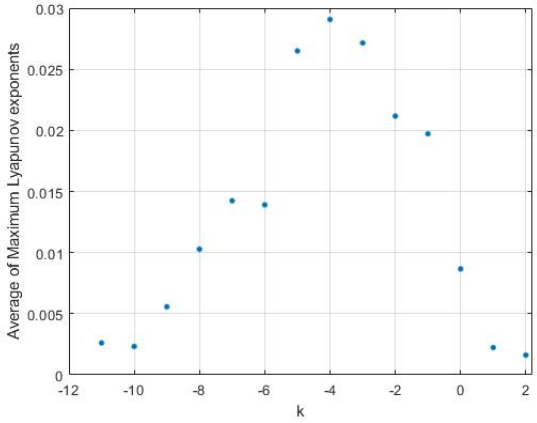

(c) $p_\phi = 2$

Figure 3.4: Lyapunov spectra at $p_\phi = 0, p_\phi = 1$ and $p_\phi = 2$

CHAPTER 4

TWO MATRIX MODEL WITH A MASS TERM

In this short chapter, we examine the changes in chaotic dynamics due to a mass deformation in the two matrix model. As we will see shortly the mass term does not break the gauge and the global symmetries. We, therefore follow the same approach and if necessary use results from chapter 2 to present the developments in this chapter.

4.1 Two matrix model with mass terms

Adding a mass term to the Lagrangian (2.3.1) is modified to

$$L = \frac{1}{2}\,\mathrm{Tr}\big((D_0X_1)^2 + (D_0X_2)^2 + [X_1, X_2]^2 - \mu^2X_1^2 - \mu^2X_2^2\big)\,, \tag{4.1.1}$$

where μ^2 is a dimensionless parameter governing the mass deformation. Clearly, $\mathrm{Tr}\,\mu^2X_i^2$ is invariant under both the local gauge transformations $U^\dagger X_i U$ and the global $SO(2)$ rigid rotations $X_i \to R_{ij}X_j$. By using equation (2.3.2), X_i^2 can be expressed as

$$\begin{aligned} X_i^2 &= \frac{1}{2}x_i^\alpha x_i^\beta \sigma^\alpha \sigma^\beta \\ &= \frac{1}{2}x_i^\alpha x_i^\beta (\delta_{\alpha\beta}\mathbb{1}_2 + i\epsilon_{\alpha\beta\gamma}\sigma_\gamma) \\ &= \frac{1}{2}x_i^2\mathbb{1}_2\,. \end{aligned} \tag{4.1.2}$$

The mass term L_μ is then

$$\begin{aligned} L_\mu &= -\frac{1}{2}\,\mathrm{Tr}\left(\mu^2\frac{1}{2}\vec{\mathbf{x}}_1^2\mathbb{1}_2 + \mu^2\frac{1}{2}\vec{\mathbf{x}}_2^2\mathbb{1}_2\right) \\ &= -\frac{1}{2}\mu^2(\vec{\mathbf{x}}_1^2 + \vec{\mathbf{x}}_2^2)\,. \end{aligned} \tag{4.1.3}$$

We have expressed the Lagrangian L_{YM} in terms of $\vec{\mathbf{x}}_1$ and $\vec{\mathbf{x}}_2$ in the equation (2.3.4). Thus, the Lagrangian with the mass deformation is

$$L = \frac{1}{2}(\dot{\vec{\mathbf{x}}}_1)^2 + \frac{1}{2}(\dot{\vec{\mathbf{x}}}_2)^2 - (\vec{\mathbf{x}}_1 \times \vec{\mathbf{x}}_2)^2 - \frac{1}{2}\mu^2\vec{\mathbf{x}}_1^2 - \frac{1}{2}\mu^2\vec{\mathbf{x}}_2^2 \,. \tag{4.1.4}$$

This yields the Hamiltonian,

$$\begin{aligned} H &= \frac{1}{2}\vec{\mathbf{p}}_i^2 + (\vec{\mathbf{x}}_1 \times \vec{\mathbf{x}}_2)^2 + \frac{1}{2}\mu^2\vec{\mathbf{x}}_1^2 + \frac{1}{2}\mu^2\vec{\mathbf{x}}_2^2 \\ &= \frac{1}{2}(\vec{\mathbf{p}}_i^2 + \mu^2\vec{\mathbf{x}}_i^2) + (\vec{\mathbf{x}}_1 \times \vec{\mathbf{x}}_2)^2 \,. \end{aligned} \tag{4.1.5}$$

Hamilton's equations of motion are

$$\begin{aligned} \dot{\vec{\mathbf{p}}}_1 &:= -\frac{\partial H}{\partial \vec{\mathbf{x}}_1} = 2\vec{\mathbf{x}}_2 \times (\vec{\mathbf{x}}_1 \times \vec{\mathbf{x}}_2) - \mu^2\vec{\mathbf{x}}_1 \,, \\ \dot{\vec{\mathbf{p}}}_2 &:= -\frac{\partial H}{\partial \vec{\mathbf{x}}_2} = -2\vec{\mathbf{x}}_2 \times (\vec{\mathbf{x}}_1 \times \vec{\mathbf{x}}_2) - \mu^2\vec{\mathbf{x}}_2 \,, \\ \dot{\vec{\mathbf{x}}}_1 &:= \frac{\partial H}{\partial \vec{\mathbf{p}}_1} = \vec{\mathbf{p_1}} \,, \\ \dot{\vec{\mathbf{x}}}_1 &:= \frac{\partial H}{\partial \vec{\mathbf{p}}_2} = \vec{\mathbf{p_2}} \,, \end{aligned} \tag{4.1.6}$$

while time derivative of the angular momentum

$$\begin{aligned} \dot{\vec{\mathbf{L}}}_1 &= \dot{\vec{\mathbf{x}}}_1 \times \vec{\mathbf{p}}_1 + \vec{\mathbf{x}}_1 \times \dot{\vec{\mathbf{p}}}_1 \\ &= 2\vec{\mathbf{x}}_1 \times (\vec{\mathbf{x}}_2 \times (\vec{\mathbf{x}}_1 \times \vec{\mathbf{x}}_2)) - \mu^2\vec{\mathbf{x}}_1 \times \vec{\mathbf{x}}_1 \\ &= 2\vec{\mathbf{x}}_1 \times (\vec{\mathbf{x}}_2 \times (\vec{\mathbf{x}}_1 \times \vec{\mathbf{x}}_2)) \,. \end{aligned} \tag{4.1.7}$$

Using the fact that $\vec{\mathbf{L}}_1$ and $\vec{\mathbf{L}}_2$ are anti parallel vectors we see that $\dot{\vec{\mathbf{L}}}_i$ is in the same direction with $\vec{\mathbf{L}}$ as in the section 2.3.

Using the coordinate transformation between $\vec{\mathbf{x}}_1$ and $\vec{\mathbf{x}}_2$, and the new coordinates (r, θ, ϕ, χ) gives simply

$$x_1^2 + x_2^2 = r^2 \,. \tag{4.1.8}$$

Therefore, the Hamiltonian in (2.3.31) is simply modified by an additive term $\frac{1}{2}\mu^2 r^2$ and has the form

$$H = \frac{1}{2}p_r^2 + \frac{2}{r^2}p_\theta^2 + \frac{p_\phi^2}{2r^2\cos^2(\theta)} + \frac{1}{4}r^4\sin^2(\theta) + \hbar r + \frac{1}{2}\mu^2 r^2 \,. \tag{4.1.9}$$

The Hamiltonian equations of motion are

$$\begin{aligned}
\dot{r} &= \frac{\partial H}{\partial p_r} = p_r \,, \\
\dot{p}_r &= -\frac{\partial H}{\partial r} = \frac{4}{r^3} p_\theta^2 - r^3 \sin^2(\theta) + \frac{p_\phi^2}{r^3 \cos^2(\theta)} - \hbar - \mu^2 r \,, \\
\dot{\theta} &= \frac{\partial H}{\partial p_\theta} = \frac{4}{r^2} p_\theta \,, \\
\dot{p_\theta} &= -\frac{\partial H}{\partial \theta} = -\frac{p_\phi^2 \tan(\theta)}{r^2 \cos^2(\theta)} - \frac{1}{2} r^4 \sin(\theta) \cos(\theta) \,.
\end{aligned} \tag{4.1.10}$$

4.1.1 Numerical Results and Chaos

Effect of the mass term on the chaotic behavior of this model will be examined through studying the Poincaré sections and the Lyapunov spectrum. Initial conditions are chosen as in section 2.3 which are $\theta = 0$, $p_r = 0$ and r values are chosen randomly as initially making p_θ real for a given energy,

$$p_\theta = \sqrt{\frac{r^2}{2}\left(E - \frac{p_\phi^2}{2r^2} - \hbar r - \frac{1}{2}\mu^2 r^2\right)} \,. \tag{4.1.11}$$

Energy and the constant resembling $\hbar$ are again taken to be 1 and 0.1, respectively as in section 2.3. We take p_ϕ fixed, at the value $p_\phi = 1$, and vary the mass parameter μ.

Figure 4.1 (a,b,c,d) show the Poincaré sections at $\mu = 0.15, 0.30, 0.45, 0.60$ respectively. In figure 4.1a, there are KAM tori around $p_\theta = 0.8$ for $p_r \in [0, 0.2]$. In figure 2.2a, we have the corresponding situation without the mass term and KAM tori were also seen around the some region in the phase space. Effect of the mass term is to narrow down this region in the phase space. Since the areas of the KAM tori in figures 2.2a and 4.1a are approximately same and the region outside of the KAM tori is chaotic, smaller Poincaré section means smaller chaotic region in this comparison. This fact implies that figure 4.1a is less chaotic than figure 2.2a. Increasing μ to 0.30 in figure 4.1b does not lead to a significant difference in the pattern, but chaotic region in phase space tends to become gradually smaller. In figure 4.1c, there are more KAM tori at various coordinates of the phase space and chaotic regions occupy less area in Poincaré section. At $\mu = 0.60$, KAM tori spread almost all over the phase space, thus no chaos remains in the phase space.

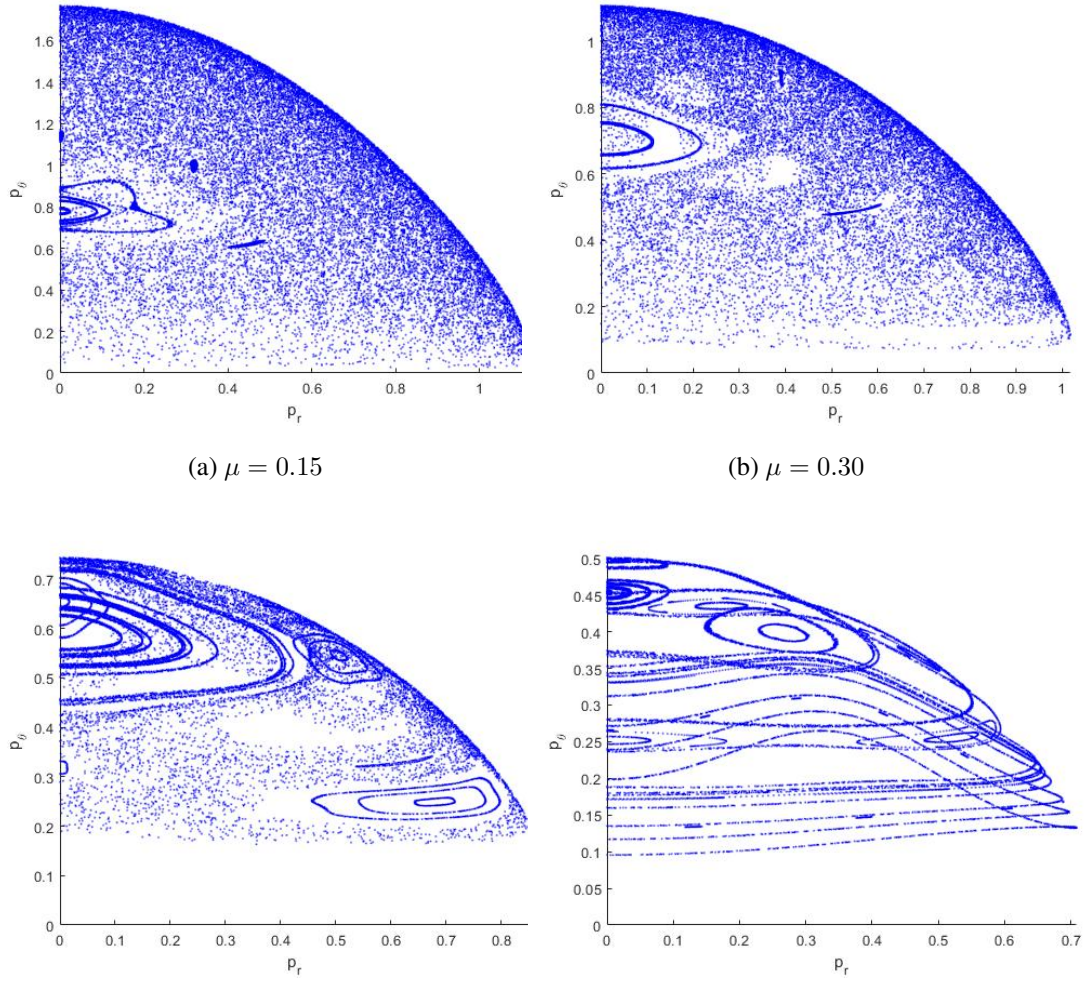

(a) $\mu = 0.15$

(b) $\mu = 0.30$

(c) $\mu = 0.45$

(d) $\mu = 0.60$

Figure 4.1: Poincaré sections at $p_\phi = 1$

Lyapunov spectrum in figure 4.2 also shows that increasing μ suppresses chaos corroborating with the results inferred from the Poincaré sections. The system with mass term becomes less chaotic than the one without the mass term as the value of the mass parameter is increased. This can be seen by the fact that the largest Lyapunov exponent at $p_\phi = 1$ in figure 2.3 is larger than the one at say $\mu = 0.1$ in figure 4.2.

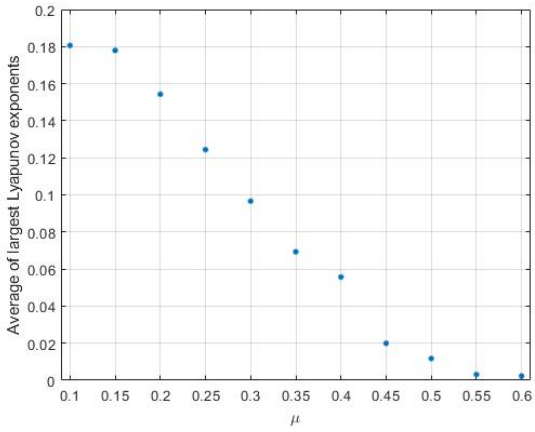

Figure 4.2: Lyapunov spectrum at $p_\phi = 1$

CHAPTER 5

BFSS MATRIX MODEL WITH MASS DEFORMATIONS

In this chapter, we consider a double mass deformation of the BFSS matrix model which breaks the global $SO(9)$ symmetry first to $SO(5) \times SO(4)$ and subsequently down to the product group $SO(5) \times SO(4) \times \mathbb{Z}_2$. The second step here is a consequence of a particular choice for an ansatz configuration composed of fuzzy four and two spheres with collective time dependence, which allows us to specialize to effective models with 4-dimensional phase space and gives us access to study the emerging chaotic dynamics in a simplified setting.

5.1 Mass Deformed Action

Let us consider the double mass deformation of the BFSS model, whose Lagrangian reads

$$S = \frac{1}{g^2} \int \mathrm{d}t \, \mathrm{Tr} \left(\frac{1}{2}(D_0 X_i)^2 + \frac{1}{4}[X_i, X_j]^2 - \frac{1}{2}\mu_1^2 (X_a)^2 - \frac{1}{2}\mu_2^2 (X_b)^2 \right), \quad (5.1.1)$$

where $i, j = 1, ..., 9$; $a = 1, ..., 5$ and $b = 6, ..., 9$. μ_1 and μ_2 are mass deformation parameters. The global $SO(9)$ gauge symmetry is broken to $SO(5) \times SO(4)$ by the last two terms in the action. We have found the equation of motion of BFSS matrix model in section 2.1 as explicitly given in (2.1.23). Contribution of the mass

deformations to the equation of motion can be found as follows

$$\begin{aligned} L_{\mu_1}(X_a) \longrightarrow & L_{\mu_1}(X_a + \delta X_a) \\ \mathrm{Tr}\left(-\frac{1}{2}\mu_1^2 (X_a)^2\right) \longrightarrow & \mathrm{Tr}\left(-\frac{1}{2}\mu_1^2 (X_a + \delta X_a)^2\right) \\ = & \mathrm{Tr}\left(-\frac{1}{2}\mu_1^2 (X_a^2 + 2X_a \delta X_a + (\delta X_a)^2)\right) \\ = & L_{\mu_1}(X_a) - \mu_1^2 \,\mathrm{Tr}(\delta X_a X_a)\,. \end{aligned} \tag{5.1.2}$$

In like fashion, the variation of the second mass deformation is simply

$$L_{\mu_2}(X_b) = \mathrm{Tr}\left(-\frac{1}{2}\mu_2^2 (X_b)^2\right) \longrightarrow L_{\mu_2}(X_b) - \mu_2^2 \,\mathrm{Tr}(\delta X_b X_b)\,. \tag{5.1.3}$$

In the $A_0 = 0$ gauge, the equations of motion with respect to X_a and X_b are therefore

$$\begin{aligned} \ddot{X}_a + [[X_a, X_j], X_j] + \mu_1^2 X_a = 0\,, \\ \ddot{X}_b + [[X_b, X_j], X_j] + \mu_2^2 X_b = 0\,. \end{aligned} \tag{5.1.4}$$

Equation (5.1.4) form a rather complicated set of coupled non-linear differential equations, which cannot be easily solved. Further, the system is subject to the Gauss law constraint $\left[X_i, \dot{X}_i\right] = 0$ due to the A_0 equation of motion.

In section 5.4 we propose an ansatz configuration that is formed from matrices configuring fuzzy 4-spheres and fuzzy 2-spheres at several increasing matrix levels and with collective time dependence. To motivate these developments we discuss fuzzy 2-sphere and 4-sphere in the next two sections.

5.2 Fuzzy Two Sphere

Fuzzy S^2 [21] can be obtained by the quantization of the map $S^3 \to S^2$. Consider the two dimensional complex plane $\mathbb{C}^2$ without the origin, $\mathbb{C}^2 \setminus \{0\}$. The coordinates $z = (\alpha_1 + i\beta_1, \alpha_2 + i\beta_2)$ can be written as $\xi = \frac{z}{|z|}$, then $|\xi|^2$ is normalized to 1. In this way, we see that ξ can be used to describe the 3-sphere as

$$|\xi|^2 = \alpha_1^2 + \beta_1^2 + \alpha_2^2 + \beta_2^2 = 1\,. \tag{5.2.1}$$

Consider the projection map $x_i(\xi) = \xi^\dagger \sigma_i \xi$, which is invariant under the $U(1)$ transformations $\xi \to \xi e^{i\theta}$. Clearly x_i forms the components of a 3-vector $\vec{\mathbf{x}}(\xi)$. Let us

compute the norm of $\vec{\mathbf{x}}(\xi)$. We have

$$\begin{aligned} x_i x_i &= (\xi_a^\dagger(\sigma_\alpha)_{ab}\xi_b)(\xi_c^\dagger(\sigma_\alpha)_{cd}\xi_d) \\ &= \xi_a^\dagger\xi_b\xi_c^\dagger\xi_d(\sigma_\alpha)_{ab}(\sigma_\alpha)_{cd} \\ &= \xi_a^\dagger\xi_b\xi_c^\dagger\xi_d(\delta_{ab}\delta_{cd} - 2\epsilon_{ac}\epsilon_{bd}) \\ &= \xi_a^\dagger\xi_b\xi_c^\dagger\xi_d(-\delta_{ab}\delta_{cd} + 2\delta_{ad}\delta_{bc}) \\ &= -1 + 2 \\ &= 1\,, \end{aligned} \tag{5.2.2}$$

where $\alpha = 1, ..., 3$ and $a, b, c, d = 1, 2$. Then x_i can be understood as the coordinates of S^2 embedded in $\mathbb{R}^3$. This construction is called the Hopf fibration $U(1) \to S^3 \to S^2$.

Quantization of S^3 gives the fuzzy S^3. We can obtain fuzzy S^3 by replacing z_i and z_i^* by annihilation operators a_i and creation operators $a_i^\dagger$, which satisfy the following commutation relation

$$\left[a_\alpha, a_\beta^\dagger\right] = \delta_{\alpha\beta}\,. \tag{5.2.3}$$

The number operator $\widehat{N}$ is defined as

$$\widehat{N} = a_\alpha^\dagger a_\alpha\,. \tag{5.2.4}$$

Using $\widehat{N}$, ξ_α can be formally quantized as

$$\widehat{\xi_\alpha} = \frac{1}{\sqrt{\widehat{N}}}a_\alpha\,, \qquad \widehat{\xi_\alpha}^\dagger = \frac{1}{\sqrt{\widehat{N}}}a_\alpha^\dagger\,, \tag{5.2.5}$$

for not taking the zero eigenvalue i.e. $N = 0$. This condition on the number operator removes the vacuum from the Hilbert space. However, a_α can create vacuum from any $|n\rangle$ state. This complication does not arise for the quantization of the 2-sphere.

We can quantize fuzzy S^2 by quantizing the $S^3 \to S^2$ map as follows

$$\begin{aligned} \widehat{x_i} &= \widehat{\xi^\dagger}\sigma_i\widehat{\xi} \\ &= \frac{1}{\sqrt{\widehat{N}}}a^\dagger\sigma_i a\frac{1}{\sqrt{\widehat{N}}} \\ &= \frac{1}{\widehat{N}}a^\dagger\sigma_i a\,. \end{aligned} \tag{5.2.6}$$

The last step follows from the fact that $\left[a_i^\dagger a_j, \frac{1}{\sqrt{N}}\right] = 0$. Since $\left[\widehat{x_i}, \widehat{N}\right] = 0$, $\widehat{x_i}$ can be restricted to act on the $(n+1)$-dimensional subspace of the Fock space spanned

by the vectors

$$|n_1, n_2\rangle = \frac{(a_1^\dagger)^{n_1}}{\sqrt{n_1!}} \frac{(a_2^\dagger)^{n_2}}{\sqrt{n_2!}} |0,0\rangle \ , \tag{5.2.7}$$

where $n_1 + n_2 = n$. Then, $\widehat{x}_i$ are linear operators on this finite-dimensional space and act on it as $(n+1) \times (n+1)$ Hermitian matrices.

$SU(2)$ generators L_i in terms of Schwinger construction [22] are given as

$$L_i = \frac{1}{2} a^\dagger \sigma_i a \tag{5.2.8}$$

and satisfy the commutation relations

$$[L_i, L_j] = i\epsilon_{ijk} L_k \, . \tag{5.2.9}$$

The coordinates of fuzzy S^2 can therefore be expressed in the form

$$\widehat{x}_i = \frac{2}{n} L_i \, , \tag{5.2.10}$$

where $\frac{2}{n}$ is the noncommutative scaling factor. The commutation relation of the coordinates of fuzzy S^2 is

$$[\widehat{x}_i, \widehat{x}_j] = \frac{2}{n} i\epsilon_{ijk} \widehat{x}_k \, . \tag{5.2.11}$$

When n goes to infinity, this commutator vanishes identically and the standard S^2 is recovered. The Casimir operator for $SU(2)$ is L_i^2 and has the eigenvalues $\frac{n}{2}\left(\frac{n}{2}+1\right)$ on the spin $j = \frac{n}{2}$ representation of $SU(2)$. We therefore have

$$L_i^2 = \frac{n}{2}(\frac{n}{2}+1)\mathbb{1}_{n+1} \tag{5.2.12}$$

on any state of a $SU(2)$ irreducible representations with spin $J = \frac{n}{2}$. By using this equation, radius of fuzzy S^2 is found as

$$\begin{aligned} x_i^2 &= \left(\frac{2}{n}\right)^2 \frac{n}{2}\left(\frac{n}{2}+1\right)\mathbb{1}_{n+1} \\ &= \left(1 + \frac{2}{n}\right)\mathbb{1}_{n+1} \, . \end{aligned} \tag{5.2.13}$$

5.3 Fuzzy Four Sphere

The generators of the group $SO(5)$ in the fundamental spinor representation with Dynkin labels $(0,1)$ are

$$G_{ab} = -\frac{i}{4}[\gamma_a, \gamma_b] \, , \tag{5.3.1}$$

where $a, b = 1, ..., 5$, and γ_a are gamma matrices acting on $\mathbb{C}^4$ and associated to $SO(5)$ group. They are defined by the anti-commutation relations $\{\gamma_a, \gamma_b\} = 2\delta_{ab}$ and we pick them in the following basis

$$\begin{aligned}
\gamma_1 = \sigma_1 \otimes \sigma_1 = \begin{pmatrix} 0 & \sigma_1 \\ \sigma_1 & 0 \end{pmatrix}, \\
\gamma_2 = \sigma_1 \otimes \sigma_2 = \begin{pmatrix} 0 & \sigma_2 \\ \sigma_2 & 0 \end{pmatrix}, \\
\gamma_3 = -\sigma_1 \otimes \sigma_3 = - \begin{pmatrix} 0 & \sigma_3 \\ \sigma_3 & 0 \end{pmatrix}, \\
\gamma_4 = -\sigma_2 \otimes \mathbb{1}_2 = i \begin{pmatrix} 0 & \mathbb{1}_2 \\ -\mathbb{1}_2 & 0 \end{pmatrix}, \\
\gamma_5 = \gamma_1\gamma_2\gamma_3\gamma_4 = -\sigma_3 \otimes \mathbb{1}_2 = \begin{pmatrix} -\mathbb{1}_2 & 0 \\ 0 & \mathbb{1}_2 \end{pmatrix},
\end{aligned} \tag{5.3.2}$$

where $\sigma_1, \sigma_2, \sigma_3$ are the Pauli matrices.

$SO(5)$ commutation relations are given in the standard form in 4-dimensional spinor representation

$$[G_{ab}, G_{cd}] = i(\delta_{ac}G_{bd} + \delta_{bd}G_{ac} - \delta_{ad}G_{bc} - \delta_{bc}G_{ad}) . \tag{5.3.3}$$

Let us form the Hilbert space $\mathcal{H}_n$ as

$$\mathcal{H}_n = (\mathbb{C}^4 \otimes ... \otimes \mathbb{C}^4)_{sym} . \tag{5.3.4}$$

This is the n-fold symmetric tensor product of $\mathbb{C}^4$. $\mathcal{H}_n$ is the carrier space of the $(0, n)$ irreducible representations of $SO(5)$ and has the dimension

$$N = \dim(0, n) = \frac{1}{6}(n + 1)(n + 2)(n + 3) . \tag{5.3.5}$$

Fuzzy S^4 [23, 24] is constructed such that its "coordinates" are matrices, X_a acting on $\mathcal{H}_n$. Thus, we can define X_a as follows

$$X_a = (\gamma_a \otimes \mathbb{1}_4 \otimes ... \otimes \mathbb{1}_4 + ... + \mathbb{1}_4 \otimes ... \otimes \mathbb{1}_4 \otimes \gamma_a) . \tag{5.3.6}$$

X_a are $N \times N$ Hermitian matrices with N given in (5.3.5), satisfying

$$X_aX_a = n(n + 4)\mathbb{1}_n , \tag{5.3.7}$$

$$\epsilon^{abcde}X_aX_bX_cX_d = 8(n + 2)X_e , \tag{5.3.8}$$

where the equation (5.3.7) gives the radius of fuzzy S^4 as

$$r_n = \sqrt{n(n+4)}\,. \tag{5.3.9}$$

The commutation relation of fuzzy S^4 is given as

$$[X_a, X_b] = 4iM_{ab}\,, \tag{5.3.10}$$

where M_{ab} are generators of $SO(5)$ in the $(0, n)$ irreducible representation. They satisfy the $SO(5)$ algebra

$$[M_{ab}, M_{cd}] = 4i(\delta_{ac}M_{bd} + \delta_{bd}M_{ac} - \delta_{ad}M_{bc} - \delta_{bc}M_{ad})\,. \tag{5.3.11}$$

The commutation relation of M_{ab} and X_c is

$$[M_{ab}, X_c] = 4i(\delta_{ac}X_b - \delta_{bc}X_a)\,, \tag{5.3.12}$$

which shows that X_a transform as vectors of $SO(5)$.

5.4 A Configuration with Collective Time Dependence and Fuzzy 4 and Fuzzy 2 Spheres

We use fuzzy S^4 and fuzzy S^2 configurations to build an ansatz for the matrices X_i $(i : 1...9)$ with collective time dependence. In particular, we take

$$\begin{aligned} X_a &= r(t)\tilde{X}_a\,, \qquad a = 1, ..., 5\,, \\ X_b &= y(t)\tilde{X}_b\,, \qquad b = 6, ..., 8\,, \\ X_9 &= 0\,, \end{aligned} \tag{5.4.1}$$

where $r(t)$ and $y(t)$ are time dependent real functions. Here $\tilde{X}_a$ are fuzzy S^4 matrices which are given in equation (5.3.6) and their dimension is given in equation (5.3.5). $\tilde{X}_b$ are fuzzy S^2 matrices which are taken as spin-j irreducible representations of $SU(2)$ with the dimension $2j + 1$. These matrices must have the same dimension $N \times N$. Thus, we have the following consistency condition

$$\begin{aligned} 2j + 1 &= \frac{1}{6}(n+1)(n+2)(n+3) \\ j &= \frac{1}{12}n(n^2 + 6n + 11)\,, \end{aligned} \tag{5.4.2}$$

for the levels (i.e. matrix sizes) of fuzzy S^4 and fuzzy S^2. Substituting the ansatz (5.4.1) into the action (5.1.1) and performing the trace operation we find the corresponding reduced effective action. The corresponding Lagrangians are

$$L_n = c_1\dot{r}^2 + c_2\dot{y}^2 - 8c_1r^4 - c_2y^4 - c_1\mu_1^2r^2 - c_2\mu_2^2y^2 - c_3r^2y^2\,. \tag{5.4.3}$$

Here we have used normalized trace $\mathrm{Tr}_N = \frac{1}{N}\,\mathrm{Tr}$. The values of the coefficients c_1, c_2, c_3 appearing in (5.4.3) are given in the table 5.1 at different values of n from $n = 1$ to $n = 6$. In other words, we have obtained a family of effective actions by using the ansatz (5.4.1) at the matrix levels $N = 4, 10, 20, 35, 56, 84$.

	$n=1$	$n=2$	$n=3$	$n=4$	$n=5$	$n=6$
c_1	2.5	6	10.5	16	22.5	30
c_2	1.88	12.38	49.88	153	391.88	881.88
c_3	21	207.66	1080.38	3970.31	11691.15	29493.06

Table 5.1

Corresponding Hamiltonian is

$$H = \frac{p_r^2}{4c_1} + \frac{p_y^2}{4c_2} + 8c_1r^4 + c_2y^4 + c_1\mu_1^2r^2 + c_2\mu_2^2y^2 + c_3r^2y^2 + 2c_1\,. \tag{5.4.4}$$

The constant term $2c_1$ is included here to ensure that the minimum energy is zero. Stability analysis given in the next section will reveal how the term $2c_1$ comes about.

The equations of motion are

$$\begin{aligned}
\dot{r} &= \frac{p_r}{2c_1}\,,\\
\dot{y} &= \frac{p_y}{2c_2}\,,\\
\dot{p_r} &= -32c_1r^3 - 2c_1\mu_1^2r - 2c_3ry^2\,,\\
\dot{p_y} &= -4c_2y^3 - 2c_2\mu_2^2y - 2c_3r^2y\,,
\end{aligned} \tag{5.4.5}$$

which describe a non-linear system of coupled differential equations. μ_1 and μ_2 are essentially free parameters. To probe the chaotic dynamics, we consider the possibility that mass parameters could also be tachyonic, in particular we focus on the choice $\mu_1^2 = -8$ and $\mu_2^2 = 1$. Other choices can be made and can have non-trivial effects on the chaotic dynamics, but several essential features appear to be the same.

5.5 Stability Analysis

The fixed points of the system described by Hamiltonian (5.4.4) are found by equating the Hamiltonian equations of motion (5.4.5) to zero:

$$\begin{aligned} \frac{p_r}{2c_1} &= 0\,, \\ \frac{p_y}{2c_2} &= 0\,, \\ -32c_1r^3 - 2c_1\mu_1^2 r - 2c_3 r y^2 &= 0\,, \\ -4c_2y^3 - 2c_2\mu_2^2 y - 2c_3 r^2 y &= 0\,. \end{aligned} \tag{5.5.1}$$

First two of the equations are trivially solved by $p_r = p_y = 0$. Solutions of the remaining two algebraic equations for r and y are found using Mathematica to be

$$(r,y) = \left\{ \Big(0,0\Big), \Big(\pm\frac{1}{\sqrt{2}},0\Big), \Big(0,\pm\frac{i}{\sqrt{2}}\Big), \Big(\pm f_1, \pm f_2\Big), \Big(\pm f_1, \mp f_2\Big) \right\}\,, \tag{5.5.2}$$

where

$$f_1 = \sqrt{\frac{c_2(16c_1+c_3)}{32c_1c_2-c_3^2}}\,, \quad f_2 = 2i\sqrt{\frac{2c_1(2c_2+c_3)}{32c_1c_2-c_3^2}}\,. \tag{5.5.3}$$

For the values of c_1, c_2, c_3 given in table 5.1 for $n = 1, ..., 6$, f_1 and f_2 in (5.5.3) form complex sets, therefore the only real solutions for r and y giving the fixed points are

$$(r,y,p_r,p_y) = \left\{ \Big(0,0,0,0\Big), \Big(\frac{1}{\sqrt{2}},0,0,0\Big), \Big(-\frac{1}{\sqrt{2}},0,0,0\Big) \right\}\,. \tag{5.5.4}$$

The energies of the fixed points can be found by substituting these solutions into the Hamiltonian

$$\begin{aligned} E_1^F &= E^F(0,0,0,0) = 2c_1\,, \\ E_2^F &= E^F\left(\frac{1}{\sqrt{2}},0,0,0\right) = 0\,, \\ E_3^F &= E^F\left(-\frac{1}{\sqrt{2}},0,0,0\right) = 0\,. \end{aligned} \tag{5.5.5}$$

These energies are indeed the values of the potential at the critical points. We see that without the addition of the last term $2c_1$ to the Hamiltonian in (5.4.4) we would have found $E_2^F = E_3^F = -2c_1$.

In order to study the stability of the system at these critical points, we may proceed as follows[15]. First let us label the phase space coordinates as $(x_1, x_2, x_3, x_4) = (r, y, p_r, p_y)$ for notational ease. Correspondingly left hand side of all equations in

(5.4.5) are denoted as $(\dot{x}_1, \dot{x}_2, \dot{x}_3, \dot{x}_4)$. From the derivatives of $\dot{x}_\alpha$ $(\alpha : 1, ..., 4)$ with respect to x_β we may form the Jacobian matrix $J_{\alpha\beta} = \frac{\partial \dot{x}_\alpha}{\partial x_\beta}$ and it reads

$$J(r, y) = \begin{pmatrix} 0 & 0 & \frac{1}{2c_1} & 0 \\ 0 & 0 & 0 & \frac{1}{2c_2} \\ J_{31} & -4c_3 ry & 0 & 0 \\ -4c_3 ry & J_{42} & 0 & 0 \end{pmatrix} , \tag{5.5.6}$$

where

$$\begin{aligned} J_{31} &= -96c_1 r^2 - 2c_3 y^2 + 16c_1 \,, \\ J_{42} &= -12c_2 y^2 - 2c_3 r^2 - 2c_2 \,. \end{aligned} \tag{5.5.7}$$

Eigenvalues of the Jacobian $J_{\alpha\beta}$ are used to determine the stability of the corresponding fixed points. According to the results given in [15, 25] we have,

i) If at least one real positive eigenvalue exists, the corresponding fixed point is unstable.

ii) If all real eigenvalues are negative, the corresponding fixed point is stable.

iii) If there are no real eigenvalues, the corresponding fixed point may be stable or unstable depending on the higher order terms, and this is the borderline case.

The eigenvalues of $J_{\alpha\beta}$ for the fixed points in (5.5.4) are

$$\begin{aligned} \lambda_1 &= \lambda(0,0,0,0) = (-i, i, -2\sqrt{2}, 2\sqrt{2}) \,, \\ \lambda_2 &= \lambda\left(\frac{1}{\sqrt{2}}, 0, 0, 0\right) = \left(-4i, 4i, \frac{-i\sqrt{2c_2 + c_3}}{\sqrt{2c_2}}, \frac{i\sqrt{2c_2 + c_3}}{\sqrt{2c_2}}\right) , \\ \lambda_3 &= \lambda\left(-\frac{1}{\sqrt{2}}, 0, 0, 0\right) = \lambda_2 \,. \end{aligned} \tag{5.5.8}$$

Therefore, we conclude that $(0, 0, 0, 0)$ is an unstable fixed point while $\left(\pm\frac{1}{\sqrt{2}}, 0, 0, 0\right)$ are borderline cases for deciding on the issue of stability as all the eigenvalues of $J_{\alpha\beta}$ are purely imaginary. Higher order analysis is required to identify the stability at these points. Here, we are not going to pursue it further as we can extract sufficiently illuminating results regarding the chaotic dynamics already at this level of the analysis.

5.6 Numerical Results and Chaos

We pick the initial conditions as follows. We initially take $y = 0$. Evaluating the Hamiltonian at this point gives

$$H\Big|_{y=0} = \underbrace{\frac{p_r^2}{4c_1}}_{k_1} + \underbrace{\frac{p_y^2}{4c_2}}_{k_2} + \underbrace{8c_1r^4 - 8c_1r^2 + 2c_1}_{k_3}, \tag{5.6.1}$$

where we divide the Hamiltonian into three parts. We pick three random numbers giving the energy as $E = k_1 + k_2 + k_3$. From these random numbers, we obtain p_r and p_y as

$$p_r = \sqrt{4c_1k_1}\,, \quad p_y = \sqrt{4c_2k_2}\,. \tag{5.6.2}$$

Consequently, r is found as

$$r = \left\{ \pm \left(\frac{1 + 2\sqrt{\frac{k_3}{8c_1}}}{2} \right)^{\frac{1}{2}}, \pm \left(\frac{1 - 2\sqrt{\frac{k_3}{8c_1}}}{2} \right)^{\frac{1}{2}} \right\}. \tag{5.6.3}$$

We choose to work with the upper sign in (5.6.3). Then we have

$$r_1 = \left(\frac{1 + 2\sqrt{\frac{k_3}{8c_1}}}{2} \right)^{\frac{1}{2}}, \quad r_2 = \left(\frac{1 - 2\sqrt{\frac{k_3}{8c_1}}}{2} \right)^{\frac{1}{2}}, \tag{5.6.4}$$

where r_1 is always real and r_2 is either real or imaginary. When r_2 is imaginary, we take $r = r_1$. On the other hand, when both r_1, r_2 are real, we randomly choose one of them with equal probability. In this way, we choose all initial conditions as real and positive numbers.

5.6.1 Poincaré Sections

In figure 5.1 we have plotted the Poincaré sections on $p_r - r$ plane at $y = 0$. The left hand side column of the given plots i.e. figure 5.1 (a,c,e,g,i,k) show the Poincaré sections at the energy $2c_1$ of the unstable critical point $(0, 0, 0, 0)$ for $n = 1, 2, ..., 6$, these energies are given respectively as $E = 5, 12, 21, 32, 45, 60$. We observe from these Poincaré sections that the phase space is essentially filled by quasi periodic orbits and no chaotic dynamics appears. From the plots given in the right hand side i.e.

figure 5.1 (b,d,f,h,j,l) which are at energies $E = 6, 15, 22, 34, 47, 63$ at $n = 1, 2, ..., 6$ respectively, clearly shows the transition in the system to significantly chaotic behavior due to significant number of randomly spread points covering some or all of the Poincaré sections, although there are still some KAM tori present. Plotted Poincaré sections are due to 25 different initial condition sets. The reason of the plots not being symmetric with respect to p_r axis is due to the fact that we initially take only positive initial conditions, and hence the motion always starts in the positive r, p_r plane.

5.6.2 Lyapunov Spectrum

We also determined the Lyapunov spectrum of the system at $n = 1, ..., 6$ at the respective fixed point energies and at energies slightly larger than these to probe the transition of the system from non-chaotic to chaotic behavior. In figure 5.2 (a-l) time series of the Lyapunov exponents are given. Each time series plot is the result of averaging of the Lyapunov exponents over 40 randomly chosen initial conditions. The plots given in the left hand side i.e. figure 5.2 (a,c,e,g,i,k) are the Lyapunov exponents at the fixed point energies $2c_1$. We see that, all the Lyapunov exponents approach to zero value indicating that the system is not chaotic at the fixed point energy. The plots given in the right hand side of figure 5.2 (b,d,f,h,j,l) show that there is a positive Lyapunov exponent which is a definitive indicator of presence of chaotic dynamics. We also observe that the sum of the Lyapunov exponents add up to zero as is expected from a Hamiltonian system.

5.6.3 Largest Lyapunov Exponents versus Energy

In order to understand the structure of the chaotic dynamics in these systems, we have performed a numerical study to reveal how the largest Lyapunov exponent responds to increase in the energy given in figure 5.3.

We find that the response of the largest Lyapunov exponent above the critical value of the energy (i.e. above the critical energies for which they become non-zero) appears to be changing logarithmically with energy except for $n = 1$. The latter is a special case in which the dynamics is chaotic only for a particular range of energies.

We find that the functional form

$$\lambda_n(E) = a_n \log(E) + b_n \tag{5.6.5}$$

fits very well with the numerical results with the coefficients provided in the table below.

n	a_n	b_n
2	0.3448	-0.8369
3	0.3517	-0.7926
4	0.3716	-0.8183
5	0.5557	-2.197
6	0.5826	-2.47

Table 5.2

We see from table 5.2 that for $n = 2, 3, 4$ there are only slight variations in the values of a_n and b_n, indicating that the largest Lyapunov exponents in these models at the levels show essentially the same universal response: to the increasing. The same conclusions can be made for $n = 5, 6$. However, we cannot immediately infer if and how this pattern could alter with increasing n, although it seems reasonable to think that a similar logarithmic dependence of the largest Lyapunov exponents on energy could be expected.

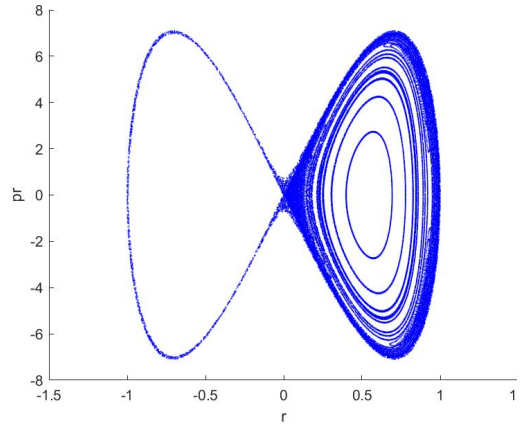

(a) $n = 1, E = 5$

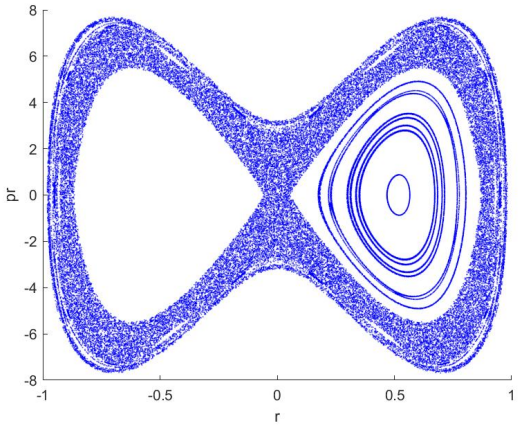

(b) $n = 1, E = 6$

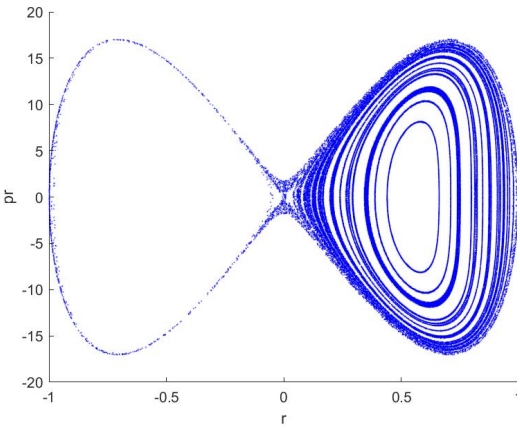

(c) $n = 2, E = 12$

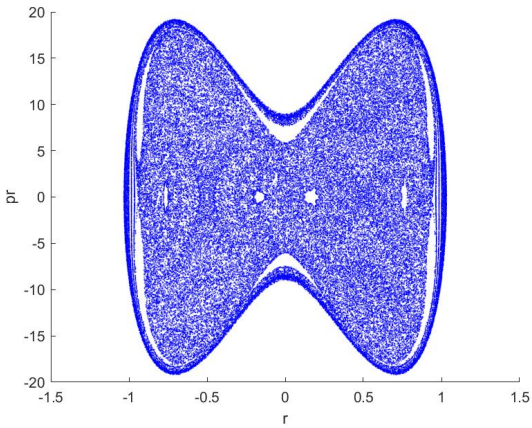

(d) $n = 2, E = 15$

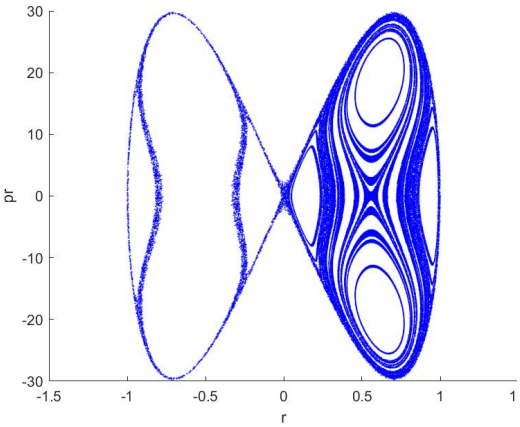

(e) $n = 3, E = 21$

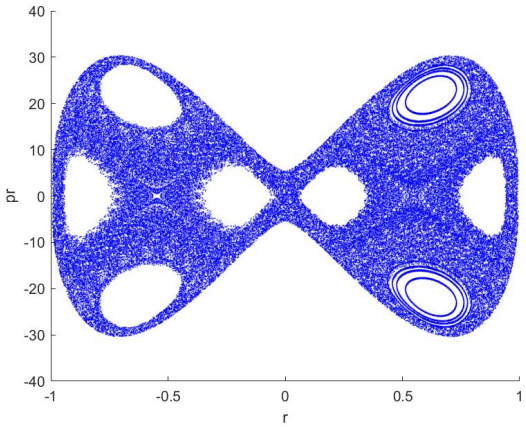

(f) $n = 3, E = 22$

Figure 5.1: Poincarè sections for $n = 1, 2, 3$

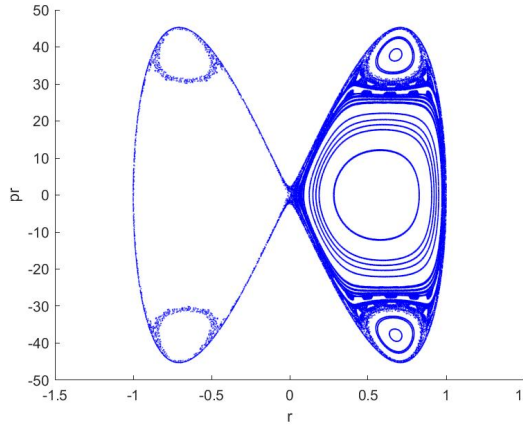

(g) $n = 4, E = 32$

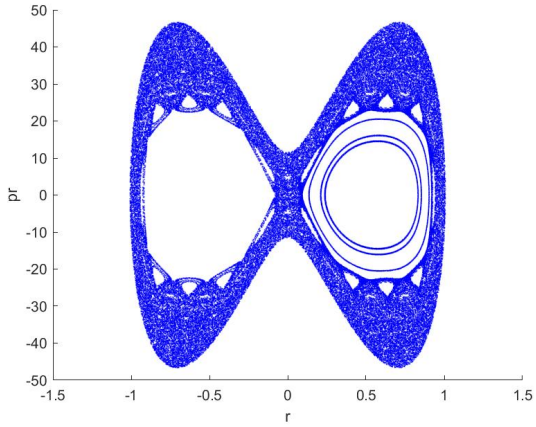

(h) $n = 4, E = 34$

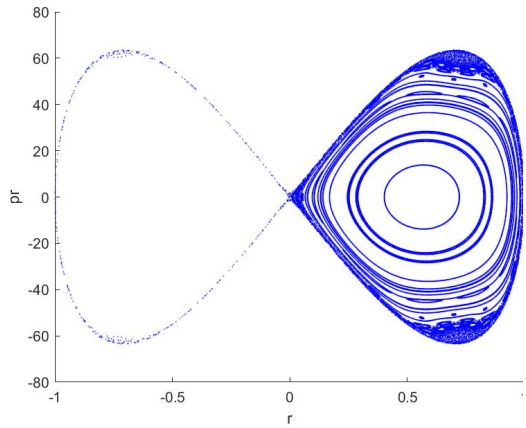

(i) $n = 5, E = 45$

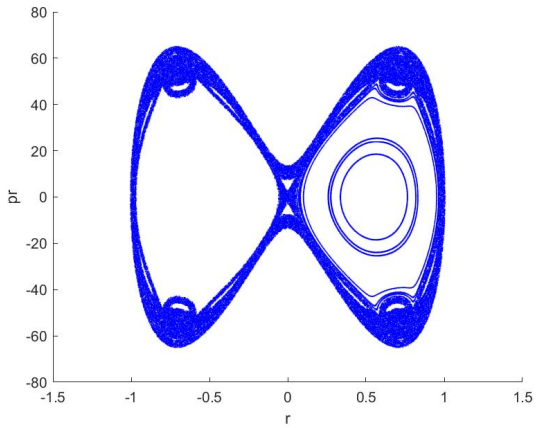

(j) $n = 5, E = 47$

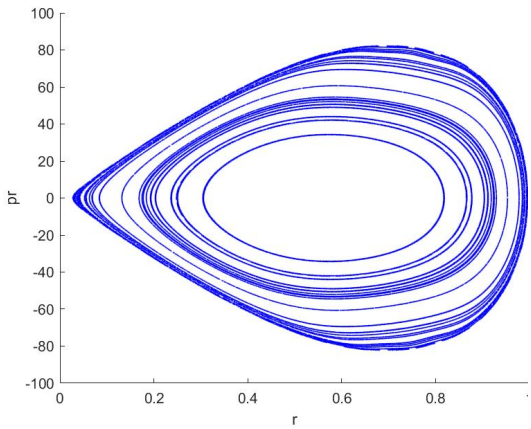

(k) $n = 6, E = 60$

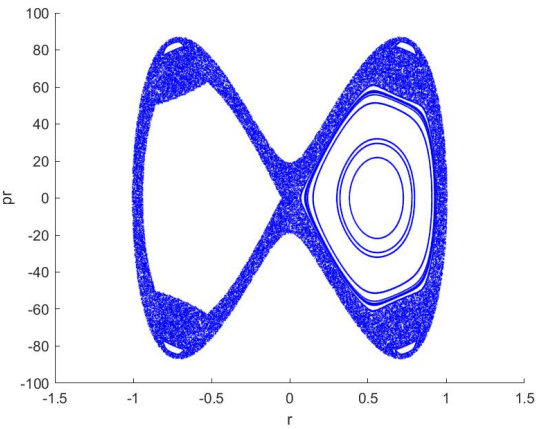

(l) $n = 6, E = 63$

Figure 5.1: Poincarè sections for $n = 4, 5, 6$

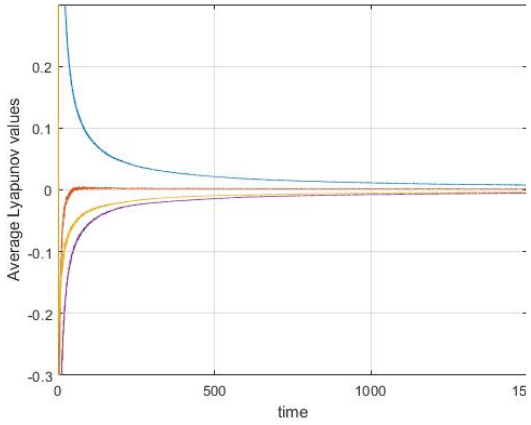

(a) $n = 1, E = 5$

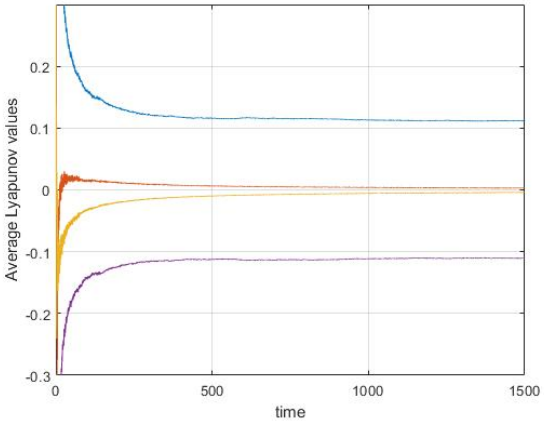

(b) $n = 1, E = 6$

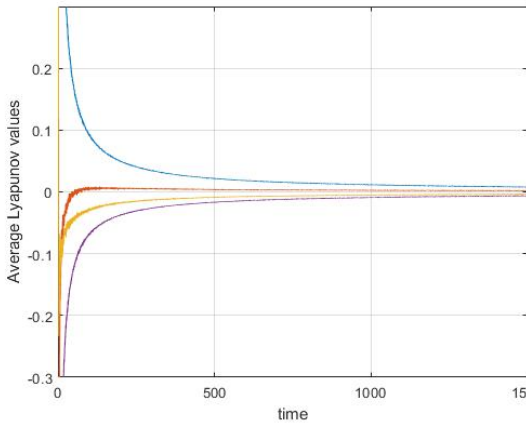

(c) $n = 2, E = 12$

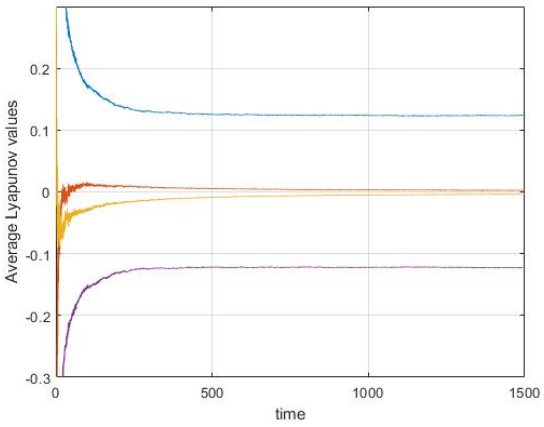

(d) $n = 2, E = 15$

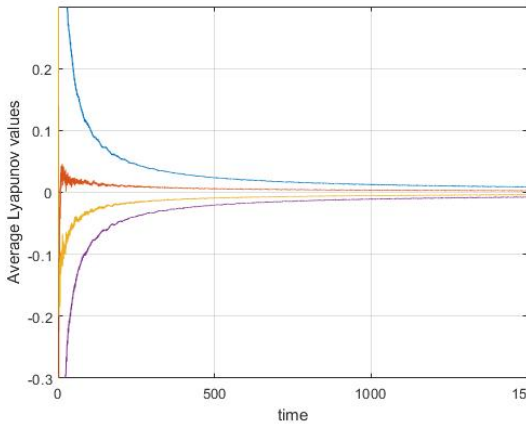

(e) $n = 3, E = 21$

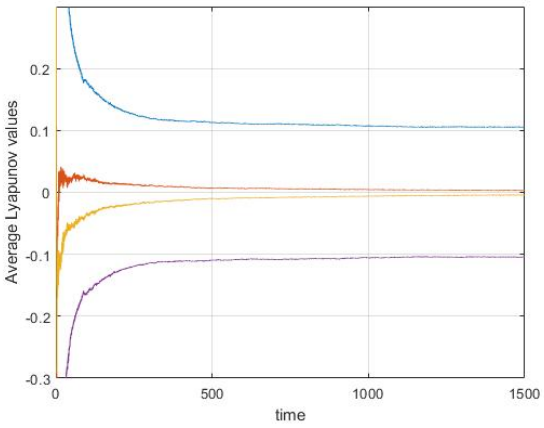

(f) $n = 3, E = 22$

Figure 5.2: Lyapunov exponents vs. time for $n = 1, 2, 3$

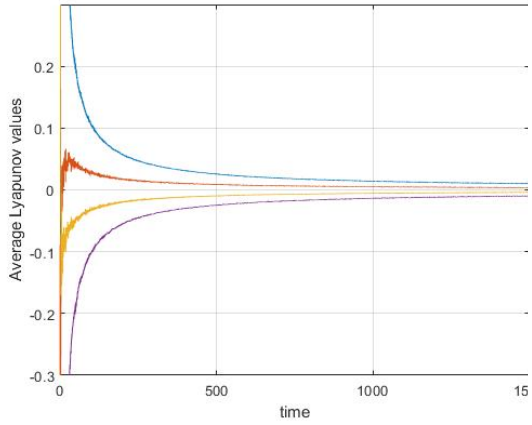

(g) $n = 4, E = 32$

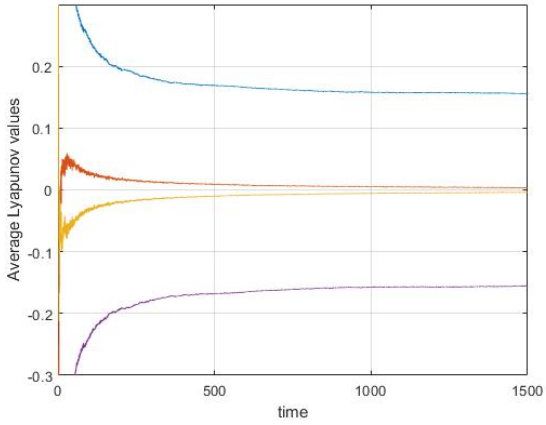

(h) $n = 4, E = 34$

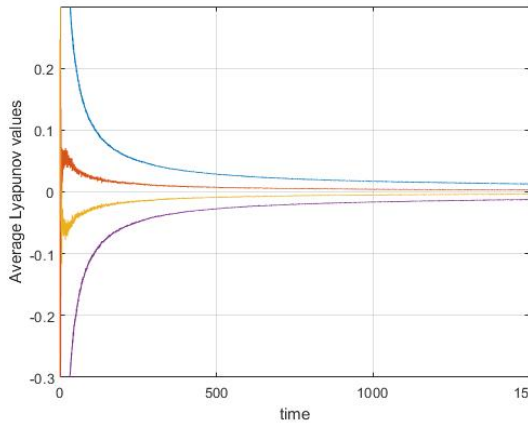

(i) $n = 5, E = 45$

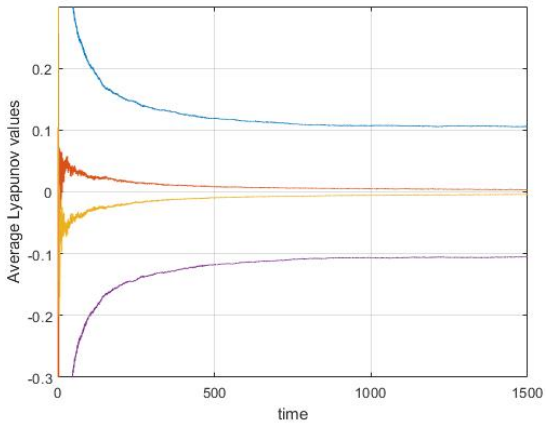

(j) $n = 5, E = 47$

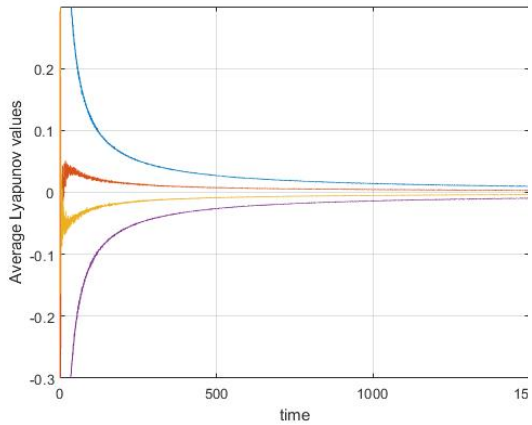

(k) $n = 6, E = 60$

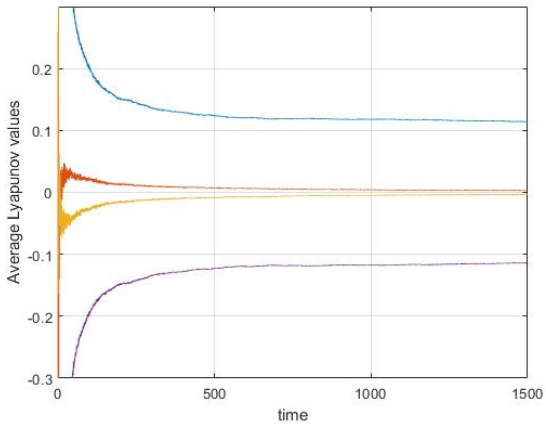

(l) $n = 6, E = 63$

Figure 5.2: Lyapunov exponents vs. time for $n = 4, 5, 6$

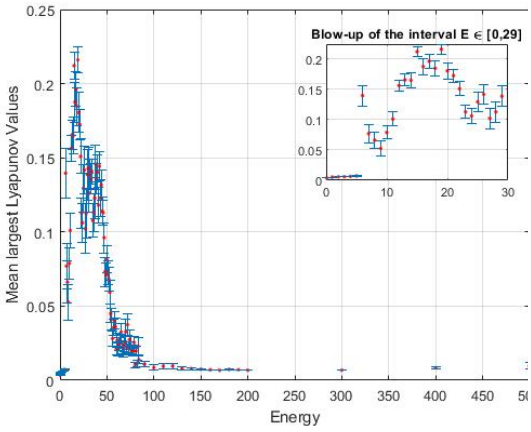

(a) $n = 1$

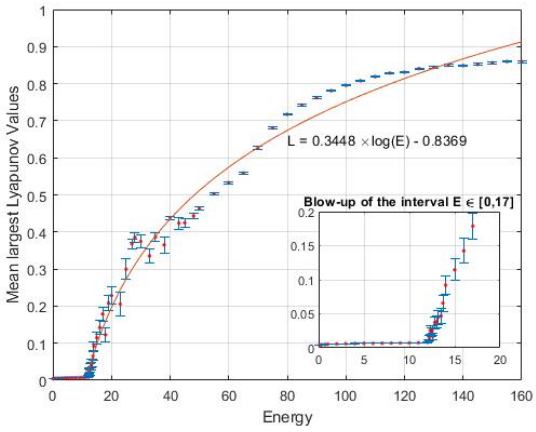

(b) $n = 2$

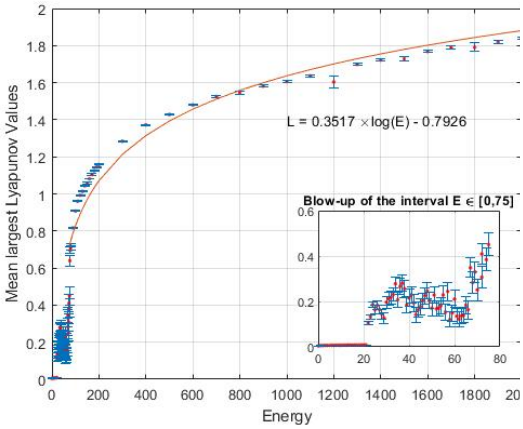

(c) $n = 3$

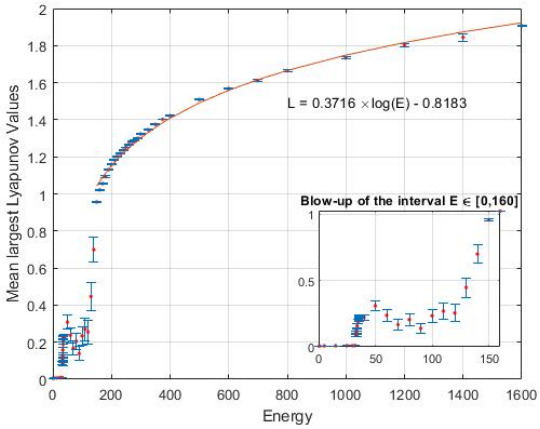

(d) $n = 4$

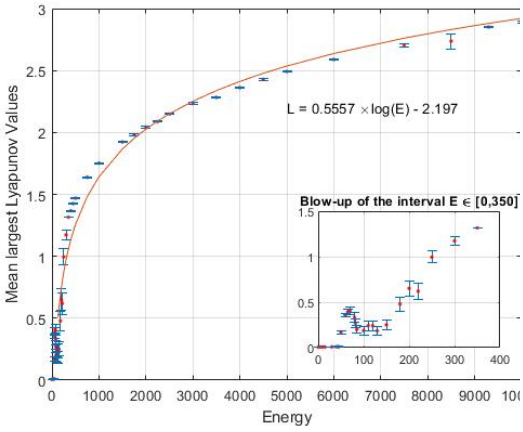

(e) $n = 5$

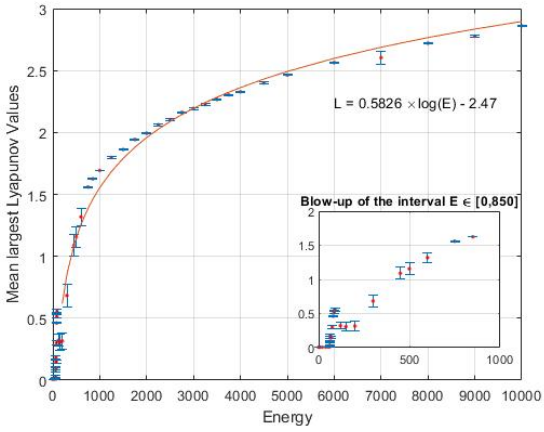

(f) $n = 6$

Figure 5.3: Mean largest Lyapunov exponents for different energy values

CHAPTER 6

CONCLUSION

In this thesis we have presented the results of two original research projects. The main theme of the works have been the exploration of chaotic dynamics emerging from matrix gauge theories. We first gave a review of the bosonic part of the BFSS matrix model and a related two matrix model in chapter 2. For the latter, we have reproduced numerical analysis given in [8] using our own code and revealed the chaotic dynamics. In particular, we have demonstrated and verified how a conserved component of angular momentum, p_ϕ, impact the chaotic dynamics, and how the system ceases to transit from chaos to no-chaos as the value of p_ϕ is modified as originally discussed in [8].

In chapter 3 we have focused our attention on the Yang-Mills Chern-Simons matrix model with two matrices which is a variant of the two matrix model reviewed in chapter 2, supplemented by the Chern-Simons term. The latter is first order in time derivatives and we presented a careful and detailed analysis of the formulation of this model. In this model too p_ϕ is conserved. Nevertheless, there is another parameter in the model, namely the Chern-Simons coupling or the Chern-Simons level which have quantized for non-abelian Chern-Simons theories. For a set of values of p_ϕ we analyzed how the Chern-Simons level $k \in \mathbb{Z}$ affects the chaos. From the Poincaré sections and Lyapunov spectrum we have found that for the completely chaotic case of $p_\phi = 0$ without the Chern-Simons term, increasing the value of $|k|$ results in driving the system to be less chaotic. We have seen from the largest Lyapunov exponents in figure 3.4a that the chaos is sustained quite well in the range $|k| \leq 10$, while the system transits to non-chaotic phase for $|k| \geq 10$ essentially. At $p_\phi = 1$, chaotic dynamics of the model is still sustained at the range $-6 < k < 2$ of values of k as

can be seen from the figure 3.4b. In fact, we see that there is even an increase in chaos for $-4 \leq k \leq -1$ which is seen from figure 3.4b, and also figure 3.4c. The reason for this new effect can already be understood from (3.7.1), which tells us that for $-4 \leq k \leq -1$ increasing $|k|$ amounts to increasing the energy of the two matrix model without the Chern-Simons term, leading to larger positive Lyapunov exponents as an indicator of more chaos.

Finally, at $p_\phi = 2$, we see that the system behaves in an almost non-chaotic manner regardless of the value of k, and even more so with increasing values of $|k|$. This is to be expected as the pure Yang-Mills model also ceases to be chaotic essentially for $p_\phi > 2$ and the same profile is sustained for the model with the Chern-Simons term too.

We have examined the effects of mass term on the structure of two matrix model in chapter 4. The Poincaré sections and Lyapunov spectrum have demonstrated the fact that increase of the mass term suppresses the chaos.

Chapter 5 has devoted to the study of a double mass deformation of the BFSS model configurations with collective time dependence to obtain a family of effective actions in this model. After performing an analysis of the fixed points and their stability for the corresponding effective Hamiltonians we have directed our studies to explore the transition to chaos once the system exceeds the energy of the unstable fixed point. Poincaré sections and Lyapunov spectrum are obtained at fuzzy sphere levels $n = 1, ..., 6$ and reveals the transition to chaos in these systems after the fixed point energy is exceeded. Finally, we have shown that largest Lyapunov exponents vary logarithmically with the energy of the system.

REFERENCES

[1] T. Banks, W. Fischler, S. H. Shenker, and L. Susskind, "M theory as a matrix model: A conjecture," *Phys. Rev. D*, vol. 55, pp. 5112–5128, Apr 1997.

[2] B. Ydri, *Matrix Models of String Theory*. 2053-2563, IOP Publishing, 2018.

[3] E. Kiritsis, *String theory in a nutshell*, vol. 21. Princeton University Press, 2019.

[4] B. Zwiebach, *A first course in string theory*. Cambridge University Press, 2004.

[5] C. V. Johnson, *D-branes*. Cambridge University Press, 2002.

[6] H. Năstase, *Introduction to the AdS/CFT Correspondence*. Cambridge University Press, 2015.

[7] M. Ammon and J. Erdmenger, *Gauge/Gravity Duality: Foundations and Applications*. Cambridge University Press, 2015.

[8] D. Berenstein and D. Kawai, "Smallest matrix black hole model in the classical limit," *Phys. Rev. D*, vol. 95, p. 106004, May 2017.

[9] Y. Asano, D. Kawai, and K. Yoshida, "Chaos in the BMN matrix model," *Journal of High Energy Physics*, vol. 2015, p. 191, Jun 2015.

[10] G. Gur-Ari, M. Hanada, and S. H. Shenker, "Chaos in classical d0-brane mechanics," *Journal of High Energy Physics*, vol. 2016, p. 91, Feb 2016.

[11] A. P. Balachandran, G. Marmo, B. S. Skagerstam, and A. Stern, *Classical Topology and Quantum States*. WORLD SCIENTIFIC, 1991.

[12] K. Başkan and S. Kürkcüoğlu, "In preparation,"

[13] K. Başkan, S. Kürkcüoğlu, O. Oktay, and C. Taşcı, "In preparation,"

[14] L. Landau, E. Lifshitz, J. Sykes, and J. Bell, *Mechanics*. Butterworth-Heinemann, Elsevier Science, 1976.

[15] E. Ott, *Chaos in Dynamical Systems*. Cambridge University Press, 2 ed., 2002.

[16] R. Hilborn, *Chaos and Nonlinear Dynamics: An Introduction for Scientists and Engineers*. Oxford University Press, 1994.

[17] S. Thornton and J. Marion, *Classical Dynamics of Particles and Systems*. Brooks/Cole, 2004.

[18] G. V. Dunne, "Aspects of Chern-Simons theory," *Aspects topologiques de la physique en basse dimension. Topological aspects of low dimensional systems Les Houches - Ecole d'Ete de Physique Theorique*, p. 177–263, 1999.

[19] H. Goldstein, C. P Poole, and J. L Safko, *Classical Mechanics (3rd Edition)*. 06 2001.

[20] J. E. Marsden and T. S. Ratiu, *Introduction to Mechanics and Symmetry: A Basic Exposition of Classical Mechanical Systems*. Springer Publishing Company, Incorporated, 2010.

[21] A. P. Balachandran, S. Kürkçüoğlu, and S. Vaidya, *Lectures on Fuzzy and Fuzzy SUSY Physics*. World Scientific, 2007.

[22] J. J. Sakurai and J. Napolitano, *Modern quantum mechanics*. Addison-Wesley, 2nd ed., international ed., 2011.

[23] Ü. H. Coşkun, S. Kürkçüoğlu, G. C. Toga, and G. Ünal, "Chaos from equivariant fields on fuzzy s4," *Journal of High Energy Physics*, vol. 2018, 12 2018.

[24] H. C. Steinacker, "One-loop stabilization of the fuzzy four-sphere via softly broken susy," *Journal of High Energy Physics*, vol. 2015, pp. 1–29, Dec 2015.

[25] S. L. Campbell and R. Haberman, *Introduction to differential equations with dynamical systems*. Princeton University Press, 2011.

[26] "Quasi-periodic motion." Encyclopedia of Mathematics. URL: `http://www.encyclopediaofmath.org/index.php?title=Quasi-periodic_motion&oldid=16781`.

[27] A. Wolf, J. B. Swift, H. Swinney, and J. A. Vastano, "Determining lyapunov exponents from a time series," *Physica D: Nonlinear Phenomena*, vol. 16, pp. 285–317, 07 1985.

[28] S. H. Strogatz, *Nonlinear dynamics and chaos: with applications to physics, biology, chemistry, and engineering*. CRC Press, 2018.

APPENDIX A

CALCULATIONS ON CHERN-SIMONS THEORY

A.1 X Matrix

The result of the matrix multiplication in (3.6.3) is

$$X = \begin{pmatrix} X_{11} & X_{12} \\ X_{21} & X_{22} \\ X_{31} & X_{32} \end{pmatrix}, \tag{A.1.1}$$

where the entries are

$$\begin{aligned}
X_{11} =& -\frac{r\sin(\alpha)\cos(\beta)\sin(\gamma)\cos(\theta)\sin(\phi)}{\sqrt{2}} - \frac{r\sin(\alpha)\cos(\beta)\cos(\gamma)\sin(\theta)\sin(\phi)}{\sqrt{2}} \\
&- \frac{r\sin(\alpha)\cos(\beta)\sin(\gamma)\cos(\phi)}{\sqrt{2}} + \frac{r\cos(\alpha)\cos(\gamma)\cos(\theta)\sin(\phi)}{\sqrt{2}} \\
&- \frac{r\cos(\alpha)\sin(\gamma)\sin(\theta)\sin(\phi)}{\sqrt{2}} + \frac{r\cos(\alpha)\cos(\gamma)\cos(\phi)}{\sqrt{2}}, \\
X_{21} =& \frac{r\cos(\alpha)\cos(\beta)\sin(\gamma)\cos(\theta)\sin(\phi)}{\sqrt{2}} + \frac{r\cos(\alpha)\cos(\beta)\cos(\gamma)\sin(\theta)\sin(\phi)}{\sqrt{2}} \\
&+ \frac{r\cos(\alpha)\cos(\beta)\sin(\gamma)\cos(\phi)}{\sqrt{2}} - \frac{r\sin(\alpha)\sin(\gamma)\sin(\theta)\sin(\phi)}{\sqrt{2}} \\
&+ \frac{r\sin(\alpha)\cos(\gamma)\cos(\theta)\sin(\phi)}{\sqrt{2}} + \frac{r\sin(\alpha)\cos(\gamma)\cos(\phi)}{\sqrt{2}}, \\
X_{31} =& \frac{r\sin(\beta)\sin(\gamma)\cos(\theta)\sin(\phi)}{\sqrt{2}} + \frac{r\sin(\beta)\cos(\gamma)\sin(\theta)\sin(\phi)}{\sqrt{2}} \\
&+ \frac{r\sin(\beta)\sin(\gamma)\cos(\phi)}{\sqrt{2}},
\end{aligned} \tag{A.1.2}$$

$$
\begin{aligned}
X_{12} =& -\frac{r\sin(\alpha)\cos(\beta)\sin(\gamma)\cos(\theta)\cos(\phi)}{\sqrt{2}} - \frac{r\sin(\alpha)\cos(\beta)\cos(\gamma)\sin(\theta)\cos(\phi)}{\sqrt{2}} \\
&+ \frac{r\sin(\alpha)\cos(\beta)\sin(\gamma)\sin(\phi)}{\sqrt{2}} + \frac{r\cos(\alpha)\cos(\gamma)\cos(\theta)\cos(\phi)}{\sqrt{2}} \\
&- \frac{r\cos(\alpha)\sin(\gamma)\sin(\theta)\cos(\phi)}{\sqrt{2}} - \frac{r\cos(\alpha)\cos(\gamma)\sin(\phi)}{\sqrt{2}}, \\
X_{22} =& \frac{r\cos(\alpha)\cos(\beta)\sin(\gamma)\cos(\theta)\cos(\phi)}{\sqrt{2}} + \frac{r\cos(\alpha)\cos(\beta)\cos(\gamma)\sin(\theta)\cos(\phi)}{\sqrt{2}} \\
&- \frac{r\cos(\alpha)\cos(\beta)\sin(\gamma)\sin(\phi)}{\sqrt{2}} + \frac{r\sin(\alpha)\cos(\gamma)\cos(\theta)\cos(\phi)}{\sqrt{2}} \\
&- \frac{r\sin(\alpha)\sin(\gamma)\sin(\theta)\cos(\phi)}{\sqrt{2}} - \frac{r\sin(\alpha)\cos(\gamma)\sin(\phi)}{\sqrt{2}}, \\
X_{32} =& \frac{r\sin(\beta)\sin(\gamma)\cos(\theta)\cos(\phi)}{\sqrt{2}} + \frac{r\sin(\beta)\cos(\gamma)\sin(\theta)\cos(\phi)}{\sqrt{2}} \\
&- \frac{r\sin(\beta)\sin(\gamma)\sin(\phi)}{\sqrt{2}}.
\end{aligned}
$$

The first column of this matrix is $\vec{\mathbf{x}}_1$ and the second column is $\vec{\mathbf{x}}_2$. We also use this matrix for the evaluation of the metric.

A.2 Metric

The metric of the two matrix model with Chern-Simons terms is more general than the two matrix model metric since we have used the full Euler angles and additional parameters appear. We have used this metric in the coordinate transformation for the $(r, \theta, \phi, \alpha, \beta, \gamma)$ coordinates. The metric is found by the equation $g_{ij} = \mathrm{Tr}\big(\partial_i X^\dagger \partial_j X\big)$ as follows

$$
g_{ij} = \begin{pmatrix}
1 & 0 & 0 & 0 & 0 & 0 \\
0 & \frac{r^2}{2} & \frac{1}{2}r^2\sin(\theta) & \frac{1}{2}r^2\cos(\beta) & 0 & \frac{r^2}{2} \\
0 & \frac{1}{2}r^2\sin(\theta) & r^2 & r^2\cos(\beta)\sin(\theta) & 0 & r^2\sin(\theta) \\
0 & \frac{1}{2}r^2\cos(\beta) & g_{34} & g_{44} & g_{45} & r^2\cos(\beta) \\
0 & 0 & 0 & g_{54} & g_{55} & 0 \\
0 & \frac{r^2}{2} & r^2\sin(\theta) & r^2\cos(\beta) & 0 & r^2
\end{pmatrix}, \quad \text{(A.2.1)}
$$

where

$$
\begin{aligned}
g_{34} =& r^2 \cos(\beta)\sin(\theta)\,, \\
g_{44} =& -\frac{1}{8}r^2\cos(2\beta)\cos(2(\gamma+\theta)) - \frac{1}{16}r^2\cos(2(\beta-\gamma)) \\
& -\frac{1}{16}r^2\cos(2(\beta+\gamma)) + \frac{1}{4}r^2\cos(2\beta) \\
& +\frac{1}{4}r^2\cos(\theta)\cos(2\gamma+\theta) + \frac{3r^2}{4}\,, \\
g_{54} =& -\frac{1}{2}r^2\sin(\beta)\cos(\theta)\sin(2\gamma+\theta)\,, \\
g_{45} =& -\frac{1}{2}r^2\sin(\beta)\cos(\theta)\sin(2\gamma+\theta)\,, \\
g_{55} =& -\frac{1}{4}r^2\cos(2(\gamma+\theta)) - \frac{1}{4}r^2\cos(2\gamma) + \frac{r^2}{2}\,.
\end{aligned}
\tag{A.2.2}
$$

The inverse metric $g^{-1}_{ij} = g^{ij}$ is

$$
\begin{pmatrix}
1 & 0 & 0 & 0 & 0 & 0 \\
0 & \frac{4}{r^2} & 0 & 0 & 0 & -\frac{2}{r^2} \\
0 & 0 & \frac{\sec^2(\theta)}{r^2} & 0 & 0 & -\frac{\sec(\theta)\tan(\theta)}{r^2} \\
0 & 0 & 0 & g^{44} & g^{45} & g^{46} \\
0 & 0 & 0 & g^{54} & g^{55} & g^{56} \\
0 & -\frac{2}{r^2} & -\frac{\sec(\theta)\tan(\theta)}{r^2} & g^{64} & g^{65} & g^{66}
\end{pmatrix}\,,
\tag{A.2.3}
$$

where

$$
\begin{aligned}
g^{44} =& -\frac{(\cos(2\gamma)+\cos(2(\gamma+\theta))-2)\csc^2(\beta)\csc^2(\theta)}{r^2}\,, \\
g^{45} =& \frac{2\cot(\theta)\csc(\beta)\csc(\theta)\sin(2\gamma+\theta)}{r^2}\,, \\
g^{46} =& \frac{(\cos(2\gamma)+\cos(2(\gamma+\theta))-2)\cot(\beta)\csc(\beta)\csc^2(\theta)}{r^2}\,, \\
g^{54} =& \frac{2\cot(\theta)\csc(\beta)\csc(\theta)\sin(2\gamma+\theta)}{r^2}\,, \\
g^{55} =& \frac{(\cos(2\gamma)+\cos(2(\gamma+\theta))+2)\csc^2(\theta)}{r^2}\,, \\
g^{56} =& -\frac{2\cot(\beta)\cot(\theta)\csc(\theta)\sin(2\gamma+\theta)}{r^2}\,, \\
g^{64} =& \frac{(\cos(2\gamma)+\cos(2(\gamma+\theta))-2)\cot(\beta)\csc(\beta)\csc^2(\theta)}{r^2}\,, \\
g^{65} =& -\frac{2\cot(\beta)\cot(\theta)\csc(\theta)\sin(2\gamma+\theta)}{r^2}\,, \\
g^{66} =& \frac{-(\cos(2\gamma)+\cos(2(\gamma+\theta))-2)\cot^2(\beta)\csc^2(\theta)+\sec^2(\theta)+1}{r^2}\,.
\end{aligned}
\tag{A.2.4}
$$

A.3 Angular Momentum Matrix for the Euler Rotation

In general angular velocities can be expressed in terms of Euler angles and their time derivatives as [20]

$$\begin{aligned} w_1 &= \dot{\gamma}\sin(\alpha)\sin(\beta) + \dot{\beta}\cos(\alpha)\,, \\ w_2 &= \dot{\beta}\sin(\alpha) - \dot{\gamma}\cos(\alpha)\sin(\beta)\,, \\ w_3 &= \dot{\alpha} + \dot{\gamma}\cos(\beta)\,. \end{aligned} \tag{A.3.1}$$

The kinetic energy for rigid body motion is

$$\begin{aligned} T =& \frac{1}{2} I_i w_i^2 \\ =& \frac{1}{2}(I_1 w_1^2 + I_2 w_2^2 + I_3 w_3^2) \\ =& I_1(\dot{\gamma}^2\sin^2(\alpha)\sin^2(\beta) + 2\dot{\beta}\dot{\gamma}\sin(\alpha)\cos(\alpha)\sin(\beta) + \dot{\beta}^2\cos^2(\alpha)) \\ &+ I_2(\dot{\gamma}^2\cos^2(\alpha)\sin^2(\beta) - 2\dot{\beta}\dot{\gamma}\sin(\alpha)\cos(\alpha)\sin(\beta) + \dot{\beta}^2\sin^2(\alpha)) \\ &+ I_3(2\dot{\alpha}\dot{\gamma}\cos(\beta) + \dot{\alpha}^2 + \dot{\gamma}^2\cos^2(\beta))\,, \end{aligned} \tag{A.3.2}$$

where I_i are the moment of inertia with respect to the Euler angles. By using $p_\alpha = \frac{\partial T}{\partial \dot{\alpha}}$, $p_\beta = \frac{\partial T}{\partial \dot{\beta}}$, $p_\gamma = \frac{\partial T}{\partial \dot{\gamma}}$ we have

$$\begin{aligned} p_\alpha =& I_3\left(\dot{\alpha} + \dot{\gamma}\cos(\beta)\right)\,, \\ p_\beta =& \frac{1}{2}\Big(2I_1\cos(\alpha)\left(\dot{\gamma}\sin(\alpha)\sin(\beta) + \dot{\beta}\cos(\alpha)\right) \\ &+2I_2\sin(\alpha)\left(\dot{\beta}\sin(\alpha) - \dot{\gamma}\cos(\alpha)\sin(\beta)\right)\Big)\,, \\ p_\gamma =& \frac{1}{2}\Big(2I_1\sin(\alpha)\sin(\beta)\left(\dot{\gamma}\sin(\alpha)\sin(\beta) + \dot{\beta}\cos(\alpha)\right) \\ &-2I_2\cos(\alpha)\sin(\beta)\left(\dot{\beta}\sin(\alpha) - \dot{\gamma}\cos(\alpha)\sin(\beta)\right) \\ &+2I_3\cos(\beta)\left(\dot{\alpha} + \dot{\gamma}\cos(\beta)\right)\Big)\,. \end{aligned} \tag{A.3.3}$$

Equation (A.3.3) can be written in matrix form as

$$\begin{pmatrix} p_\alpha \\ p_\beta \\ p_\gamma \end{pmatrix} = \begin{pmatrix} 0 & I_3 & I_3\cos(\beta) \\ 0 & A_{22} & A_{23} \\ I_3\cos(\beta) & A_{32} & A_{33} \end{pmatrix} \begin{pmatrix} \dot{\alpha} \\ \dot{\beta} \\ \dot{\gamma} \end{pmatrix} \tag{A.3.4}$$

where

$$
\begin{aligned}
A_{22} &= I_1 \cos^2(\alpha) + I_2 \sin^2(\alpha)\,, \\
A_{23} &= I_1 \cos(\alpha)\sin(\alpha)\sin(\beta) - I_2 \cos(\alpha)\sin(\alpha)\sin(\beta)\,, \\
A_{32} &= I_1 \cos(\alpha)\sin(\alpha)\sin(\beta) - I_2 \cos(\alpha)\sin(\alpha)\sin(\beta)\,, \\
A_{33} &= I_3 \cos^2(\beta) + I_2 \cos^2(\alpha)\sin^2(\beta) + I_1 \sin^2(\alpha)\sin^2(\beta)\,.
\end{aligned}
\tag{A.3.5}
$$

We write (A.3.4) as $P = A \cdot \dot{\Theta}$ for notational ease. The column matrix $(\dot{\alpha}, \dot{\beta}, \dot{\gamma})^T = \dot{\Theta}$ can be obtained from the equation $\dot{\Theta} = A^{-1} \cdot P$. Substituting $\dot{\alpha}, \dot{\beta}, \dot{\gamma}$ coming from this equation into (A.3.1) yields w_1, w_2, w_3 in terms of $p_\alpha, p_\beta, p_\gamma$, and we obtain the angular momentum $L_i = \frac{\partial T}{\partial w_i} = I_i w_i$ as follows

$$
\begin{aligned}
L_1 &= \sin(\alpha)(p_\gamma \csc(\beta) - p_\alpha \cot(\beta)) + p_\beta \cos(\alpha)\,, \\
L_2 &= \cos(\alpha)\csc(\beta)(p_\alpha \cos(\beta) - p_\gamma) + p_\beta \sin(\alpha)\,, \\
L_3 &= p_\alpha\,,
\end{aligned}
\tag{A.3.6}
$$

or in the matrix form

$$
\vec{\mathbf{L}} = \begin{pmatrix}
\sin(\alpha)(p_\gamma \csc(\beta) - p_\alpha \cot(\beta)) + p_\beta \cos(\alpha) \\
\cos(\alpha)\csc(\beta)(p_\alpha \cos(\beta) - p_\gamma) + p_\beta \sin(\alpha) \\
p_\alpha
\end{pmatrix}. \tag{A.3.7}
$$

APPENDIX B

METHODS OF EXAMINING CHAOS

B.1 Poincaré Sections

N dimensional phase space can be equivalently reduced to $N-1$ dimensional surface by taking the intersection of the flow in the phase space and a surface of section, which is called as Poincaré section[9, 15, 16, 17]. The flow of the phase space is seen as dots in the Poincaré section. The dynamics of the system can be examined by the pattern of these dots. In a periodic motion, the flow of the phase space intersects the surface at the same points after a while. Different initial conditions change the place of these points. Each flow for different initial conditions can be projected onto the same surface of section. In this way, Poincaré sections yield more comprehensive analysis of the dynamics. For each different initial conditions, neighboring points are formed in a periodic motion and they all form a closed contour.

Quasi-periodic motion consists of $N \geq 2$ different frequencies such that no frequency can be written as a linear combination of others by using rational coefficients. In other words, ratio of the frequencies are not rational numbers, they have to be incommensurable. Quasi-periodic motion of N frequencies can be regarded to form a phase space, which is an N-dimensional torus, which is also called the invariant torus in the context of the Kolmogorov-Arnold-Moser (KAM) theorem [15, 26]. The latter is a celebrated theorem in mathematics, which can be briefly stated as the result that for a small enough perturbation of a Hamiltonian system, there exists invariant torus of the perturbed system which is close enough to that of the unperturbed system. The details and proof of this theorem are quite complicated and beyond the scope of this thesis. Nevertheless, a simple example can briefly illustrate these remarks. If a

Hamiltonian system of say a point particle has T^2, i.e. as it invariant torus, this means that the particle exhibits quasi-periodic motion with frequency w_1 and w_2 as long as $\frac{w_1}{w_2}$ is an irrational number. The latter ensures that the trajectory of the particle never overlaps and eventually passes through every point of the invariant torus. Therefore, quasi-periodic orbits in Poincaré sections can be seen by dots forming denser closed contours. In this context, denser means that closed contours are like continuous lines instead of separated dots. These contours are usually called KAM tori. On the other hand, chaotic motion appears in Poincaré sections as randomly scattered dots.

As a simple example in which Poincaré sections can be illustrated, we may consider the two dimensional simple harmonic oscillator with the Hamiltonian

$$H = \frac{p_x^2}{2m} + \frac{p_y^2}{2m} + \frac{1}{2}k(x^2 + y^2)\,. \tag{B.1.1}$$

Let's take $m = \frac{1}{2}$ and $k = 2$, then the Hamiltonian becomes

$$H = p_x^2 + p_y^2 + x^2 + y^2\,. \tag{B.1.2}$$

The Hamiltonian equations of motion are given as

$$\dot{x} = 2p_x\,, \quad \dot{p}_x = -2x\,, \tag{B.1.3}$$

$$\dot{y} = 2p_y\,, \quad \dot{p}_y = -2y\,. \tag{B.1.4}$$

Equations of motion are integrable and this motion is well known to periodic. Therefore, we naturally expect to see a closed contour in the Poincaré section provided that sufficient number of initial conditions are used in sampling.

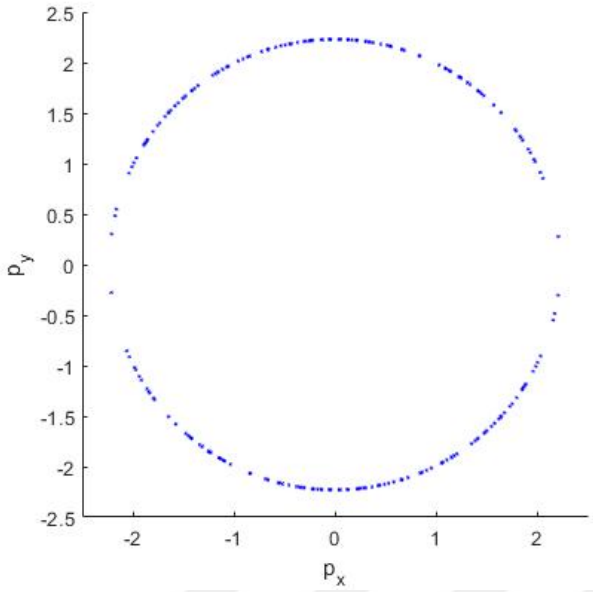

Figure B.1: Poincaré section at $E = 5$

Taking $E = 5$ and selecting initial conditions such that $(x, y) = (0, 0)$ and $p_y = \sqrt{E^2 - p_x^2}$ with p_x chosen randomly in the interval $p_x \in \left[-\sqrt{E}, \sqrt{E}\right]$ to make p_y real and using 125 different initial conditions according to this protocol, $p_x - p_y$ Poincaré section is obtained and given in figure B.1.

B.2 Lyapunov Spectrum

Lyapunov exponents[9, 27, 28] measure the sensitivity of the system to given initial conditions. Let $\mathbf{x}^i(t)$ denote an $i^{\text{th.}}$ initial condition and nearby point in the phase space be $\mathbf{x}^i(t) + \delta\mathbf{x}^i(t)$. The deviation $\delta\mathbf{x}^i(t)$ can be expressed as

$$\delta\mathbf{x}^i(t) = \delta\mathbf{x}^i(0)e^{\lambda_i t}\,, \quad i = 1, ..., N\,, \tag{B.2.1}$$

where λ_i are Lyapunov exponents for N dimensional phase space. $\delta\mathbf{x}^i(0)$ form an N dimensional infinitesimal sphere in the phase space. Time evolution of the system distorts the infinitesimal sphere into an infinitesimal ellipsoid, which $\delta\mathbf{x}^i(t)$ is the $i^{\text{th.}}$ principal axis.

Lyapunov exponents are given as

$$\lambda_i = \lim_{t\to\infty} \frac{1}{t} \log\left(\frac{\delta \mathbf{x}^i(t)}{\delta \mathbf{x}^i(0)}\right). \tag{B.2.2}$$

Let us denote the time evolution operator as

$$E_t = e^{\lambda_i t}\,. \tag{B.2.3}$$

Dividing the time t into the two steps as $t = t_1 + t_2$ we have

$$\delta \mathbf{x}^i(t_1 + t_2) = \delta \mathbf{x}^i(0) E_{t_1} E_{t_2}\,. \tag{B.2.4}$$

Therefore, dividing the time into n equal steps such that $t = n\Delta t$ gives the Lyapunov exponents as follows

$$\lambda_i = \lim_{t\to\infty} \frac{1}{n\Delta t} \log\left(\frac{E_{\Delta t} ... E_{\Delta t} \delta \mathbf{x}^i(0)}{\delta \mathbf{x}^i(0)}\right). \tag{B.2.5}$$

Let $\mathbf{v}_0^i$ be the orthonormal basis which are tangent to the trajectory of the $i^{\text{th.}}$ initial condition at $t = 0$. Time evolution of these vectors can be obtained by $\mathbf{v}_1^i = E_{\Delta t}\mathbf{v}_0^i$. However, the vectors $\mathbf{v}_1^i$ do not have to be orthogonal. Using the Gram-Schmidt orthogonalization we can obtain the orthogonal set as follows

$$\begin{aligned} \mathbf{u}_1^1 &= \mathbf{v}_1^1 \\ \mathbf{u}_1^i &= \mathbf{v}_1^i - \sum_{l=1}^{i-1} P_{\mathbf{u}_1^l}(\mathbf{v}_1^i)\,, \quad i > 1\,. \end{aligned} \tag{B.2.6}$$

$P_\alpha(\beta)$ is the projection operator defined by

$$P_\alpha(\beta) = \frac{\langle \beta, \alpha\rangle}{\langle \alpha, \alpha\rangle}\alpha\,, \tag{B.2.7}$$

where $\langle \cdot, \cdot \rangle$ is the inner product. The expansion rate of the vector $\mathbf{v}_1^i$ can be found by

$$r_1^i = \frac{\|\mathbf{u}_1^i\|}{\|\mathbf{v}_0^i\|} = \left\|\mathbf{u}_1^i\right\|, \tag{B.2.8}$$

where $\mathbf{v}_i^i$ is normalized to 1. $\mathbf{u}_1^i$ can be normalized as follows

$$\tilde{\mathbf{u}}_1^i = \frac{1}{r_1^i}\mathbf{u}_1^i\,, \tag{B.2.9}$$

This procedure defines the time evolution of one Δt. After $n\Delta t$ steps we have

$$\lambda_i = \lim_{n\to\infty} \frac{1}{n\Delta t} \sum_{k=1}^{n} \log\left(r_k^i\right). \tag{B.2.10}$$

The set $\lambda_i = \{\lambda_1, ..., \lambda_N\}$ is called as Lyapunov spectrum. The highest deviation among $\mathbf{v}_k^i$ and $\mathbf{u}_k^i$ occur for $\mathbf{u}_k^1$ as a consequence of this construction. At least one positive Lyapunov exponents is sufficient to say that the system is chaotic.